Methodological approaches to the optimization of observatory systems for the study of benthic ecological processes

by

Katleen Robert
B.Sc., McGill University, 2008

A Thesis Submitted in Partial Fulfillment
of the Requirements for the Degree of

MASTER OF SCIENCE

in the Department of Biology

Supervisory Committee

Methodological approaches to the optimization of observatory systems for the study of benthic ecological processes

by

Katleen Robert
B.Sc., McGill University, 2008

Supervisory Committee

Dr. S. Kim Juniper, (School of Earth and Ocean Sciences, Department of Biology)
Supervisor

Dr Bradley R. Anholt, (Department of Biology, Bamfield Marine Sciences Centre)
Departmental Member

Dr. Mairi M.R. Best (School of Earth and Ocean Sciences)
Outside Member

Dr. Philippe Archambault (Institut des Sciences de la Mer de Rimouski)
Additional Member

Abstract

Supervisory Committee
Dr. S. Kim Juniper, (School of Earth and Ocean Sciences, Department of Biology)
Supervisor
Dr Bradley R. Anholt, (Department of Biology, Bamfield Marine Sciences Centre)
Departmental Member
Dr. Mairi M.R. Best (School of Earth and Ocean Sciences)
Outside Member
Dr. Philippe Archambault (Institut des Sciences de la Mer de Rimouski)
Additional Member

Although the deep seafloor represents the largest biome on the planet, its benthos has remained understudied because of logistical difficulties and the cost of access. Long-term, time-series information is needed to understand the small-scale and inter-annual variations required to build predictive models of ecological processes. In this thesis, we employed three newly developed observatory systems, which coupled *in situ* imagery with environmental data to examine ecological processes in three deep-sea benthic habitats: 1) Megabenthic surface bioturbation on the upper continental slope (400m depth) near Barkley Canyon, off Vancouver Island, 2) Thermal response in polynoid taxa at Main Endeavour Hydrothermal Vent Field (2,100m depth) on the Juan de Fuca Ridge and 3) Behavioural rhythms and bacterial mat growth in Saanich Inlet (100m), a fjord in southern Vancouver Island. To ensure that the imagery collected was useful for quantitative hypothesis testing by a single observer, we employed a step-wise methodological approach, taking advantage of previously acquired knowledge and, in two cases, the interactive nature of cabled observatories, to tailor the sampling frequency to the variables of interest. The application of a diverse array of image analysis techniques and statistical models, easily extendable to other systems, was also demonstrated.

The results obtained while conducting the protocol optimization phase described organism and community level responses to environmental variations. Using a remotely operated camera connected to the NEPTUNE Canada cabled observatory, we estimated that total surface sediment turnover by sea urchins and flatfish, the two most important megafaunal contributors, within the field of view required 93 to 125 days in the absence of phytodetrital accumulations. When employing a camera-temperature array system, the most frequently observed mobile megafaunal species, two polynoid taxa, were not found to exploit the recorded temperature gradients suggesting that they employed a thermoconforming strategy to cope with thermal variability. In the aphotic, mostly hypoxic benthos of Saanich Inlet, strong behavioural entrainment, neither diel nor tidal, was not observed. However, significant changes in species composition and bacterial mat substratum coverage were observed following intrusion of oxygenated waters, a yearly event resulting from specific bathymetric features and oceanographic dynamics of this fjord. A Bayesian approach to data modeling was found to be particularly well suited to protocol optimization purposes as complex models could be more easily and intuitively implemented.

The further application of our multi-disciplinary step-wise approach will reduce the time required to approach new ecological questions and improve integration of studies carried in different locations. By carefully choosing ecosystem functions which can be used as indicators of change, the current baseline state of the system can be described. Informed long-term monitoring initiatives can then be implemented in order to quantify global ocean responses to anthropogenic factors such as climate change, resource extraction or eutrophication.

Table of Contents

List of Tables

List of Figures

Acknowledgments

Very many people helped tremendously throughout this project and this thesis would not have been possible without their help.

I would like to first thank the undergraduate students who have helped with data collection and processing; Courtney Dean, Katrina Nikolich and Sonja Kolstoe. I would also like to thank the members of my lab for their support and intellectual contributions; Annie Bourbonnais, Maéva Gauthier, Damian Grundle, Nathalie Forget, Sheryl Murdock as well as all the other graduate students in the School of Earth and Ocean Sciences, University of Victoria.

For technical support I would like to extend my sincere thanks to Jonathan Rose, Nic Scott, Kim Wallace and Jason Williams. The skills I have learned with you have already proven their use beyond the writing of this thesis. I would also like to mention the remarkable crew and staff members of NEPTUNE Canada, VENUS, DMAS, ROPOS, Alvin, R/V Thomas G. Thompson, R/V Atlantis and CCGS John P. Tully.

I am indebted to many contributors who volunteered their time, knowledge and experience to this thesis; Jaccopo Aguzzi, Amanda Bates, Corrado Costa, Alex Hay, Ray Lee, Marjolaine Matabos, Paulo Menesatti, Farouk Nathoo, Kirt Onthank and Douglas Schillinger.

For funding, I would like to acknowledge the Natural Sciences and Engineering Research Council of Canada (NSERC), le Fonds québécois de la recherche sur la nature et les technologies (FQRNT), the Canadian Healthy Ocean Network (CHONe) and the Biology department of the University of Victoria.

Finally, I would like to address a special thanks to my committee members for their availability and numerous advice; Philippe Archambault, Brad Anholt and Mairi Best; with a particular thank you for giving me the opportunity to get involved with at-sea operations. I would also like to thank Sally Leys for her role as external examiner. Of course, I would like to express my outmost gratitude to Dr. Kim Juniper, my supervisor. Your involvement has been most valuable throughout this project, I have learned a lot and I am looking forward to applying it in future endeavours.

Merci beaucoup,

Vous avez mes plus sincères remerciements et toute ma gratitude.

Dedication

To family and friends, a strong support network made all the difference
A ma famille et mes amis, un réseau de support fiable a fait toute la différence

Chapter 1
Introduction

Shooting for Picture Perfect

Our understanding of the ecology of the deep seafloor, arguably the most extensive habitat on earth, is hampered by the cost and logistic challenges associated with sampling and data gathering at great depths (Snelgrove 1999). The baseline state of the deep-sea benthos remains poorly characterized and little is known of how environmental factors influence ecological processes. With the deep sea facing threats such as increased anthropogenic disturbances from trawling or mining as well as the expansion of anoxic zones and increasing acidification from rising global CO_2 levels (Davies et al. 2007), it becomes increasingly important to understand the factors driving the functioning of deep-sea ecosystems in order to more accurately predict how they may respond to future changes.

Fortunately, our industrial and technological development is also extending our scientific reach into these distant ecosystems. In particular, the use of underwater imagery is now much more prevalent in deep-sea research. For example, the coupling of imagery and acoustic data acquired via Remotely Operated Vehicles (ROVs) and Autonomous Underwater Vehicles (AUVs) is being used for habitat mapping which can serve in spatial planning (Bett 2001, Masson 2001). These types of spatial surveys also provide insights into relationships between ecosystem properties and habitat variables that can be used in predictive modeling. However, time-series observations of ecosystem responses to environmental variation are also needed to develop and test predictive models. Cost and technical challenges have so far limited long-term studies of ecological processes in the deep sea (Glover & Smith 2003) as time-series studies have usually

involved costly and logistically challenging deployments of autonomous cameras and instrument packages.

These autonomous systems were originally limited by battery life and memory space, but incessant developments have greatly improved their ability to monitor ecological processes occurring at various temporal scales. Early, short-term deployments of baited cameras revealed the importance of carcass falls and mobile scavengers in deep-sea ecosystems (Rowe et al. 1986). Simulation of food falls still remain one of the rare types of manipulative experiments accomplished using deep-sea camera systems. Longer deployments of autonomous camera landers led to the realisation that the deep sea was also subject to seasonal variations in sedimentation of particulate organic matter from the surface ocean, including strong pulses of phytodetritus input (Billett et al. 1983). Higher sampling frequencies allowed documentation of megabenthos movement patterns, revealing responses to organic matter pulses and permitted the estimation of surface bioturbation rates (Smith et al. 1993b, Kaufmann & Smith 1997, Bett et al. 2001). The contribution of macrofauna to vertical sediment mixing was also estimated using observations from autonomous cameras (Smith et al. 1986), and this capability was later enhanced by the development of sediment profile imagery and by further increasing image acquisition frequency (Solan & Kennedy 2002, Solan et al. 2004). Specifically designed platforms, such as the 'Eye-in-the-Sea' (EITS) or the 'Intensified Silicon Intensified Target' (ISIT) lander, have been used to document other processes such as bioluminescence (Gillibrand et al. 2007, Raymond 2008). The introduction of fixed-position benthic video camera systems in deep-sea ecological studies has finally made it possible to monitor behavioural activities occurring over the time scales of seconds to

minutes. Examples include swimming behaviours and muscle performance in deep-sea fish (Bailey et al. 2003), feeding behaviour of scavengers at simulated food falls (Jeffreys et al. 2011), shrimp predation on amphipods (Jamieson et al. 2009) as well as community responses to physico-chemical changes at hydrothermal vents (Sarrazin et al. 2007, Auffret et al. 2010).

Further technological advances resulted in the recent development of cabled seafloor observatories on which a suite of instruments are connected to land by communication and power cables, now offering cost-effective opportunities for continuous monitoring of oceanographic systems with real-time data transfer to shore (Delaney et al. 2000, Service 2007). As far as benthic ecosystems are concerned, these instrument arrays provide opportunities for *in situ* observation of key organisms in real-time using remotely operated video or still cameras which can be coupled with data on physical and chemical properties measured by other nearby sensors for the study of processes at local scales (Sherman & Smith 2009). On the west coast of Canada, two such observatories, VENUS (Victoria Experimental Network Under the Sea, 2006, www.venus.uvic.ca/) and NEPTUNE Canada (NorthEast Pacific Time Series Undersea Networked Experiments, 2009, www.neptunecanada.ca/), have been deployed in recent years. Similar observatories are also planned for the west coast of Washington and Oregon, USA (Isern & Clark 2003) as well as all in different regions of Europe (Priede et al. 2004) as part of the Ocean Observatories Initiative (OOI, USA) and the European Seas Observatory NETwork (ESONET). By providing long-term time-series data, these cabled observatories will enable documentation of the baseline state of the deep-sea

benthos, which is essential to detecting responses to environmental change, be they natural or anthropogenic in nature (Glover & Smith 2003).

For observational studies, the main advantage of these cabled observatories when compared to autonomous observatory systems is their interactivity whereby sampling frequencies can be adjusted based on an adaptive approach which builds on new knowledge acquired continuously. As such, the successful use of cabled observatory instruments for ecological research questions requires the optimization of instrument placement and the development of observation protocols. First and foremost, previous knowledge of benthic communities and their environment, acquired via complementary means such as submersible surveys or shipboard sampling will provide information on general site selection for instrument placement. Important technical considerations for determining final instrument locations include constraints such as cabled length, substratum type, predisposition to fouling and the level of risk to the equipment. Once positioning has been finalized, careful thought needs to be given to determining the appropriate sampling protocol, particularly in the case of camera systems. Continuous, unlimited acquisition of imagery is not practical for several reasons. Storage and processing of large quantities of image data are a major challenge for all observatory projects; particularly when manual image processing remains the most reliable analysis technique (Solan et al. 2003). The use of artificial lighting to acquire imagery in an otherwise aphotic environment is a potential environmental impact issue (Herring et al. 1999, Widder et al. 2005) that places time constraints on the use of cameras. Too few observations, on the other hand, will fail to capture episodic or short-lived phenomena

that can be critical to ecosystem function; hence, the need to customize observational protocols when first employing these technologies in a new environment.

Once this has been achieved, methodological development needs to focus on the extraction of quantitative information from the collected imagery in order to move beyond a solely descriptive approach. In addition to simply counting and identifying species, techniques such as perspective grids (Wakefield & Genin 1987), polar coordinate systems (Norris et al. 1997), fractal analysis (Mandelbrot 1983) and particle tracking techniques (Lard et al. 2010) can be employed to estimate parameters of interest and yield predictive models. Collaboration with software engineers will improve video annotation tools and image analysis techniques; hopefully eventually alleviating the current bottleneck resulting from reliance on manual processing (Solan et al. 2003). Bayesian modeling approaches are particularly well suited to optimization questions as they can easily handle missing data points and allow for the inclusion of previous information through the use of priors (Gelman et al. 1995). The use of quantitative approaches and standardized observation protocols will expedite answering large-scale ecological questions by facilitating comparison between locations.

The main objective of this thesis was to develop methodological approaches to quantitatively study ecological processes using time-series, deep-sea imagery; more specifically, to investigate how environmental variation affects the behaviour of megabenthic organisms. We sought to develop and test methods for the characterization of three different processes involving individual organisms or benthic communities. 1) We used the NEPTUNE Canada observatory cameras to quantify megafaunal surface bioturbation rates near Barkley Canyon (400m); 2) We studied the relationship between

locomotion patterns and thermoregulating behaviour in two polynoid taxa at Main Endeavour Vent Field (2,100m) using an autonomous camera and temperature sensors; 3) We used the VENUS observatory camera and sensors in Saanich Inlet (100m) to study behavioural rhythms in specific taxa and their responses to fluctuating environmental variables. In each chapter of this thesis, a different observing system was employed and new methodological approaches were developed, applied and tested, creating a set of tools easily applicable to other benthic processes and camera systems.

Chapter and Appendix Summary

Megafaunal Surface Bioturbation

In Chapter 2, I examined surface bioturbation, a process of ecological importance (Lohrer et al. 2004) which provides valuable ecosystem services (Beaumont et al. 2007). In the deepsea, little is known regarding how bioturbation may vary over short time scales, but seasonal trends are expected. In the northeast Pacific, increased summer and fall primary productivity in surface waters lead to higher quantities of phytodetritus reaching the benthos (Drazen et al. 1998, Lauerman & Kaufmann 1998, Smith et al. 2008). This increased food supply has been shown to influence composition and activity rates in megabenthic organisms (Kaufmann & Smith 1997).

This process was examined using a remotely operated camera system connected to the Barkley Canyon node of the NEPTUNE Canada cabled observatory. Approaches to observation protocol optimization, extraction of quantitative information and Bayesian modeling are presented. A description of ROV video transect analysis used to position two instrument platforms on a mid-depth plateau as well as a time-series observation of surface chlorophyll concentrations obtained through satellite imagery are included in

Appendix A. Appendix A was included as part of a collective work led by Dr M. Matabos which yielded Chapter 14, 'Seafloor Observatories' of the Wiley-Blackwell book entitled 'Biological sampling in the deepsea'.

Thermal response of Vent Polynoids

In Chapter 3, we addressed the question of whether marine ectotherms have evolved the ability to exploit small-scale gradients in substratum temperature. Movement patterns restricted to a narrower range of temperatures than available in the environment would suggest habitat selection as a result of active thermoregulating behaviours or following foraging decisions. Hydrothermal vents represent a unique ecosystem to address such questions as they are one of the only marine habitat where large temperature fluctuations are observed over short temporal and spatial scales (Bates et al. 2010).

These questions were investigated using autonomous camera-temperature array systems deployed with the submersible Alvin. This camera system was developed and tested by Dr. R. W. Lee (Rinke & Lee 2009). Co-author K. L. Onthank applied his knowledge of image analysis to create a routine which automatically selected organisms based on their colour and subtracted the background. This allowed for quick processing of the large quantity of image acquired during the deployments. As first author, I made use of interpolation techniques to create temperature maps and extract the temperature experienced by organisms as they moved across the field of view. I also applied a two state hidden Markov model (Patterson et al. 2009) whose results were used to discuss optimization of image acquisition frequency, deployment duration and size of the field of view. In Appendix B, differences in temperature interpolation estimates between linear and ordinary kriging techniques were investigated. These estimates were obtained using

the same camera-temperature array systems, but sulphide worms, *Paralvinella sulfincola*, individuals were observed in this instance. Presentation of differences between position estimates from two independent observers as well as behavioural classification of individual sulphide worms (Grelon et al. 2006) were also assessed. The temperature interpolation, position estimates and behavioural classification were contributed to a manuscript authored by Dr A. E. Bates. Only the figures from this manuscript appear in Appendix B.

Behavioural Responses to Environmental Cycles

In Chapter 4, we presented the work carried on the behavioural rhythms of taxa representing the benthic community of Saanich Inlet, a fjord on the southern portion of Vancouver Island, BC. We examined geophysical factors associated with diurnal and tidal cycles. On a longer time scale, oxygen concentration fluctuations resulting from deep-water renewal was also analyzed. This event occurs in fall when waters from Haro Straight cascade over the shallow sill (70m in depth) at the mouth of the inlet and displace the lower layer of hypoxic waters ($< 2 ml\ l^{-1}$) (Anderson & Devol 1973).

This study was conducted using the camera connected to the VENUS cabled observatory and was part of a collaborative project between VENUS, Dr Juniper's laboratory (University of Victoria), the Instituto de Ciencias del Mar (Spain) and the Agricultural and Engineering Research Unit of the Agriculture Research Council (Italy). It yielded the article by Matabos et al. (2011a) comprising Chapter 4. As first author, Dr M. Matabos analyzed the collected images to obtain abundance estimates for the two species of decapod observed, compiled the data regarding the environmental variables and carried the cross-correlation analyses. She also assembled the contributed sections

and composed the manuscript. Dr J. Aguzzi was responsible for the periodogram and waveform analysis of the decapod abundance data. My contribution as co-author included the application of optical techniques, described in Chapter 2, to create perspective grids used to quantify seafloor surface area (Wakefield & Genin 1987). I also contributed i) a description of fractal analysis (Mandelbrot 1983) techniques for the surface coverage quantification of macroscopic mats of chemosynthetic bacteria, *Beggiatoa* spp., over time and ii) an analyses of ROV video transects collected from 2005 to 2009 under both oxic and hypoxic conditions used to determine optimal camera placement. A brief summary of these results is included in Appendix C. A short technical note on the creation of a computer simulation used to examine the effect of the number of visible squares of a perspective grid at varying bacterial mat densities is outlined in Appendix D.

Chapter 2
Quantifying megafaunal surface bioturbation using cameras on the NEPTUNE Canada cabled observatory: Observational protocol development and Bayesian modeling

Robert, K.[1*] and Juniper, S.K.[1, 2]

[1]Department of Biology, University of Victoria, PO Box 3020 STN CSC, Victoria, BC V8W 3N5, Canada

[2] School of Earth and Ocean Sciences, University of Victoria, PO Box 3065 STN CSC, Victoria, B.C. V8W 3V6, Canada

Submitted to Marine Ecology Progress Series, April 2011

Second round of review, August 2011

*Corresponding author: katleenr@uvic.ca
Department of Biology, University of Victoria, PO Box 3020 STN CSC,
Victoria, V8W 3N5, Canada
Tel: (+1) 778-430-0332

Abstract

The mixing of deep-sea sediments by the benthic megafauna is an important ecological service that influences biogeochemical processes. Quantifying the contribution of individual species to bioturbation and their responses to environmental variations both require experimental manipulations or direct observations, both of which are logistically challenging in the deep sea. Emerging cabled seafloor observatories now permit real-time data transfer to shore and interactive sampling, providing a new tool for long-term studies of the benthos at high temporal resolutions. We report here on the development of a methodological approach to studying bioturbation in a submarine canyon using video cameras remotely operated over the internet, through the NEPTUNE Canada observatory. A step-wise process was used to determine optimal observation schedule and image analysis techniques were developed to extract quantitative measures for flatfish and sea urchins. Application of a Bayesian model to extrapolate data quantifying megafaunal locomotion patterns and appearance rates indicated complete sediment surface turnover in 93 to 125 days. Our proposed model provides an initial step in building a long-term program for monitoring ecological processes on the seafloor.

Introduction

The floor of the deep ocean, arguably the most extensive habitat on earth, remains markedly understudied particularly with regard to phenomena requiring time-series observations. Deploying instruments and cameras in the deep sea for times-series studies is costly and logistically challenging. A relatively small number of studies to date have provided some key insights into the functioning and dynamics of deep-sea ecosystems. For example, time-lapse camera deployments have revealed the role of scavengers and carcass falls (Witte 1999) in deep-sea food webs as well as ecosystem responses to seasonal inputs of phytodetritus (Lampitt et al. 2001, Smith et al. 2008). Another important deep-sea ecosystem process that can be studied in time-series imagery is bioturbation, the mixing of sediment by benthic organisms (Smith et al. 1993b, Kaufmann & Smith 1997, Bett et al. 2001, Belley et al. 2010). Deposit-feeders ingest sediments, absorb their organic content and excrete pellets, while burrowing organisms, through bioirrigation and vertical mixing of particles (Meysman et al. 2006), can directly alter sediment properties both physically (Rhoads & Boyer 1982) and chemically (Aller 1982). The role of bioturbators is of enough importance to warrant them the name of ecosystem engineers (Mermillod-Blondin & Rosenberg 2006, Meysman et al. 2006). A recent analysis of global bioturbation in soft sediment identified a clear lack of information regarding sources and levels of bioturbation in the deep sea (Teal et al. 2008).

Bioturbation has most commonly been studied through the use of vertical tracers or time-lapse imagery. In the former, natural or artificial tracers deposited at the surface are eventually buried deeper within the sediment column as a result of faunal activity

(Maire et al. 2008). Sediment cores are then taken and sliced. A mathematical model is fitted to the resulting profile of tracer quantity over depth to yield bioturbation coefficients (D_b) or mixed layer depth (L) (Meysman et al. 2008). Naturally occurring tracers, such as radionuclides (Smith et al. 1993a, Gerino et al. 1998), or artificially introduced tracers, such as luminophores or isotopically labelled particles (Bradshaw et al. 2006, Maire et al. 2006), have been used to resolve different timescales of vertical mixing of sediments. Regardless of the tracer method used, the obtained biodiffusion coefficients only provide a time-averaged estimate of bioturbation. Although limited to the observation of larger organisms moving over the sediment surface, time-series image analysis does allow a better resolution of short-term variations (Maire et al. 2008) and the partitioning of contributions by species. This approach has been used to quantify bioturbation in imagery obtained with autonomous cameras at deep-sea sites; Station M in the northeast Pacific (Smith et al. 1993b, Kaufmann & Smith 1997) and the Porcupine Abyssal Plain in the northeast Atlantic (Bett et al. 2001) as well as in the lower estuary and Gulf of St-Lawrence (Belley et al. 2010). In addition to cameras that view the seafloor surface, sediment profile imaging systems inserted directly into the sediment provide supplementary information by allowing for the direct observation of burrowing behaviour as well as the vertical movement of luminophores (Solan et al. 2004).

Recently, two cabled seafloor observatories, VENUS (Victoria Experimental Network Under the Sea, 2006) and NEPTUNE Canada (NorthEast Pacific Time Series Undersea Networked Experiments, 2009), have been deployed off the west coast of Canada. As these technologies come into use, there is a need to develop methodological approaches and optimize observational protocols in order to make productive use of

online observatory cameras and accompanying instruments for ecological studies. Acquiring continuous video streams is operationally simple, but impractically large quantities of data would need to be stored and processed. Although significant advances are being made in automated image analysis (Walther et al. 2004, Aguzzi et al. 2009b, Purser et al. 2009) there are few, if any software tools that can reliably be employed for *in situ* benthic studies. Most analyses still require labour-intensive manual processing of imagery by trained observers. In many cases, the amount of time required to process the imagery surpasses the real-time duration of the footage; severely limiting the use of extensive video or photo records for ecological studies (Solan et al. 2003). In the deep sea where sunlight never penetrates, additional considerations related to light pollution from artificial sources must also be taken into account. The prolonged presence of unnatural lighting has the potential to negatively affect deep-sea organisms (Herring et al. 1999), influence the behaviour of the animals under study (Widder et al. 2005, Raymond & Widder 2007) and accelerate biofouling of instruments.

The duration of all autonomous camera studies has been limited by data storage capacity as well as by battery life but these two technologies have improved considerably in recent years. Cabled observatory cameras are free of data or energy storage constraints, but their greatest advantage lies in their real-time and interactive capabilities. Their sampling frequency does not need to be determined before deployment; it can be refined based upon incrementally improving knowledge of the system or triggered in response to an unpredicted event (Delaney et al. 2000, Service 2007, Sherman & Smith 2009). Remotely-controlled pan and tilt mechanisms afford a larger field of view (FOV) and allow for precise positioning and repositioning to study small features such as inhabited

burrows. *In situ* observation of key benthic organisms in real-time can then be coupled with data on physical and chemical properties measured by nearby sensors (Sherman & Smith 2009).

This paper describes the development of a combined observational and modeling protocol for the quantitative study of surface sediment bioturbation by megafaunal organisms at a NEPTUNE Canada cabled observatory site on the upper continental slope in the northeast Pacific Ocean, off Vancouver Island, Canada. We present the newly deployed observatory camera system and our approach to optimizing its use for the quantitative study of surface bioturbation. Techniques for extracting quantitative information from the imagery acquired during the first year of deployment are described, as is the development of a Bayesian model to estimate the rate of sediment reworking by the megafauna. Bayesian inference is particularly well suited to research questions requiring methodological optimization because previous knowledge (acquired as methods are refined) can be incorporated in the prior distributions (Dennis 1996, Ellison 1996, Ellison 2004). A quantitative model of bioturbation rates can thus be created and improved upon as additional observations are made. Bayesian modeling is still relatively new in ecology, but recent years have seen an increasing number of studies making use of this approach (Choy et al. 2009, Ogle 2009).

Methods and Results

Study Area

Barkley Canyon, located 100 km off the coast of Vancouver Island, British Columbia, Canada, is a submarine canyon connecting the continental margin to the abyssal plains. It was chosen as a site for one of the regional nodes of the NEPTUNE

Canada cabled observatory because of its suitability for the study of bentho-pelagic couplings as well as nutrient and sediment fluxes across the continental slope. In 2009, the Barkley Canyon node was connected to the backbone fiber optic cable, allowing for real-time data streaming back to a shore station located in Port Alberni, BC and the operations centre at the University of Victoria. Three instrument platforms (IP) with black and white video cameras were deployed at three depths near to or within the canyon; the first observation site was located at the shelf-break (396 m, 48°25'37.18" N, 126°10'29.72" W), the second camera was positioned mid-canyon on a plateau (891 m, 48°18'54.23" N, 126°3'31.16" W) while the third camera was installed within the canyon's axis (984 m, 48°19'0.02" N, 126°3'0.64" W).

Instruments

The video cameras used for this study were low-light, black and white Multi-SeaCam® from DeepSea Power & Light with a depth of field in water of 57° horizontal and 45° vertical, it yielded a surface of observation of ~ 0.9 m^2 per frame. The centre of the lens was positioned 61 cm above the base of the platform's legs. The cameras were mounted on pan and tilt mechanisms, which allowed for remote control. The total field of view (FOV) was evaluated as having a radius of 200 cm, for a total of 8.8 m^2. Physical limitations of the pan mechanism reduced camera rotation to less than a full 360˚, creating a blind spot near the rear left leg of the platform that accounted for 30% of the FOV. The camera control web interface allowed for semi-automated observations using predetermined camera positions. All cameras were also equipped with two 635 nm laser beams positioned 10 cm apart and used for image scaling. In addition, the lighting

system was composed of a pair of ROS SmartLIGHT II strobe equipped with seven adjustable LED lights (5,500° K , 570 lux at 1 m) positioned 24 cm on either side of the lens. A 2 m long scaling ruler marked at 10 cm intervals was laid on the seafloor perpendicular to the long axis of the IP, with one end directly below the camera on the seafloor (Nadir point) and the other extending away from the study area. The video stream was recorded in .mov files and stored by NEPTUNE Canada's data archiving system DMAS. These archived videos can also be downloaded online and interested individuals can also view live streams from the cameras using the web interface (http://dmas.uvic.ca/Camera).

Spatial Considerations

Video surveys were conducted around each IP during the maintenance cruise of May 2010 with the remotely operated vehicle (ROV) ROPOS (operated by the Canadian Scientific Submersible Facility), in order to develop a more spatially extensive understanding of the local benthic megafauna observed by the cameras. Starting over the IPs, eight 50 m long radial transects separated by 45° angles were surveyed. While the ROV flew at a height of 1-3 m, a down-mounted camera, including in its FOV two laser beams separated by 10 cm, recorded video imagery that was used to identify megabenthic organisms to the lowest taxonomic unit. During each transect, the ROV's navigation system reported its position every second, so that the position of organisms on the seafloor could be geo-referenced. During a subsequent cruise in September 2010, a multi-beam survey of the area surrounding the Shelf-break IP was also carried out with the ROV flying at an altitude of 5 m above bottom. In addition, to characterize decimetre

scale changes in the sediment surface, images from Kongsberg Mesotech Rotary sonars with 1071 heads deployed on all three IPs were also examined. These instruments collected images at 675 kHz, and these were then analyzed for the formation and turnover rates of sediment structures.

A Principal Component Analysis (PCA) of the ROV video transects clearly indicated a difference in species composition between the three camera sites. The clustering of species (Table 1) reflected the three sites with the first principal component loading explained 35% of the variation and the second representing 23.5% of the variation. The first principal component loading was found to be highly correlated to depth based on linear regression ($r^2 = 0.85$, $p < 0.001$) while the second component could be explained using the number of cobbles present along a transect ($r^2 = 0.26$, $p = 0.006$).

Table 1: Species composition surrounding the three instrument platforms based on clusters identified using a Q-type PCA.

Shelf-Break	**Axis**	**Mid-Canyon**
Rockfish, *Sebastes* sp.	Sun Star, *Solaster* sp.	Tanner Crab, *Chinocetes* sp.
Fragile Pink Sea Urchin, *Allocentrotus fragilis*	Blood Star, *Henricia* sp.	Snail, Buccinidae
Orange Anemone, Actiniaria	Thornyhead, *Sebastolobus* sp.	Droopy Sea Pen, *Umbellula* sp.
Holothurian, *Pseudostichopus mollis*	Eelpout, *Lycenchelys*sp.	Holothurian, *Pannychia* sp.
	Sand Star, *Luidia foliolata*	

Preliminary analysis of the sonar imagery indicated further differences between the IP sites. Abundant ~50 cm diameter pits were observed surrounding the Shelf-break IP, but not at the two deeper sites. Pit location did not change over time (Hay et al. *in prep.*). These pits were also observed over a larger spatial scale during ROV surveys. Their depth was visually estimated at 3-7 cm, but because of their shallowness, they could not be resolved using the multi-beam sonar on ROPOS. Since significant differences in species composition existed between the IPs, faunal information collected

for the three IPs was not combined for analysis. As more time-series data were available for the Shelf-break site, further analysis focused on this particular IP where flatfish (Dover sole, *Microstomus pacificus* and halibut, *Hippoglossus stenolepis*) and sea urchins (*Allocentrotus fragilis*) were the primary sources of megafaunal surface bioturbation.

Temporal Considerations

As a precaution against the potential negative effects of light pollution, lighting was limited to one hour per day at each IP, but could be allocated as desired throughout the day. Different observation regimes were tested to determine the one most effective at capturing sea urchin movement patterns and flatfish abundance at the shelf-break site. The daily sampling strategies consisted of one consecutive hour, two 30 min periods or 5 min every second hour.

A step-wise approach used to optimize the sampling design yielded additional information following each iteration. The insights provided enabled a more informed choice of observation regime for the next period. The three regimes were found to optimize the sampling of different variables (Table 2). The hour-long observations provided first-order familiarity with the system; the residence time of flatfish was determined to be less than 60 min whereas this same time period did not permit detection of displacement by sea urchins. Doubling the sampling frequency (2 x 30 min per day) allowed us to observe individual sea urchins more than once each day, but was insufficient to describe sea urchin movement as on most occasions, individuals stayed less than 12 hrs within the FOV. We therefore elected to increase the sampling frequency while respecting the daily lighting time limit. A minimum of 5 min was required for the camera to cover the entire FOV. Twelve 5 min observation periods per day was therefore

the maximal frequency attainable without losing the increased FOV afforded by the pan and tilt mechanism. This regime allowed for movement tracking and improved overall fish abundance estimates. As the quantity of information collected could still be managed by a single observer, this regime was chosen for implementation.

Table 2: Qualitative assessment of each observation regime with respect to the collection of information necessary for estimating the parameters of interest for the bioturbation model.

	One 60 min Period	**Two 30 min Periods**	**Twelve 5 min Periods**
Echinoderms			
- Movement	Rarely observed	Not observed	Quantifiable
- Abundance	Rare	Rare	Infrequent
- Residence time	Less than 24 hrs	Less than 24 hrs	Accurate to within 2 hrs
Flatfish and Skates			
- Occurrence	Rare	Rare	Infrequent
Gastropods			
- Movement	Accurate	Within period only	Not Quantifiable
- Abundance	Common	Common	Frequent
Burrow maintenance			
- Occurrence	Common	Rare	Not observed
Pelagic Fish			
- Occurrence	Changed over time	Changed over time	Common

In addition to this regular monitoring program, interactive sampling and short bursts of increased sampling rates in response to unpredicted events were possible. In spring 2010, in contrast with the previous decade, no pronounced spring or summer phytoplankton bloom was observed in satellite imagery of the waters overlying Barkley Canyon. The historical trend was based on SeaWiF satellite data obtained through NASA's web-based GIOVANNI application developed by GES DISC (data not shown). Hence, a high-resolution sampling protocol was not implemented and the data collected were not partitioned based on seasonality.

Construction of perspective grids

Perspective grids were constructed to measure objects in the oblique images, based on the method of Wakefield and Genin (1987). We made *in situ* optical measurements to compensate for any sinking of the camera platform legs into the sediment following deployment. For each deployment, perspective grids were built using the paired lasers mounted on the camera, and the scaling ruler placed on the seafloor within the FOV. The distance between the laser beams varied predictably with the tilt position of the camera (Figure 1 A). With the graduated pole clearly visible in the center of the image, the horizontal scale, or relationship between laser beam separation and distance from the Nadir point, was established. Based on this information, the meridian lines of the perspective grid were traced. Horizontal lines for the perspective grid were drawn based on the vertical scale obtained using the position of the scaling ruler's 10 cm increments (Figure 2). Starting at the Nadir point, the number of pixels separating each horizontal line was then measured on screen using the image analysis software ImageJ (freely available online; http://rsbweb.nih.gov/ij/) developed by the National Institute of Health, USA. The exponential relationship (Figure 1 B) thus created was used to measure the vertical dimension of objects present within the FOV. Because IPs changed locations following the maintenance cruise in May 2010, separate relationships were established for each deployment year. The differences between years illustrate the difference in camera height from the seafloor resulting from the legs sinking within the soft sediment.

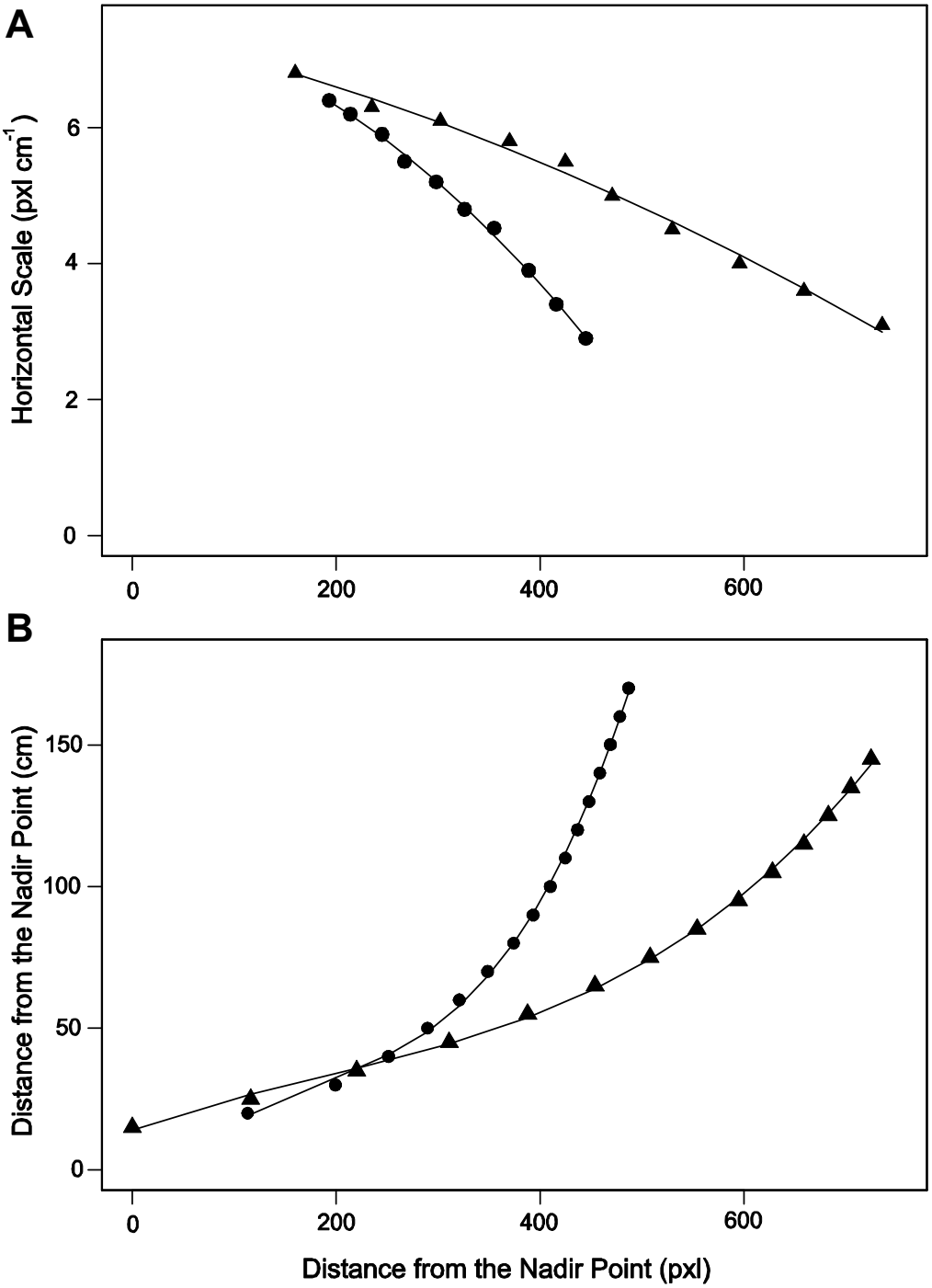

Figure 1: A) Relationship between the horizontal scale as determined by the number of pixels separating the laser beams and the pixel distance from the Nadir point. B) Relationship between the actual distance in centimetres from the Nadir point and the pixel length. The pixel representing the Nadir point was set to zero. Circles indicate the 2009 deployment and triangles the 2010 deployment.

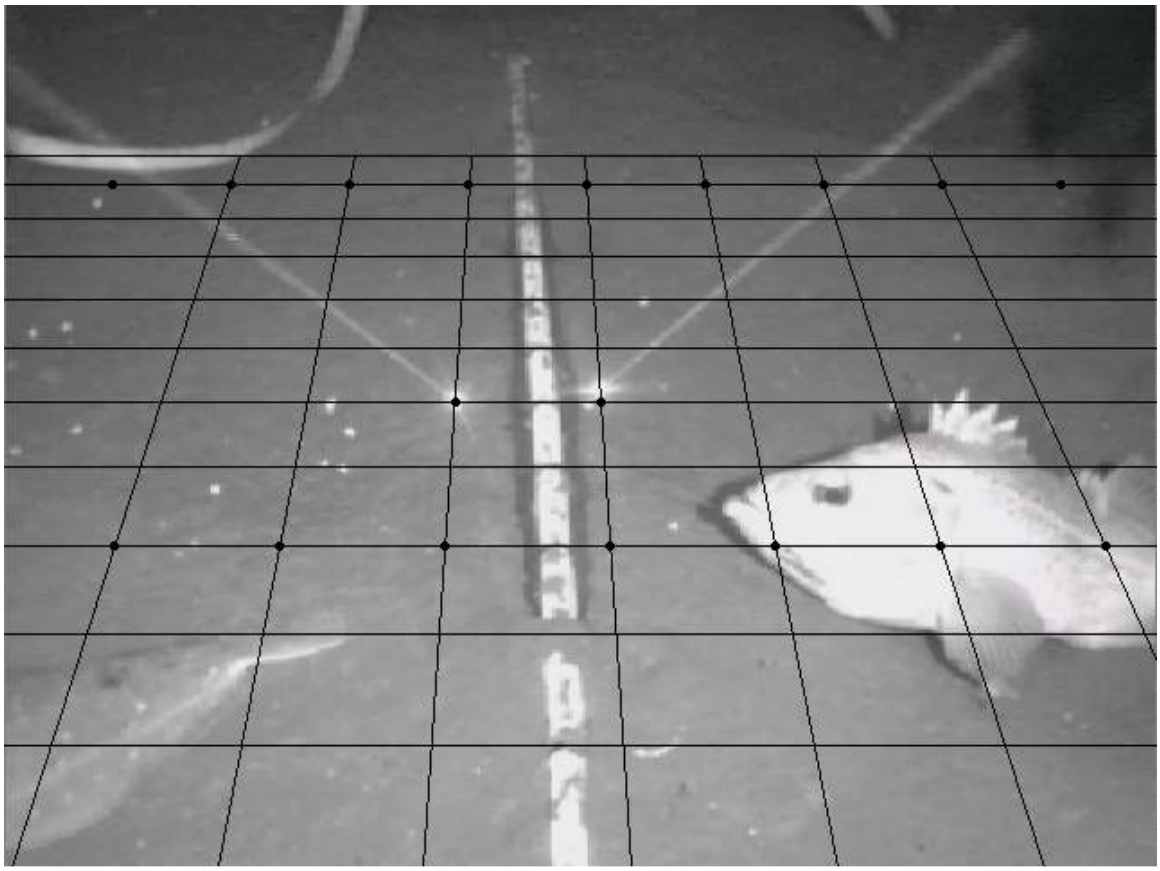

Figure 2: Perspective grid for the Axis site with a tilt = 30. The scaling ruler with 10 cm increment is visible in the center of the image and the laser beams are separated by 10 cm. Hence, each square represents 100 cm^2 on the seafloor.

Horizontal measurements were obtained using the number of pixels separating the laser points and the "Set Scale" option in Image J. To determine the vertical distance between two points (A, B) (Figure 3), we used the relationship between laser separation and distance from the Nadir point. By positioning the lasers next to each point in turn, the distance between each point and the Nadir point ($\overline{NA}$, $\overline{NB}$) could be obtained. These two distances were then subtracted to yield their vertical separation ($\overline{AB}$).

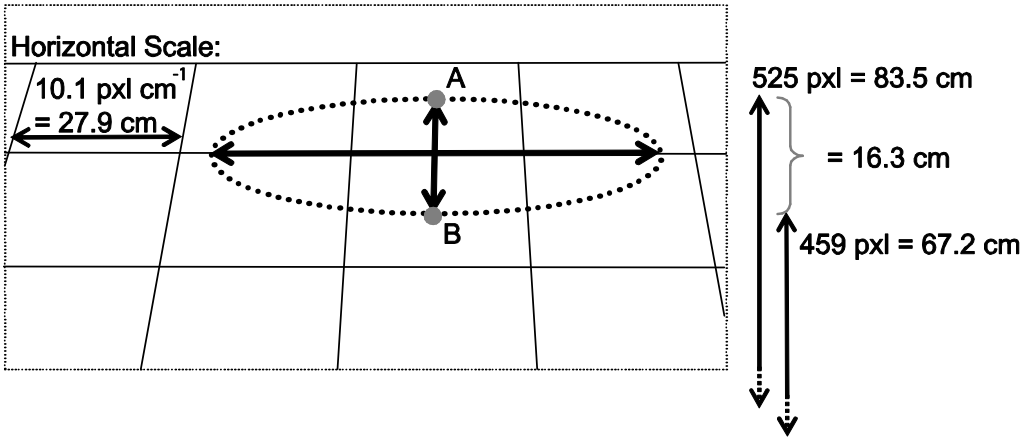

Figure 3: Measuring of objects using a perspective grid method.

Smith *et al*.(1993b) used perspective grids to follow the movement of organisms from one observation period to the next, but slight modifications were once again carried in order to accommodate the circular study area. A polar coordinate system was developed so that the position of an object could be described based on its distance from a fixed point and its azimuth (angle away from a reference direction) (Figure 4). Polar coordinate systems have been used in both terrestrial and marine ecology where study areas have been circular (Craig & Ebert 1994, Norris et al. 1997). In this case, the fixed point was the Nadir point and the reference direction was considered to be a pan value of zero. The position of each individual was recorded based on pan and tilt values, transferred to a polar coordinate system and plotted on a circular map representing the study area. The Euclidean distance between two subsequent positions was used as an estimate of the minimum distance travelled. The vertical component was calculated using the previously described techniques. For the horizontal component, a relationship between actual distances moved for degree panned at various distances from the Nadir point was established (Figure 5).

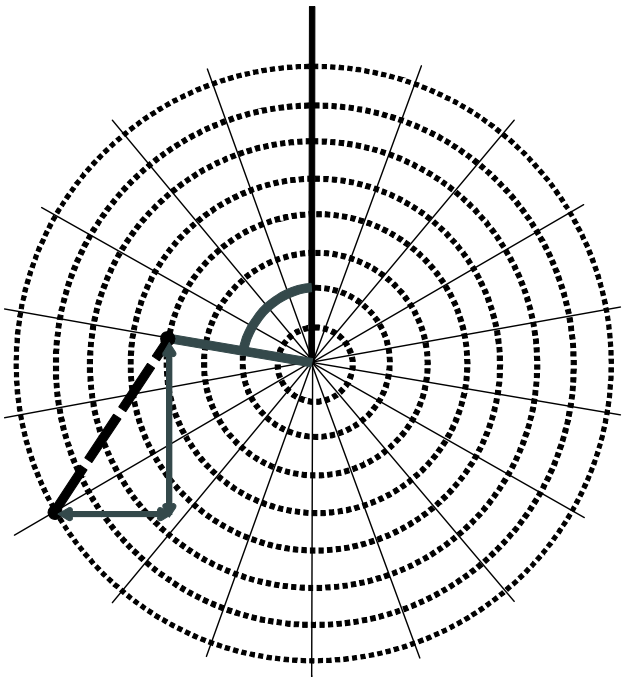

Figure 4: Polar coordinate system representing the circular field of view. The black line is the reference direction (0°) and the position of the object can be determined based on the radius and the azimuth. The horizontal and vertical components of the minimum distance travelled (black dashed line) are shown as arrows.

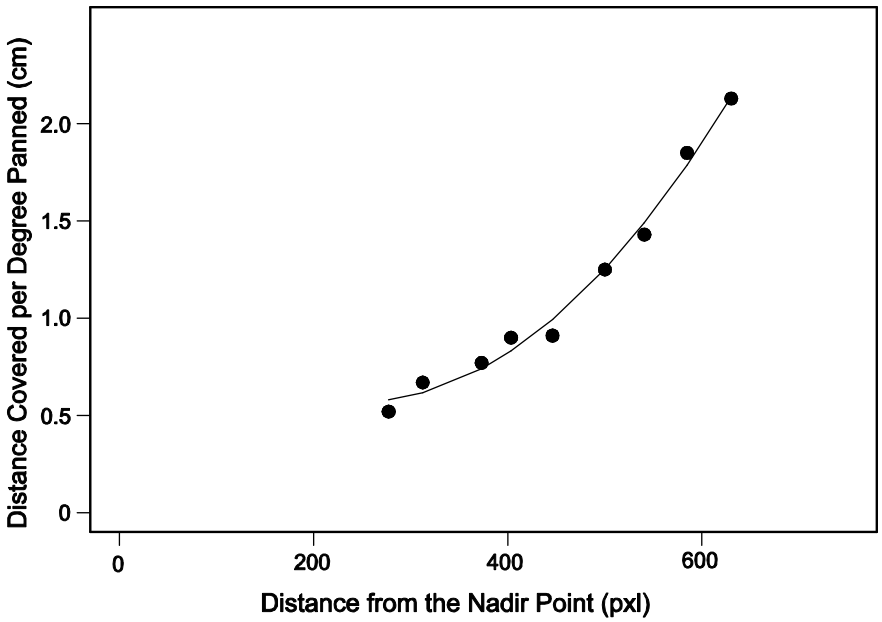

Figure 5: Relationship between distances covered in centimetres for each degree of pan moved at various distances from the Nadir point for the 2010 deployments at the Shelf-break site.

Quantifying bioturbation

Only fish species observed to frequently rest on the seafloor and cause sediment disturbance upon leaving were included as bioturbators; these mainly consisted of Dover sole (*Microstomus pacificus*) and halibut (*Hippoglossus stenolepis*). None of the skates (*Raja rhina* and *Bathyraja kincaidii*) were observed to bury themselves or otherwise disturb the sediment; hence, they were not included in the bioturbation model. The main variables of interest for analysis of flatfish effects were the surface area of the footprint left on the sediment and the frequency at which fish were observed to lie in the sediment. In order to facilitate measurements, footprint shape for flatfish was represented as an ellipse enclosing the body of the fish, but excluding the tail and dorsal fins.

The most important variables for determining the influence of sea urchin movement on the mixing of surface sediments included organism abundance and trace dimensions (e.g. width, length and depth) (Hollertz & Duchêne 2001, Belley et al. 2010). Likely due to the shallowness of sea urchin traces, these could not be resolved using the present camera system. Instead, the width of the organisms combined with the minimal distanced travelled between sightings were used to determine the area tracked during locomotion (Kaufmann & Smith 1997). Distance travelled by sea urchins between observations was converted to distance travelled per hour, to allow for comparisons between estimates obtained using each of the observation regimes. Measurements were conducted on screen from extracted video frames using the previously described technique.

Bayesian Model

A statistical model was used to quantitatively describe the contribution of the two faunal subgroups (sea urchins and flatfish) to bioturbation at the Shelf-break site. This model was similar in many aspects to the one described in Lohrer et al. (2005) except that the present model utilized a Bayesian approach. Bayesian inference is based on Bayes' theorem (Bayes 1763):

$$P(\theta|Y) = \frac{f(Y|\theta)\,P(\theta)}{P(Y)}$$

where $P(\Theta|Y)$ represents the *posterior* or probability of obtaining the parameter Θ given the data, $P(\Theta)$ is the *prior* containing previous information regarding the hypothesis, $f(Y|\Theta)$ is the *likelihood* function and $P(Y)$ is a normalizing constant (Gelman et al. 1995, Ellison 1996). It differs from a frequentist approach to hypothesis testing in a few significant ways. The most fundamental of which, is to condition probability statements on the observed data and not to estimate the probability of the obtained data given the null hypothesis. Furthermore, with a Bayesian approach, it is appropriate to state there is p% probability that the parameter is found within the limits of the credible interval. Bayesian inference also allows for the inclusion of previous knowledge in the form of priors. However, for the first iteration of the model presented in this study, uninformative priors were used. The rational was that these priors could be updated with the information obtained in this study for subsequent monitoring.

For the sea urchins, the information previously collected was used to simulate 31,000 draws of the posterior distribution for the rate of sediment displacement by a single organism as well as the number of organisms encountered per observation period, using the software WinBUG (freely available online; http://www.mrc-

bsu.cam.ac.uk/bugs/). The first parameter was modeled as a function of organism width and speed (Equation 1). Width and speed were modeled to follow a bivariate normal distribution and uninformative prior distributions were used (with N ~ (0, 1E-06) and $\Sigma \sim \begin{pmatrix} 1 & 0 \\ 0 & 1 \end{pmatrix}$). The bivariate distribution allowed missing speed data to be internally computed within WinBug, based on sea urchin width and the covariance function. A Poisson distribution with uninformative prior distribution (logN ~ (0, 1E-06)) was selected for the abundance parameter. The first 1,000 draws were discarded as a burn in and thinning was applied so that only the value of every third draw was retained. Three chains with different initial values were created and used to verify that convergence had been achieved. Little information was obtained for residence time, which averaged less than 12 hrs. Complete observation cycles were rarely achieved because of frequent system interruptions. Sea urchins often left the FOV during interruptions (e.g. recording system interruption, equipment shut-down due to ground fault issues, electrical overload of the lighting system) so that accurate residence time could not be obtained. Based on the few organisms observed without interruptions, residence time was estimated to be an average of 8 hrs and was modeled as having a normal distribution (N ~ (8, 2)).

Random draws from the posterior distribution of the rate of sediment displacement as well as from the residence time distributions were carried out. The values thus obtained were selected with respect to their probability of occurrence. Using the randomly obtained values, an estimate of the area of displaced sediment generated by one random organism was calculated using Equation 2. This process was repeated for each organism encountered during an observation period; this parameter (n) was drawn from the Poisson distribution. This process was repeated thrice daily in order to scale up

to 24 hrs. The total turnover area per day was computed by summing the area of sediment displaced contributed by each individual sea urchin.

Equation 1: Rate of displaced sediment = Width of Organism (cm) * Speed (cm hrs^{-1})

Equation 2: Area of displaced sediment = Rate (cm^2 hrs^{-1}) * Residence Time (hrs)

For the flatfish, posterior distributions were computed for footprint area and number of fish present per observation period. A normal distribution was used for the first parameter with prior distributions N ~ (0, 1E-06) for the mean and Gamma ~ (1E-03, 1E-03) for the precision. A Poisson distribution with prior logN ~ (0, 1E-06) was used for fish abundance. A random draw was carried out for the number of fish observed per time period. Based on the drawn abundance value, *n* draws from the footprint area distribution were generated. Fish stayed within the FOV for less than 60 min; hence the process was repeated hourly to scale up to 24 hrs. By adding the contribution of each individual, the total area affected per day was calculated.

The total surface area of the FOV was estimated at 8.79 m^2. For sea urchin and flatfish (both separately and combined), the number of days required to track over the entire area represented in the FOV was computed based on the daily simulations. This process was repeated 500 times to account for the uncertainty associated with using small sample size for parameter estimation. The previous steps were carried using the statistical package R (freely available online; http://www.r-project.org/). The parameters obtained for the posterior distributions for sea urchins and flatfish are summarized in Table 3.

Table 3: For two taxa of bioturbators, parameter estimates base on 31,000 draws of the posterior distribution with a 1,000 burn-in and thinning where only values for every third draws were selected.

	Sea Urchin	**Flatfish**
Width (cm)	N ~ (3.953, 0.955) n = 99	__
Speed (cm/h)	N ~ (7.316, 12.23) n = 50	__
Area (cm^2)	N ~ (33.9,6.79)	N ~ (162.5, 68.81) n= 49
Abundance per sampling period	Pois ~ (0.599) n = 125	Pois ~ (0.086) n = 231

In general, sea urchins were observed more frequently than flatfish and their contribution to bioturbation was the largest. However, the short residence time of flatfish, resulted in their abundance being underestimated. Hence, the present estimates represent their minimum contribution to bioturbation. The estimated number of days required to rework the entire surface area of the FOV by sea urchins and flatfish is presented in Figure 6. Based on the model, sea urchins have the ability to completely track the surface within 153 to 213 days. The contribution by flatfish was slightly less; ranging from 227 to 294 days. Taken together, sea urchin and flatfish are expected to turnover the entire area within 93 to 125 days.

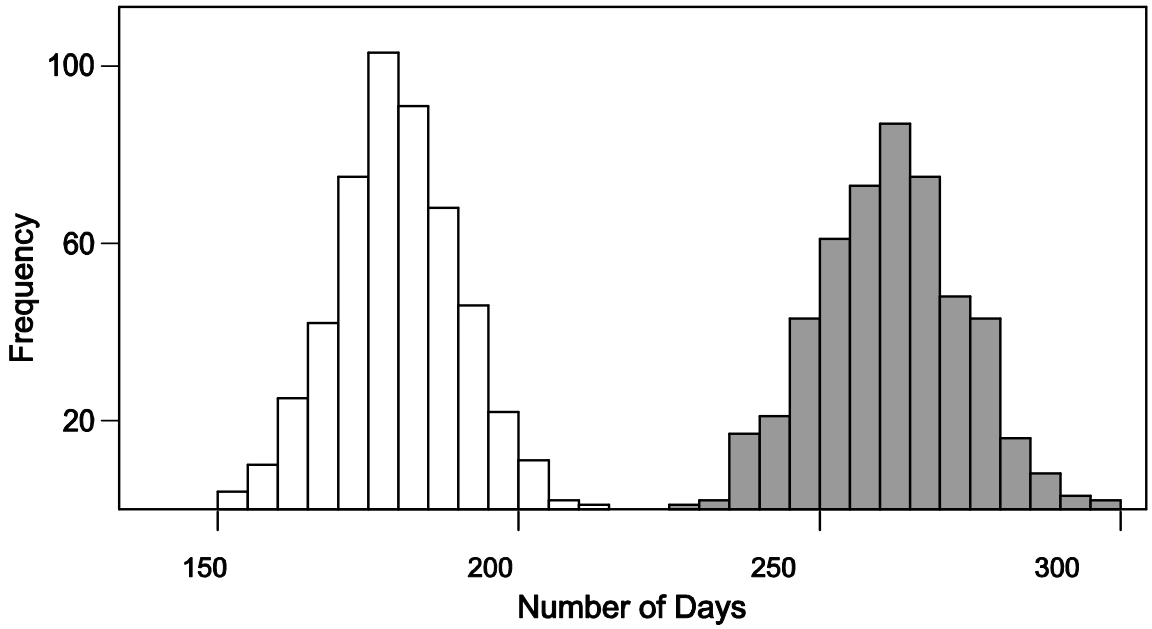

Figure 6: Frequency histogram based on 500 simulations showing the number of days required for two bioturbator taxa (flatfish, *Microstomus pacificus* and *Hippoglossus stenolepis*, (grey) and sea urchin, *Allocentrotus fragilis* (white)) to fully rework the sediments surface within the 8.79 m^2 of the study area.

Discussion

Sampling Design and Model Review

The daily 60 min observational period permitted thorough testing of the camera system and software limitations. However, the slow locomotion of the echinoderms, which comprised the majority of observations, resulted in limited detection of movements within a single hour. By the next day, the individual had usually left the field of view (FOV). When speed was calculated, it was greatly influenced by short rapid bursts of movement which were not representative of sustained locomotion speeds. On the other hand, the initial 60 min observation regime was appropriate for faster moving organisms such as buccinid snails. Other behavioural activities such as burrow maintenance could also be followed with this sampling design, but would require interpolation to complete

the remainder of the day. Recent documentation of behavioural rhythms in deep-sea organisms (Aguzzi et al. 2003b, Matabos et al. 2011a) suggested that this type of interpolation needs to be done with caution because behavioural rhythms can lead to error in abundance or activity rate estimates when observations are not appropriately distributed.

The transition to two daily observation blocks increased the number of fish recorded, but individuals rarely stayed for 30 min. None of the flatfish species encountered appeared to respond to the artificial lighting used during the observations. However, at our Mid-canyon site sablefish (black cod), *Anoplopoma fimbria*, commonly swam toward the camera when the video lights were turned on, to the point where increasing densities of these fish over the course of the observation period occasionally impaired monitoring of the benthic fauna. This contrasts with a study by Widder et al. (2005) that found sablefish to be more likely to exit the FOV once white light had been activated. There are few other published studies of the responses of deep-water organisms to artificial lighting (Raymond & Widder 2007).

By making five-minute observations every two hours, we were able to estimate speeds for slow moving megabenthic species. In addition, movement patterns within the FOV could be recorded and the likelihood of an individual going undetected was reduced. This observation regime also increased the number of flatfish observed, but an even higher sampling frequency would be advantageous for these species. Because movement patterns have only been described for a small number of individuals, we opted to employ speed estimates in the first version of the bioturbation model, so that we could include all accumulated data. An individual sea urchin was assumed to move randomly

at a constant speed across the FOV during a given residence time. This approach likely resulted in an over-estimation of the area covered because crossing over freshly tracked sediment was not taken into account and the constant speed assumption is inconsistent with what is known of the foraging behaviour of echinoderms. Their movement pattern can better be described as ranging, which involves an initial long-distance searching phase not guided by sensory organs that can be followed by a choice to stay in a high quality patch (Dusenbery 1989). As more information on movement patterns becomes available, calculating the actual area tracked by individual animals will provide a more accurate model.

This capacity for iterative model building is the reason why a Bayesian approach was chosen for this study. The initial estimates collected in this study can now be incorporated into longer term studies to be carried on the NEPTUNE Canada cabled observatory. The ease with which a Bayesian approach can handle missing data, through sampling the posterior distributions (Gelman et al. 1995), was an additional reason to opt for this less conventional type of model. Observatory technologies are relatively new, and interruptions in data time series are to be expected. Hierarchical designs including additional species, seasonal trends in response to chlorophyll concentrations or spatial variation based on depth can also be incorporated into the model, once supplementary environmental data have been collected.

Although extrapolations based on small data sets need to be viewed carefully, the estimated 93 to 125 days required for complete surficial sediment turnover is in the range of values reported in the literature using similar techniques at other deep-sea locations. At station M at 4,100 m in depth in the northeast Pacific, estimates of turnover rates for a

20 m^2 section of seafloor ranged from 45 days (Smith et al. 1993b) to 202 days (Kaufmann & Smith 1997). At 4,850 m in depth, at the Porcupine Plain of the northeast Atlantic, turnover rates for an area 2.2 m^2 were estimated at 306 to 1,332 days in the 1991-1994 period and at 27 to 69 days from 1997-2000 (Bett et al. 2001). However, seafloor morphology, depth, organic matter fluxes and species assemblages all differed between studies; rendering any further comparison impractical. The addition of data obtained from the other two NEPTUNE Canada IPs in the area will generate a more thorough description of the spatial variation in bioturbation levels particularly with respect to depth and topographic features. The use of multiple sites will provide a better appreciation of the spatial scale to which bioturbation levels can be extrapolated.

Bioturbation at the Shelf-break Site

Echinoderms often dominate deep-sea habitats and have been given much consideration in discussions of bioturbation. The sea urchin *Allocentrotus fragilis*, the most common echinoderm observed at the Shelf-break site, likely influences sediment organic matter content when feeding on phytodetritus (Giese 1961), but no obvious trails or burrowing behaviours have been reported for this species. Their contribution to particle mixing is likely limited to horizontal transport of the upper surface with very little subduction. This species is known to form high density aggregations (Boolootian et al. 1959) in which case their contribution to bioturbation will exhibit high spatial variability at scales greater than the patch size. No such aggregations were observed using the NEPTUNE Canada cameras, but some were observed during general ROV maintenance surveys of the NEPTUNE Canada installations (K. Robert, pers. obs.). The

movement rates determined for *A. fragilis* (average: 8.45 cm h^{-1}, maximum: 324.8 cm h^{-1}) were consistent with laboratory observations by Salazar (1970) who also found *A. fragilis* to respond to light stimulation with its maximal speed observed during illumination periods, underlining the need to limit artificial light exposure in deep-sea studies. The occurrence of behavioural rhythms has not been investigated for *A. fragilis*.

Both Dover sole, *Microstomus pacificus,* and halibut, *Hippoglossus stenolepis,* were observed to bury themselves in the upper layer of sediment and leave shallow oval imprints upon departure. A similar contribution of small flatfish to bioturbation in a shallower soft sediment system (~100 m) was documented by Yahel et al. (2008). Rays are also known as major bioturbators in certain coastal systems. These elasmobranchs lie on the seafloor covered in sediment with only their eyes visible, or flap their pectoral fins to excavate burrowed organisms; leaving oval imprints 6 to 10 cm deep in the sediment (Howard et al. 1977, Gregory et al. 1979, Thrush et al. 1991, Martinell et al. 2001). Fossil oval traces have been described in a sandstone bed at densities of one pit per square meter, and higher pit densities of 2 to 3 per square meter have also been recorded in present day tidal flats (Martinell et al. 2001).

Skates of the genera *Raja* and *Bathyraja* occur in the northeast Pacific to depths of at least 400 m (Bizzarro et al. 2009). Although, pit formation in these species has not been reported in the literature or recorded by our cameras; the above information could be consistent with the pits observed by rotary sonar and ROV in the area surrounding the Shelf-break site. A total of 17 individual skates were recorded at the Shelf-break site while none were observed at the two deeper sites where depressions were absent. Literature estimates of daily bioturbation in shallow areas by elasmobranch populations

available in the literature for shallow areas vary widely from10 to 11.4 m^2 on the west coast of New Zealand (Thrush et al. 1991) to less than 1 m^2 in the Gulf of California (Myrick & Flessa 1996). These studies also report rapid infilling of these pits, while the ones observed in this study did not significantly vary in location over nearly three months (A. Hay, pers. comm.). This long survival time contrasts with that of other biogenic sedimentary features, such as openings of abandoned burrows and buccinid trails, which lasted no more than a few days (K. Robert, pers. obs.), presumably erased by the action of bottom currents. This suggests that a maintenance mechanism must be at work to permit the persistence of these shallow oval depressions.

There is some support in the literature for an explanation wherein the depressions around the Shelf-break IP could be maintained, or even originate, through micro-scale habitat selection by flatfish. Flatfish associations with depressions produced by other species have been reported and mechanisms such as protection against predators and enhanced prey capture have been suggested to explain this behaviour (Auster et al. 1995). Behavioural studies of flatfish have also found them to significantly associate with sediment structures such as depressions or sand waves (Norcross & Mueter 1999, Busby et al. 2005, Stoner et al. 2007). In addition, during ROV operations carried around the Shelf-break site, many individual flatfish were observed lying in the centre of depressions (K. Robert, pers. obs.). Our results already suggested that flatfish reworked the entire study area in a matter of months. If instead their activity was focused in depressions, these would be visited on more frequent basis.

System Improvement and Future Use

Although the present system provides the basic hardware necessary for long-term, high frequency documentation of bioturbation and other ecological processes, improvements to the system are required before more extensive studies are practical. Zooming capabilities, color imagery and high video resolution are the simplest improvements needed for the current system. These would facilitate detection and identification of small cryptic species and improve the overall quality of observations. On a more developmental note, automated image acquisition software will be needed to take full advantage of the increased FOV provided by the pan and tilt mechanism. Coupling the video sweeps to high frequency, fixed-position snapshots of a section of the FOV will augment the amount of information collected without considerably increasing lighting time. This will be particularly useful for better definition of flatfish abundance patterns and buccinid snail movement. A better understanding of the effects of artificial light in aphotic environments might permit current precautionary restrictions on maximal observation time to be reduced. Automated object detection software will be essential for the processing of large image data sets, in order to reduce the bottleneck caused by our present reliance on manual annotations. The Monterey Bay Aquarium Research Institute (MBARI) team developed a software that allowed for automated detection of event in the water column (Walther et al. 2003). However, the increased complexity of the background as well as the partial occlusion and high density of organisms in benthic videos have retarded the implementation of automated object detection algorithms in benthic studies. Progress has been made using neuromorphic vision algorithms (Cline et al. 2008), local invariant features (Gobi 2010), Fourier descriptors (Aguzzi et al. 2009b), Canny edge detection and Delaunay triangulation (Taylor et al. 2008). However, for the

present, manual processing remains the most accurate method for analysis of complex benthic imagery.

The study presented here provides one approach to optimizing data collection and extraction of ecologically meaningful information that is extendable to other camera systems and locations. As an initial step with a new system, a single continuous observation period is appropriate to gain familiarity with the operating system as well as determine the composition and behaviour of the community present in the FOV. Once the community is characterized, the parameters needed to quantify the process of interest need to be identified. The observation frequency can then be increased incrementally until changes are perceived. Higher frequencies providing more accurate estimates can be implemented until the time required for data processing becomes impractical for long-term monitoring or technical limitations are reached. Each parameter will vary in its range of effective observation frequencies, and areas of overlap represent optimal observation frequencies for several processes of interest. Figure 7 provides a schematic representation of this approach as exemplified by bioturbation processes observed in this study. Data accumulated over the course of the iterative procedure, for the purpose of resolving the observation schedule, can be used to establish useful priors. These can later be incorporated into Bayesian models once additional information from the standardized observation protocol becomes available. The use of similar protocols will facilitate comparisons between studies.

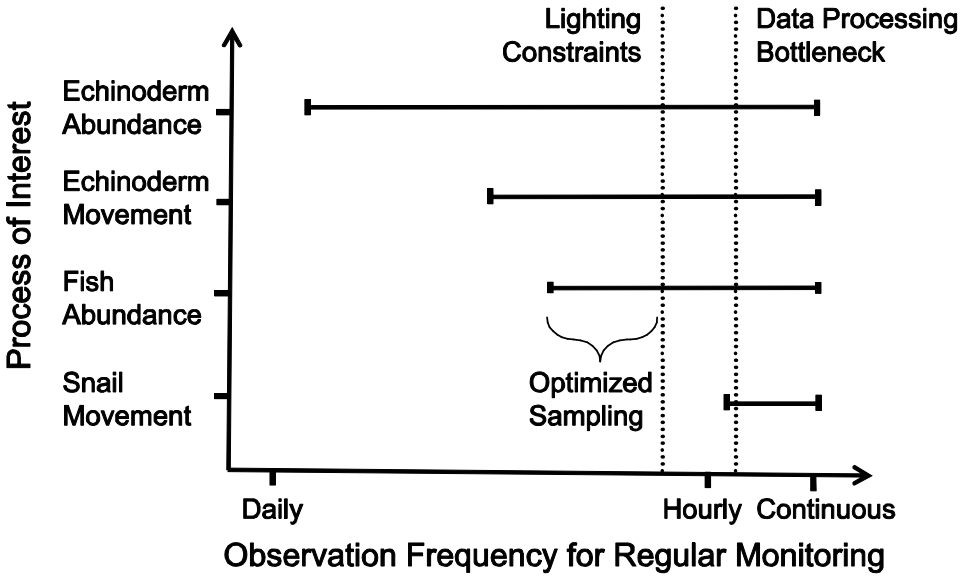

Figure 7: Schematic representation of the sampling protocol challenges for long-term regular monitoring. The goal is the find a sampling frequency that will maximize the information gathered for processes occurring at various temporal scales all the while ensuring that logistical constrains such as lighting time allocation (left dash line) are not exceeded and that data processing remains feasible (right dash line).

Conclusion

Long-term monitoring using seafloor observatories will provide valuable insights into the response of seafloor ecosystems to changes in primary productivity and organic matter sedimentation (Smith et al. 2009, Larkin et al. 2010). Changes in upper water primary productivity will propagate to the benthos which is already food-limited (Smith & Kaufmann 1999). In megabenthic species, quick behavioural responses (Kaufmann & Smith 1997, Grémare et al. 2004, Vardaro et al. 2009) as well as changes in species composition and biomass (Billett et al. 2001, Ruhl & Smith 2004, Billett et al. 2010) are to be expected; all of which are likely to influence bioturbation and other ecosystem services in the deep sea. The tools developed in the current study can now be employed to establish a baseline characterization of the current state of this biome and enable future quantitative evaluation of the impacts of global climate change and increased

anthropogenic disturbance on ecosystem processes. Bioturbation is an important ecological service influenced by a variety of environmental factors whose characterization in the deep sea requires an integrated approach well suited to cabled observatories as exemplified in this study.

Acknowledgments

We would like to thank Dr. Mairi Best and NEPTUNE Canada for the at-sea opportunities as well as the support provided for the use of the camera system. Thank you to the ROPOS team for all the expertise demonstrated installing the various pieces of equipment. A special thanks to Jason William, Kim Wallace and Nick Scott for all the trouble shooting regarding the cameras, Dr. Alex Hay and Douglas Schillinger for access to the rotary sonar data and Dr. Farouk Nathoo for the help with Baysian analyses. This research was supported by the Natural Sciences and Engineering Research Council of Canada (NSERC) through a Discovery grant to SKJ, a Strategic Networks grant to the Canadian Healthy Oceans Network (CHONe) and funds from the Canada Foundation for Innovation for NEPTUNE Canada, University of Victoria. K. Robert benefited from scholarships from the Natural Sciences and Engineering Research Council of Canada (NSERC), the Fond québécois de la recherche sur la nature et les technologies (FQRNT) and the University of Victoria.

Chapter 3
Small-scale thermal responses of hydrothermal vent polynoid polychaetes: Preliminary *in situ* experiments and methodological development

Robert, K.[1*], Onthank, K.L. [3], Juniper S.K. [1, 2] and Lee R.W. [3]

[1]Department of Biology, University of Victoria, PO Box 3020 STN CSC, Victoria, B.C., V8W 3N5, Canada

[2] School of Earth and Ocean Sciences, University of Victoria, PO Box 3065 STN CSC, Vic, B.C. V8W 3V6, Canada

[3]School of Biological Sciences, Washington State University, Pullman, Washington, 99164-4236, USA

Submitted to the Journal of Experimental Marine Biology and Ecology, August 2011

*Corresponding author: katleenr@uvic.ca
Department of Biology, University of Victoria,
PO Box 3020 STN CSC,
Victoria, V8W 3N5,
Canada
Tel: (+1) 778-430-0332

Abstract

Hydrothermal vent systems represent a unique marine environment where large temperature variations allow the studying of mobile ectotherms' responses to small-scale temperature gradient. An autonomous time-lapse camera with a temperature logger array system was deployed on four occasions to examine the thermal response of two vent endemic polynoid polychaete taxa: *Branchinotogluma* sp. and *Lepidonotopodium piscesae*. Automated image processing and particle tracking routines were used to quickly process the imagery acquired *in situ*. Kriging interpolation was employed to create temperature maps representing the field of view in which individual polynoids were tracked over time. We found that both polynoid taxa employed a thermoconforming strategy to cope with thermal variability and that temperature experienced did not influence the temperature selected at the next time interval. Applying a two state hidden Markov model with temperature as a covariate, it was possible to distinguish between resident and transient states based on movement pattern. Based on these preliminary deployments, we make suggestions regarding future studies which aim to sample at broader spatial scale, in more diverse thermal regimes, and examine responses over longer time scales.

Introduction

Hydrothermal vents are highly dynamic environments where temperatures fluctuate over small temporal and spatial scales. Hot chemically laden fluids can directly discharge from the seafloor as black smokers where temperatures can exceed 350 °C, or mix with crustal seawater prior to venting, creating complex, diffuse flow vents ranging in temperature from that of ambient seawater (> 2 ˚C) to 30-50 °C, often over centimetre distances (Delaney et al. 1992, Dover 2000). In addition to spatial gradients, diffuse flow vents also exhibit significant temperature variations at hourly scales (Tivey et al. 2002). The organisms exploiting these habitats are thus exposed to some of the highest and most variable temperatures in the marine environment (Girguis & Lee 2006, Bates et al. 2010). As such, temperature exerts a strong influence on species distribution and community structure (Sarrazin et al. 1997, Sarrazin et al. 1999, Bates et al. 2005). Vent organisms have been suggested to select temperatures conservatively with respect to their thermal limits, a strategy that may provide a safety margin against rapid temperature fluctuations (Bates et al. 2010). However, even within the tolerance range of a species, individual organisms are still exposed to small-scale temperature gradients whose exploitation may be beneficial for thermoregulation or foraging purposes.

For ectotherms, strategies for coping with temperature fluctuations range from active behavioural thermoregulation to thermoconformity (Huey & Slatkin 1976, Herczeg et al. 2003). In the former, organisms position their body to buffer environmental fluctuations and maintain a constant body temperature. In the latter, organisms have evolved the ability to function over a wide breadth of body temperatures. The major trade-offs are the time invested in maintaining a constant body temperature versus the increased performance expected when optimal body temperature can be maintained.

When not exposed to high temperature extremes, thermoregulators would be expected to select warmer areas as performance-temperature curves in ectotherms are typically negatively skewed (Angilletta et al. 2010). On the other hand, thermoconformers can be active throughout their surroundings. In hydrothermal vent systems, temperature is also expected to influence resource quality. Concentrations of reduced sulphur species (primarily HS^-), the energy source for most primary productivity by chemo-autotrophic microorganisms at vent, are positively correlated with temperature (Jannasch & Mottl 1985, Sarrazin et al. 1999, Ding et al. 2001). Hence, low temperature areas usually represent areas of low productivity and temperature may provide cues to guide habitat selection.

In the marine environment, hydrothermal vent systems represent one of the only habitats where it is possible to conduct *in situ* studies of how mobile ectotherms exploit small-scale temperature gradients (Bates et al. 2010). Cameras and temperature sensors are the primary tools for these types of studies but behavioural activities such as thermoregulation and foraging cannot always be observed directly. Instead, inferences regarding behavioural state can be made based upon movement patterns and quantifiable environmental variables (Patterson et al. 2009). This information can, in turn, be used to understand the influence of temperature on small-scale habitat selection. The highly variable nature of diffuse hydrothermal discharge necessitates centimetre-scale sampling resolutions at intervals of hours to days (Lee 2003) and customized protocols are required for individual taxa in order to ensure appropriate observation frequency and duration. *In situ* observations in the deep sea are operationally complicated, expensive and very time limited; as such, efficient taxa-specific protocol customization must be a step-wise

process wherein careful examination of prior knowledge will provide information for subsequent deployments.

The present study used an autonomous camera system and grid of temperature loggers to examine the movement patterns of two vent-endemic, polynoid polychaetes (*Branchinotogluma* sp. and *Lepidonotopodium piscesae*) in relation to substratum temperature. The camera system allowed for *in situ* time-lapse image acquisition and temperature quantification across the field of view (FOV) (Rinke & Lee 2009). The two polynoids were chosen because of their abundance and visibility in the acquired imagery. They are commonly distributed in habitats characterized by medium temperature (10-20 °C) diffuse flow (Sarrazin et al. 1997). The characteristics of the camera system as well as the sampling rate implemented varied between deployments. Automated image analysis techniques that allowed tracking of organisms and multiple statistical methods were used to determine which strategy is employed by these taxa to cope with thermal variability. Based on their movements through variable temperature fields, we tested the hypothesis that these worms used a thermoconforming strategy within their range of temperature tolerance. We also analyzed longer time series from two worms to distinguish between behavioural states using movement patterns, and to examine their relationship to temperature as a proxy of habitat quality. Finally, based on these first observations and the resultant hypotheses, we propose specific recommendations for future experimental deployments of these and other seafloor camera systems.

Methods

Camera System

Time-lapse digital cameras were deployed over the course of three Alvin dives on hydrothermal chimneys at two locations on the Juan the Fuca Ridge, in July 2010. Three deployments of the SMOKE (Submersible Macrophotography Observation Kamera Equipment) apparatus (Rinke & Lee 2009) took place on the Grotto chimney of the Main Endeavour Field (2,100 m) on Endeavour Segment, and one at Axial Volcano (1,500 m). A12.1 megapixel Nikon Coolpix P5100 time-lapse camera was set to variable image acquisition frequencies. The camera was mounted down-looking inside a titanium pressure housing and placed either 30 cm (Small) or 50 cm (Large) above a grid of Thermochron ibutton (± 0.5 °C) temperature loggers, resulting in a 300 cm^2 (Small) or 1,200 cm^2 (Large) field of view (FOV). Either 16 or 25 loggers were mounted in a 30 x 30 cm grid. All loggers appeared in the FOV of the larger set-up, but only 7 loggers were visible in the smaller FOV (Figure 8B). The temperature sampling frequency also varied between deployments (5 sec to 5 min). Deployment duration was limited by memory space and varied between dives. Characteristics for each deployment are reported in Table 4.

Table 4: Characteristics of 2010 time-lapse camera and temperature sensor deployments.

Dive	Location	FOV (HxV)	Grid Size	Image Frequency	Temperature Frequency	Duration
4619	Axial Volcano	40 x 30 cm	5.0 cm	1 min	2 min	609 min
4621	Main Endeavour	20 x 15 cm	7.5 cm	2 sec	1 min	69 min
4627	Main Endeavour	20 x 15 cm	7.5 cm	5 sec	5 sec	46 min
4627	Main Endeavour	40 x 30 cm	5.0 cm	5 min	5 min	2410 min

Data Processing

The imagery collected was adjusted to improve brightness, contrast and color saturation using Adobe® Photoshop®. The high quality of the images obtained with the small FOV made it possible to develop an automated detection routine for *Branchinotogluma* sp. individuals. In Adobe® Photoshop®, a color range characteristic of *Branchinotogluma* sp. was selected while the background was suppressed. This highlighted individual worms against the background substratum. The images were then binarized and small noise artefacts were removed through filtering; yielding black dots representing individual organisms (Figure 8 B). Tracking of individual worm movements was carried out using the image processing software Image J (freely available online; http://rsbweb.nih.gov/ij/) where the 'MTrack2' plug in (Stuurman 2003) recorded the pixel coordinate of each individual scale worm across the frames. Tracking parameters (e.g. particle size, minimum number of frames and maximum distance moved) could be altered to ensure that remaining artefacts resulting from uneven lighting were not mistaken for organisms. On deployments when the automated routine could not be applied because of suboptimal image quality or for *L. piscesae* individuals, the x and y coordinate positions for each individual was recorded manually.

A

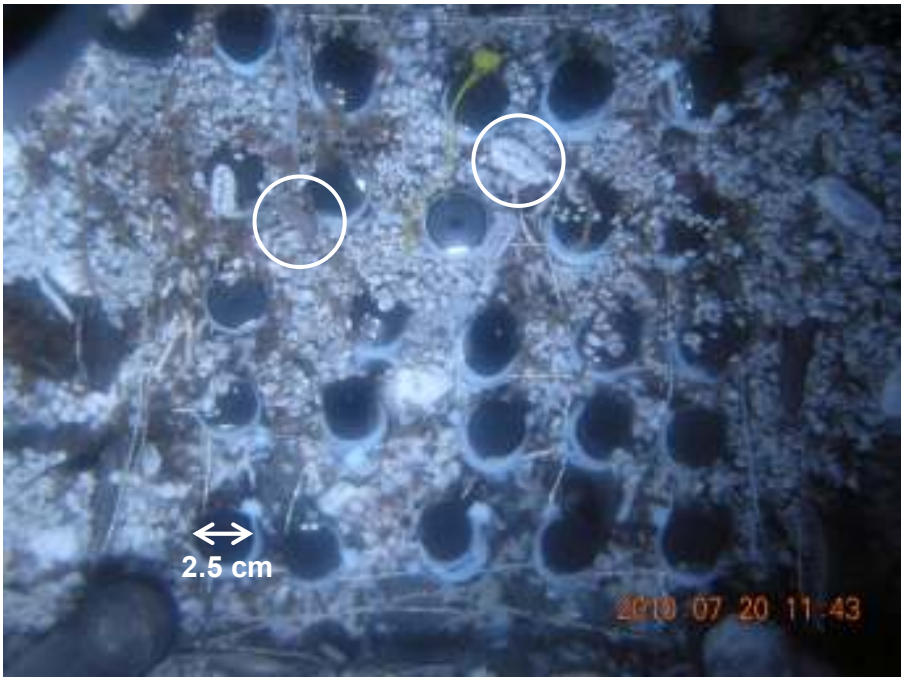

B

Figure 8: A) Image representing the large field of view with all 25 temperature loggers visible. In the left circle is a *Branchinotogluma* sp. individual and in the right circle a *Lepidonotopodium piscesae* individual. B) Image analysis process; the original image (left) obtained from the small field of view, the same image (center) following brightness, contrast and saturation correction and the resulting binary image (right) where black dots represent *Branchinotogluma* sp. individuals.

Statistical Analysis

Temperature Interpolation

Ordinary kriging was used to interpolate temperature between loggers in order to characterize the temperature field through which the scale worms travelled. Our data met the assumptions for kriging: 1st and 2nd order stationarity, isotropy and normality. Linear

interpolation of the temperature through time was also carried out to ensure exact correspondence with the time of picture acquisition. The temperature differences recorded between sampling intervals by individual loggers were much smaller than the between logger temperature differences observed within a sampling interval. Temperature maps (Figure 9) were created for each sampling interval and temperatures experienced by individual worms were estimated for each time interval, based on their pixel coordinates. Spatial interpolation and subsequent statistical analysis were carried out using the library 'fields' (Furrer et al. 2010) of the free statistical software R (R Development Core Team, 2006, online ref.: http://www.r-project.org/).

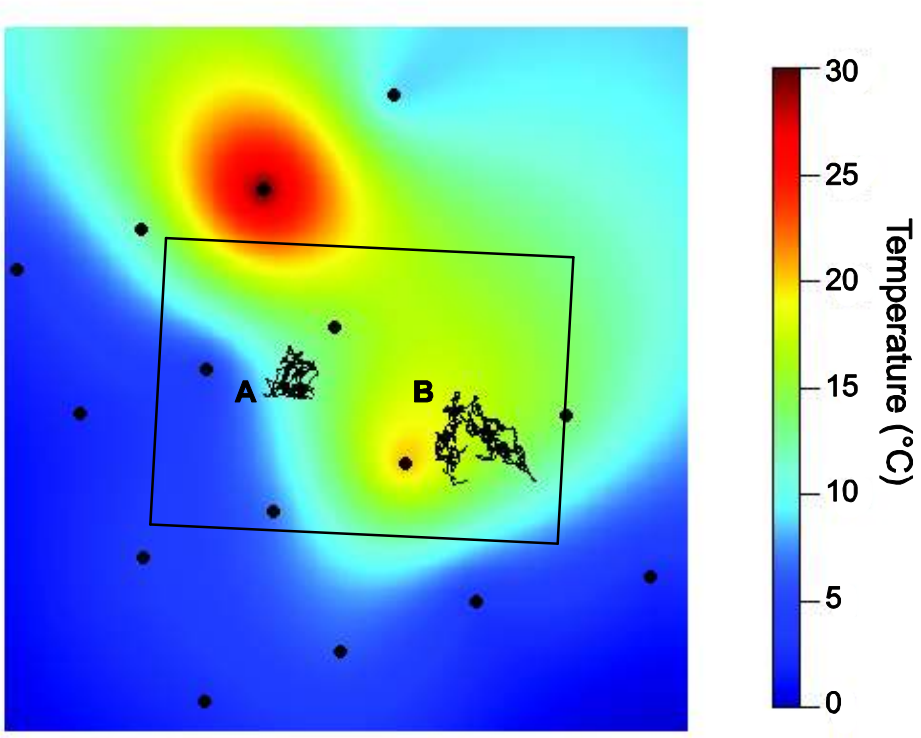

Figure 9: Temperature map obtained through kriging interpolation. The data illustrate the mean temperature recorded over the course of dive 4621. The smaller field of view is depicted by the rectangle and the trajectories of the two *Branchinotogluma* sp. individuals A and B tracked for a longer time series are also included. The black circles illustrate the positions of temperature loggers which were separated by 5 cm.

Strategy to Cope with Thermal Variation

In order to determine whether polynoids exhibited a thermoconforming strategy to cope with thermal variation, we developed a random walk model. The *step* length (Euclidean distance travelled between successive images; Turchin (1998)) was randomly sampled from a normal distribution modeled on observed polynoid movement characteristics (mean step length and standard deviation) while the angle of movement was sampled from a uniform distribution between 0 and 360 degrees. A random starting location was set for each particle, but the length of time spent within the FOV reflected that of observed individual polynoids. The number of randomly moving particles generated was equivalent to the number of individual polynoids observed in each deployment. The temperatures experienced at each time interval were then extracted using kriging interpolation.

Choice of Location in Temperature Field

To examine whether individual polynoids used temperature cues to select subsequent locations, we tested whether the temperature experienced at $time_{t-1}$ influenced the temperature experienced at $time_t$. The percent rank of the temperature experienced at $time_t$ with respect to temperatures interpolated from 1,000 randomly generated points was computed. These random positions were drawn from the step length distribution previously calculated and represented likely alternatives available to the individual scale worm. We predicted that if an individual experienced uncomfortably high temperatures at $time_{t-1}$, it would have moved to a cooler position by $time_t$. This was represented by percent rank values below 50; the null expectation. Values above 50 would illustrate a displacement towards warmer temperatures; expected if individuals were exposed to

excessively low temperatures at $time_{t-1}$. The time interval between frames varied between all four deployments (refer to Table 4).

Behavioural State Predictions

To determine if temperature could be used as a proxy for assessment of habitat quality, we fitted the data to a two state hidden Markov model. This approach attempts to predict the behavioural state of an organism based on its movement pattern (Figure 10). The two states used were resident, small movements in one area inferred as being a good quality patch, and transient, long steps through a lower quality patch. In this case, a good quality patch may represent a patch whose temperature is optimal for active thermoregulation or one exhibiting increased food availability. Temperature, as a proxy for intensity of hydrothermal discharge is likely to be an indicator of food availability since chemosynthetic productivity by free-living bacteria is dependent on hydrothermal fluid supply. Hence, its inclusion as a covariate in the model may improve behavioural state predictions. The R code employed was modified from the one generously provided by Patterson et al. (2009) in their supplementary material, and parameters were also estimated using the maximum-log likelihood method. We selected individuals from dive 4621 as it had the highest image acquisition frequency (2 sec). The sampling rate directly affects step length, where fast sampling rates lead to small step length, and in order for the model to make accurate predictions, mean differences in step length between states must be maximized (Patterson et al. 2009). In addition to the original 2 sec sampling frequency, we thinned the data and retained samples for every 6 sec and 14 sec. As a result, only 2 individual polynoids were observed in enough frames to be examined

(Figure 9). The large number of frames is a requirement for reliable inference of animal behaviour (Patterson et al. 2009).

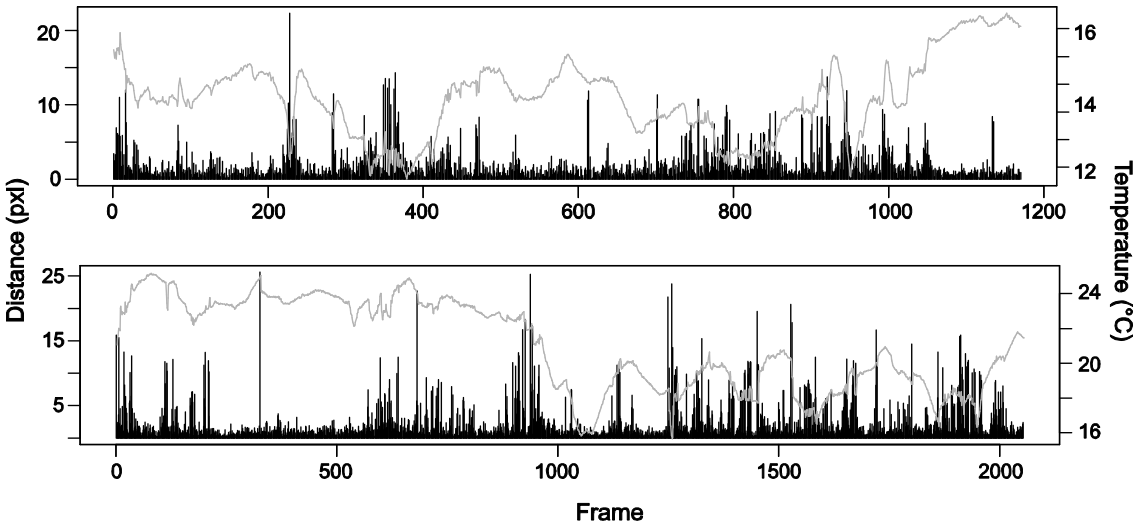

Figure 10: Plot of the temperature experienced (red line) and the step length (black bar) for Individual A (upper) and Individual B (lower).

Results

The minimum substratum temperature observed for all three deployments was similar (1.5-2.5 °C). The mean temperatures for dives 4619, 4621, 4627 (small) and 4627 (large) were respectively 9.4 °C, 11.8 °C, 14.5 °C and 23.2 °C. Warmer maximum temperatures were recorded in deployment 4627 (large) (maximum= 67 °C) while dive 4619 at Axial Volcano had overall lower maximal temperatures (maximum= 27 °C). The maximal temperature change observed over time by one sensor was 34.5 °C in 5 minutes while a difference of 60.5 °C was observed between sensors located 12 cm a part; with both occurring during the 4627 (large) deployment (Figure 11).

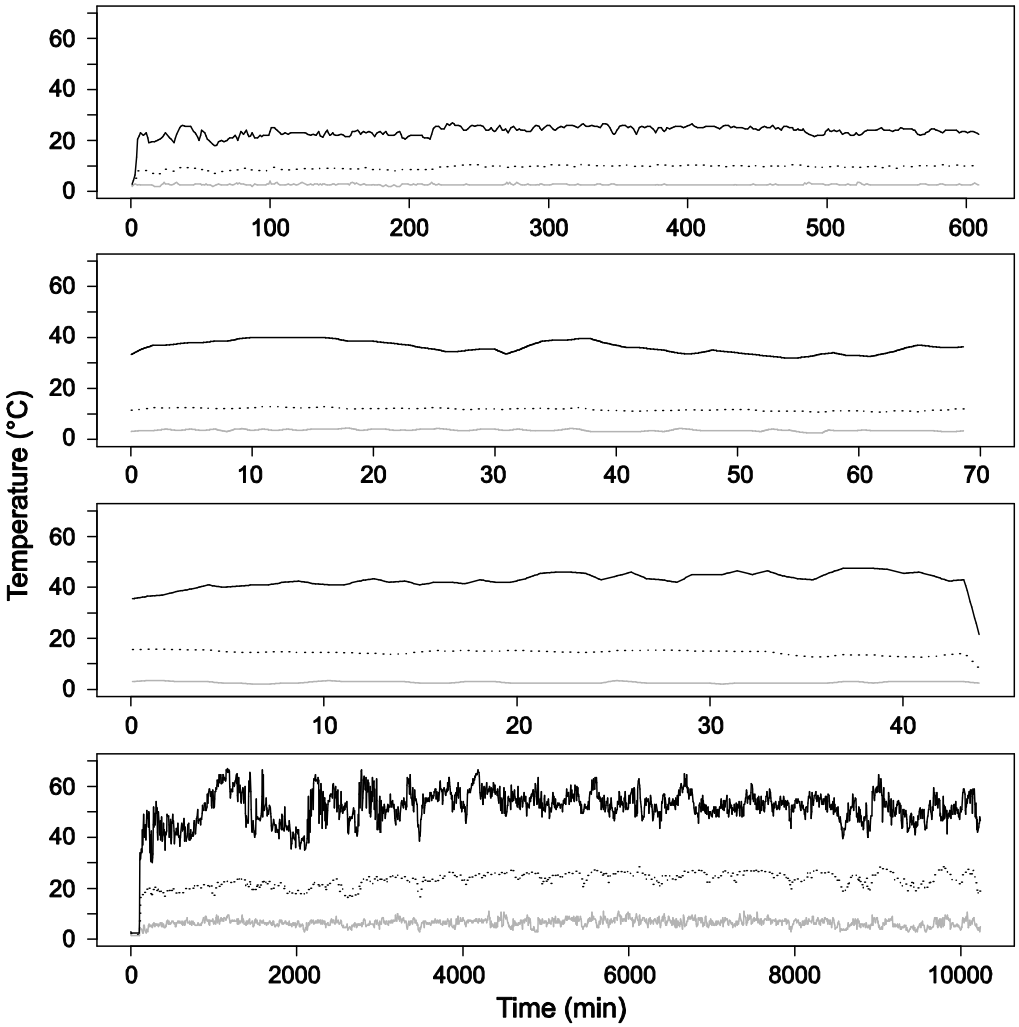

Figure 11: Mean (dotted), minimum (gray) and maximum (black) temperature observed over time for dive 4619, 4621, 4627 (small) and 4627 (large) (from top to bottom).

The temperatures experienced by *Branchinotogluma* sp. did not differ from the temperatures experienced by randomly moving particles (Figure 12). No individuals of *L. piscesae* were observed during dive 4619. For dives 4621 and 4627, the temperature range experienced by *L. piscesae* appeared barely narrower than the one encountered by the random particles. Overall, polynoid species did not experience a more constrained range of temperature than randomly moving particles nor did they select the warmer end of the available temperature gradient.

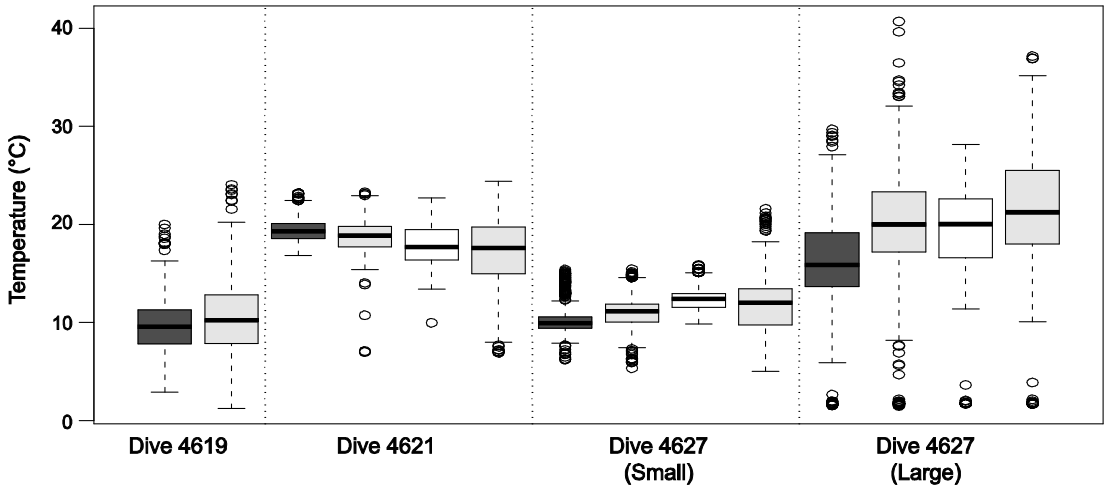

Figure 12: Boxplots illustrating the temperatures experienced by the *Branchinotogluma* sp. (dark gray) and *Lepidonotopodium piscesae* (white) when compared to randomly moving particles (light gray) for each deployment. No white scale worms were observed for dive 4619.

The temperature experienced by an individual at $time_{t-1}$ did not have an effect on its position at $time_t$ (Figure 13). Although, polynoids were exposed to temperatures ranging from 5-40 °C, organisms experiencing extreme temperatures were not more likely to have moved to areas exhibiting milder conditions by the next time interval. This trend was observed for both polynoid taxa in all four deployments (frequencies ranging from 2 to 300 sec). Hence, this result is unlikely to be an artefact of oversampling whereby observations were taken at a rate faster than the organism's capacity for repositioning.

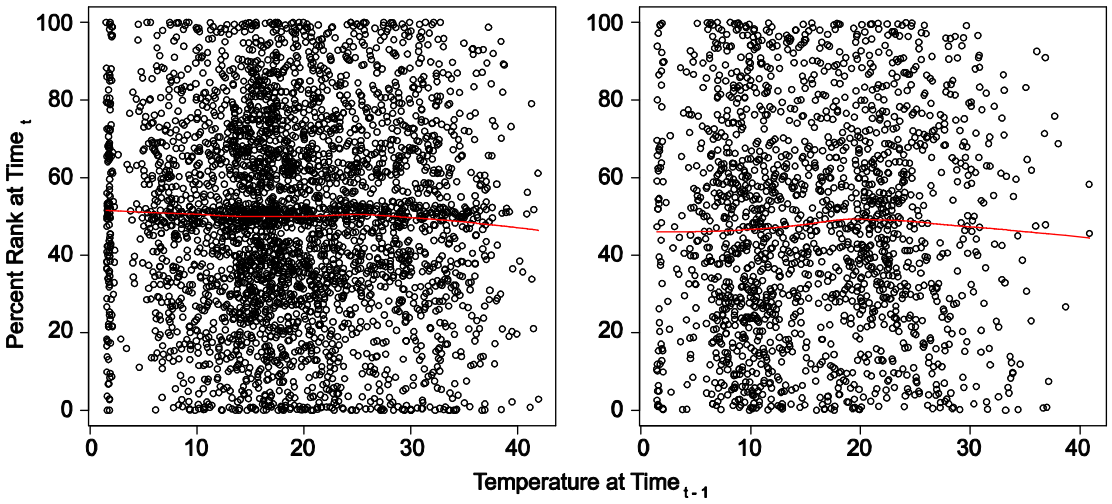

Figure 13: Based on a comparison with the temperature that would have been experienced at 1,000 randomly drawn positions, the percent rank of the actual temperature experienced by each organism with respect to the temperature experienced at $time_{t-1}$. A value of 50 represents the null expectation. The red line represents a LOWESS regression smoother. Only results from dive 4627, *Branchinotogluma* sp.(left) and *Lepidonotopodium piscesae* (right), are shown as an example.

Table 5: Parameter estimates for the two state hidden Markov model using temperature as a covariate. The Alpha and Beta parameters regulate the influence of the temperature covariate by determining the transition matrix, while Lambda represents the mean step length in pixels scaled down by a factor of four.

		Alpha		**Beta**		**Lambda**	
		Resident	**Transient**	**Resident**	**Transient**	**Resident**	**Transient**
Individual A	**2 sec**	3.3	2.9	0.4	-0.4	1.2	3.1
	6 sec	2.7	3.4	0.1	-1.1	1.8	4.5
	14 sec	3.1	2.7	0.1	-0.8	3.4	8.6
Individual B	**2 sec**	3.1	2.3	0.1	-0.2	1.1	4.4
	6 sec	2.7	2.9	0.1	-0.1	1.5	5.5
	14 sec	2.2	3.2	0.1	-0.1	1.9	8.0

The three sampling frequencies (2 sec, 6 sec and 14 sec) used in the two state hidden Markov model yielded differences in behavioural state predictions (Figure 14). The results of the parameter estimates are reported in Table 5. The 6 sec subsampling gave the clearest result by differentiating between clustered observations (resident state) and directional movement (transient state). Step lengths of 6 to 10 pxl characterized

resident behaviours and 17 to 22 pxl for the transient states. Individual A and Individual B, respectively, spent 18 and 32.4 min in resident state versus 21 and 36.1 min expressing a transient behaviour. However, the temperatures experienced by an individual in either behavioural state were similar (Figure 15). At a faster sampling rate, the step length difference between the two states was too small while at slower sampling frequencies too much information describing the trajectory was lost and the number of frames available became too small to make accurate predictions.

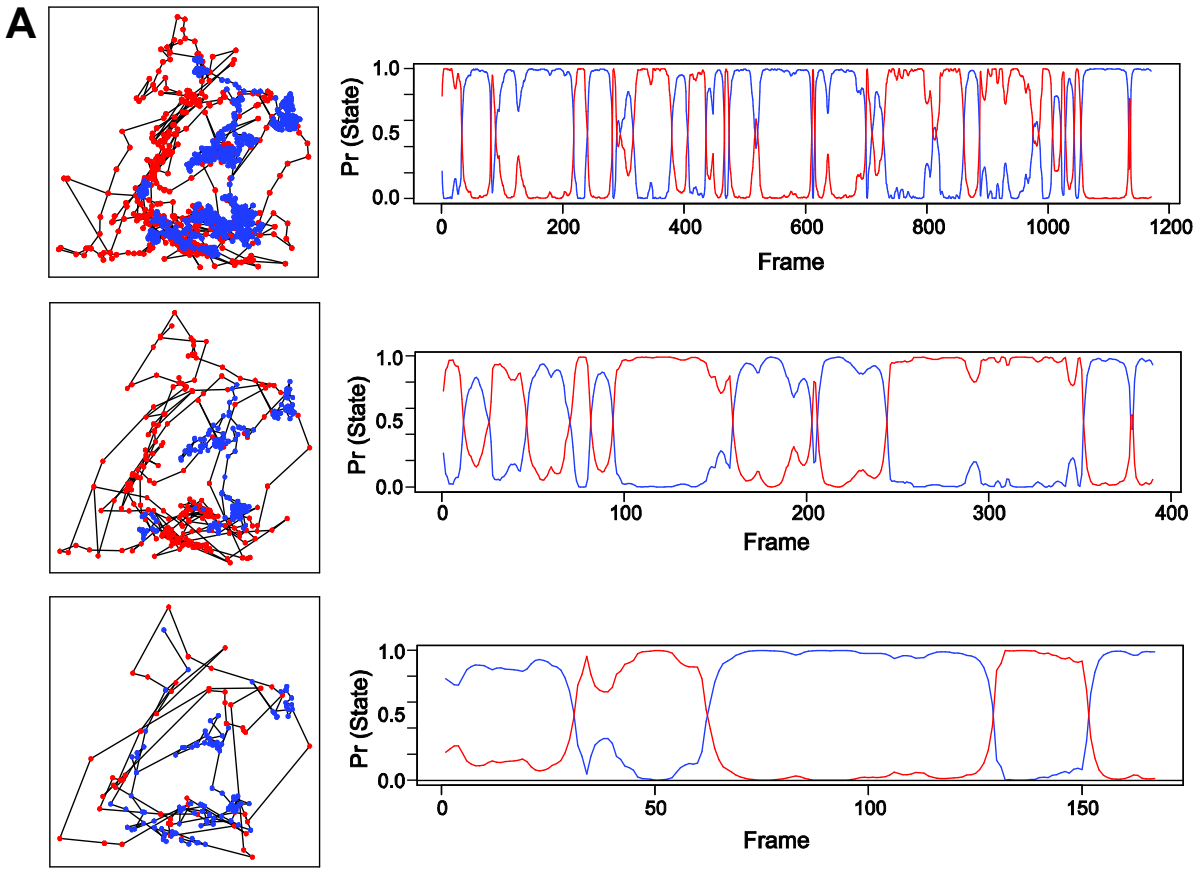

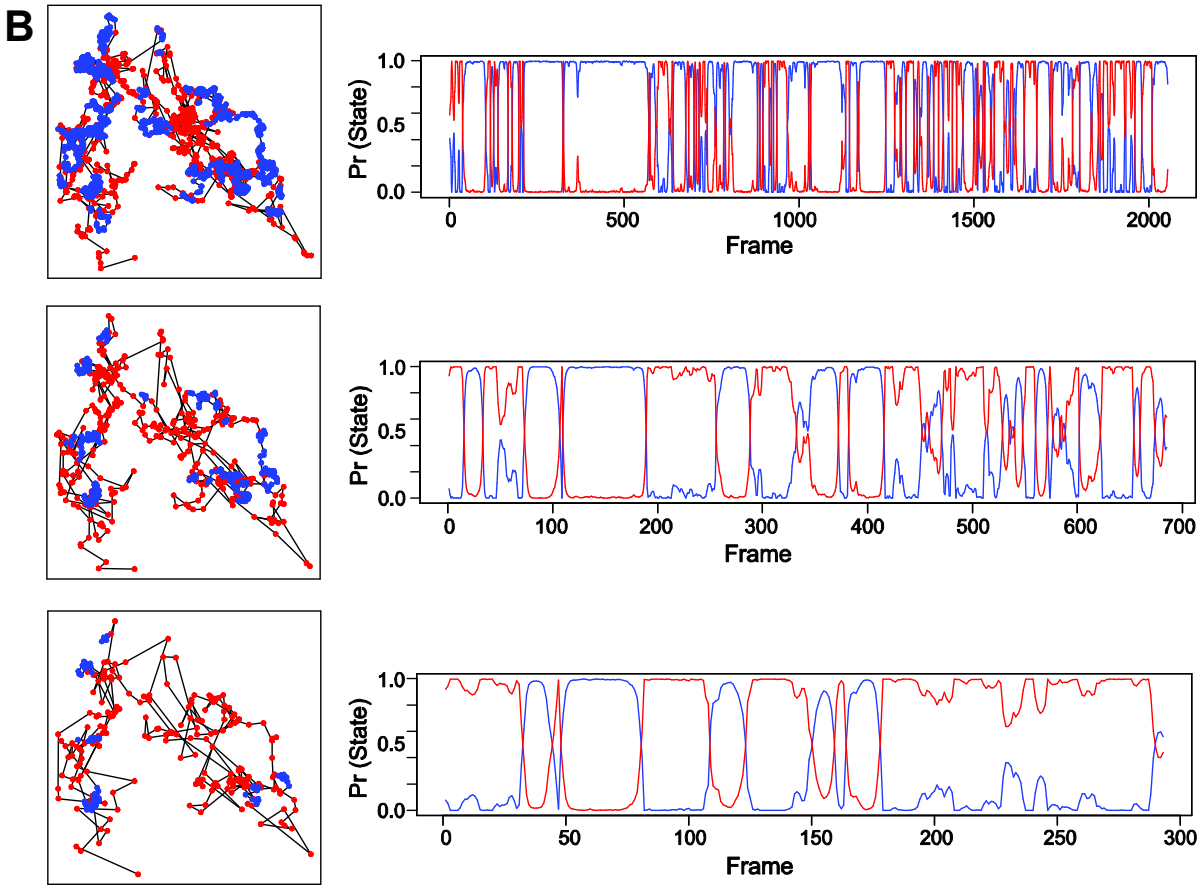

Figure 14: Spatial (left) and temporal (right) predictions of the two behavioural states, resident (blue) and transient (red), base on the hidden Markov model output. For dive 4621, Individual A and Individual B subsampled at every 2 sec (top), 6 sec (middle) and 4 sec (lower).

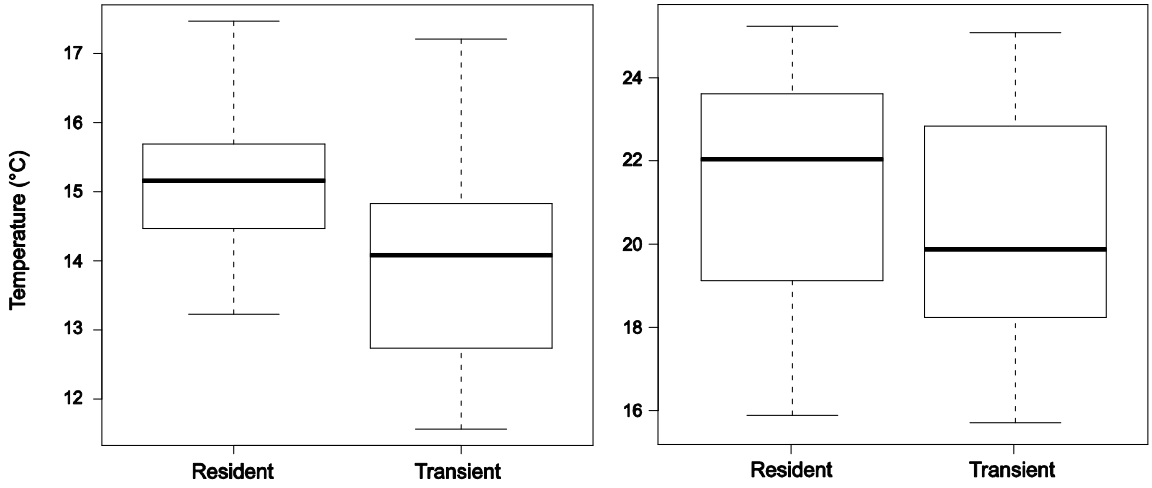

Figure 15: Temperature experienced when in resident and transient state for Individual A (left) and Individual B (right) based on 6 sec subsampling.

Discussion

Thermal Response

Hydrothermal vents offer a unique setting to examine the response of mobile marine ectotherms to small-scale changes in substratum temperature. As exemplified by the camera-temperature array system, vent organisms are exposed to steep thermal gradients over small spatial scales which also vary temporally. The efficiency of the automated image analysis and tracking techniques (>3,400 frames processed) allowed a large number of individuals (>1,700) to be identified and positioned over time. Reliance on manual processing would have greatly limited our ability to determine the *in situ* responses of these polynoid taxa (*Branchinotogluma* sp. and *Lepidonotopodium piscesae*) to thermal variability.

Based on laboratory experiments in pressurized aquaria, these taxa are known to tolerate a wide temperature range; activity has been recorded from 2.5-23 °C and their thermal limit has been established at 35-40 °C (Bates et al. 2010). Confirming the laboratory findings, we observed individual *Branchinotogluma* sp. and *L. piscesae* in areas ranging in substratum temperature from 1.5-40 °C. With the exception of temperatures surpassing their thermal limit, our modeling showed that organisms and randomly moving particles encountered similar temperatures. These results indicate that polynoid taxa at the Main Endeavour Vent Field are able to exploit a broad temperature range, indicative of a thermoconforming strategy. There is currently some uncertainty about the taxonomy of the *Branchinotogluma* genus; three similar species had originally been described for the Juan the Fuca Ridge, *B. grasslei*, *B. sandersi* and *Opisthotrochopodus tunnicliffeae* (Pettibone 1988), but in more recent publications these have been treated as a single species (Desbruyères et al. 2006, Levesque et al. 2006).

Whether habitat preferences among these three morphotypes might obscure existing trends remains unknown and cannot be resolved using imagery techniques.

Our finding that temperature experienced in a previous time interval did not affect the temperature experienced in the next time interval suggests it is unlikely that these polynoids used substratum temperature as a means to thermoregulate or as a cue to locate areas of high biomass of free-living chemosynthetic bacteria. Polynoids have been observed to feed on microbial mats and particulate organic matter (POM) (Levesque et al. 2006) whose composition is known to vary spatially (Sarrazin et al. 2002). The elytra of *L. piscesae* are covered in white bacterial filaments (Pettibone 1988, Desbruyères et al. 2006). The functional significance of these bacteria is not currently known, but might serve a role in sulphide detoxification or in contributing nutritional benefits (R. Lee, pers. comm.). However, *L. piscesae* individuals were not observed to select or exploit more sulfidic waters as a result of this relationship. Stable isotopic analyses also suggest a predatory diet for these polynoid species, likely feeding on *Ridgeia piscesae, Depressigyra globulus* and *Nicomache venticola* (Bergquist et al. 2007). More information on the thermal niche and habitat preference of prey species as well as the spatial density distribution of POM and microbial mats will be required to better understand habitat selection in these polynoids.

Other vent taxa such as *Paralvinella sulfincola* have been shown to exhibit behavioural thermoregulation and exploit small-scale temperature gradients (Bates et al. submitted). The difference in thermal response between these two taxa may reflect the lower mobility and the more extreme niche occupied by the sulphide worms (Lee 2003, Girguis & Lee 2006, Grelon et al. 2006). As such, in sulphide worms, exploitation of

small-scale temperature gradients might be more critical to avoid exposure to temperatures outside the thermal preference, particularly since a migration to a more favourable location would entail the rebuilding of a mucous tube (Grelon et al. 2006). For scale worms the ability to tolerate a wider range of temperatures as they forage may be more beneficial since the magnitude of spatial variations observed during our deployments was larger than any observed temporally. Deployments where average temperatures approach the outer thermal limits might reveal more information regarding small-scale exploitation of temperature gradients since foraging decisions would need to be carefully balanced with the risks of encountering temperatures outside the thermal tolerance of the organism (Bates et al. 2010).

When temperature was used to in a two state hidden Markov model, we could differentiate between two behavioural states using movement patterns. Evidence of a difference in temperature based on behavioural state was only observed with the single individual subjected to lower overall temperatures; suggesting that different strategies might be employed based on characteristics of the immediate surroundings. Differences in patch (food) quality significant enough to warrant a behavioural reaction may only appear near the extremities of the thermal environment. The occurrence of differing strategies would be obscured when looking at population level distributions and responses. Hence, the need to design observation protocols ensuring that individuals can be tracked for long time periods and that physical variations are sampled at a similar scale and frequency as encountered by the individual organism (Szewczyk et al. 2004). In the current study, only two such individuals were observed. These are too few to make reliable inferences regarding thermal response and habitat selection. Instead, we have

used these and the other results to develop recommendations for observational protocols for future deployments.

Recommendations for Future Deployments

The smaller (300 cm^2) FOV improved individual organism detection using the automated image processing routine. Because background complexity was reduced, better lighting, contrast and colour saturation could be achieved. On the other hand, the larger (1,200 cm^2) FOV captured the steep spatial gradients recorded by the temperature loggers, which were absent when limited to the seven loggers present in the smaller FOV (e.g. Maximal thermal gradient: 18.7°C and 16.1°C (small FOV) instead of 46.5°C and 45.0°C (large FOV)). A larger FOV would also ensure that organisms are tracked in a greater number of frames and would augment overall sample size (e.g. Residence time: 10.5 and 22.0 min (large FOV) instead of 3.2 and 4.2 min (small FOV)). Careful lighting and use of a wide-angle camera, although distortion is likely around the edges, could increase FOV size without forfeiting the efficacy of the automated image processing routine. The use of a remotely operated camera mounted on a pan and tilt mechanism would be another option to increase the FOV.

Temperature variations occurred over the scale of centimetres and a greater number of temperature loggers would improve temperature map resolution. However, this would also increase clutter and create additional disturbances within the FOV. The deployment of one very dense temperature grid would allow quantitative determination of the optimal distance between sensors. The choice of interpolation technique also

creates differences in temperature maps. However, when linear and kriging techniques were compared, they did not affect the observed results (Bates et al. submitted).

Reliable tracking of specific individuals over a long time period was required to successfully implement a two state hidden Markov model. Now that high capacity memory cards are easily available and inexpensive, even with a high sampling frequency (e.g. 6 sec, which gave the most satisfying results), day-long deployments will be feasible. Particularly since image processing can be easily automated, as we have demonstrated here. Synchronization between image and temperature acquisition frequency would avoid the need for temporal interpolation.

Conclusion

Both thermoregulation and foraging decisions likely play a role in describing movement patterns in polynoids; teasing out the relative importance of each will be difficult. Additional deployments of longer duration and covering different thermal regimes (e.g. regions where temperatures exceed thermal limits or where temporal fluctuations are stronger) as well as experimental manipulations will certainly be required. The possibility of undertaking both types of deployment will soon be improved with the addition of a remotely operated camera at the Endeavour node of the NEPTUNE Canada cabled observatory planned for summer 2011 (Robert et al. 2010). This system will allow for real-time monitoring and interactive resetting of sampling frequency based on improved knowledge of the system or in response to rare episodic events. Adaptation of the techniques proposed in this article to study thermal responses in other taxa or to link movement patterns to additional environmental variables will also be feasible. One

shortcoming of cabled observing systems is the limited spatial coverage obtained with fixed position cameras and sensors. Hence, portable and cabled observing systems should be used in a complementary way, where portable systems are first used to explore potential sites for the deployment of cabled cameras and later broaden the spatial footprint of experimental observations, while the cabled system can be used in an interactive way to refine the observational methodology.

Acknowledgments

We would like to thank Sonja Kolstoe for all her help collecting and processing the data as well as acknowledge the remarkable crew of the R/V Atlantis and the submersible Alvin. Funding for this cruise was provided by the National Science Foundation (NSF, USA) OCE-0623554. This research was supported by the Natural Sciences and Engineering Research Council of Canada (NSERC) through a Discovery grant to SKJ, a Strategic Networks grant to the Canadian Healthy Oceans Network (CHONe). K. Robert benefited from scholarships from NSERC, the Fond québécois de la recherche sur la nature et les technologies (FQRNT) and the University of Victoria.

Chapter 4
Multi-parametric study of behavioural modulation in demersal decapods at the VENUS cabled observatory in Saanich Inlet, British Columbia, Canada

Matabos M.[1*], Aguzzi J.[2], Robert K.[3], Costa C.[4], Menesatti P.[4], Company J.B.[2] and Juniper S. K.[1, 3]

[1] School of Earth and Ocean Sciences, University of Victoria, PO Box 3065 STN CSC, Vic, B.C. V8W 3V6, Canada

[2] Instituto de Ciencias del Mar (ICM-CSIC), Paseo Marítimo de la Barceloneta, 37-49. 08003 Barcelona, Spain

[3] Department of Biology, University of Victoria, PO Box 3020 STN CSC, Vic, B.C. V8W 3N5, Canada

[4]AgritechLab - Agricultural Engineering Research Unit of the Agriculture Research Council (CRA-ING), Via della Pascolare, 16. 00015 Monterotondo Scalo (Roma), Italy

Published in the Journal of Experimental Marine Biology and Ecology (2011), 401:89-96

*Corresponding author: mmatabos@uvic.ca
NEPTUNE Canada
University of Victoria
PO Box 1700 STN CSC
Victoria, BC V8W 2Y2 Canada
Tel: (+1) 250 472 5089
Fax: (+1) 250 472 5370

Abstract

Understanding biological rhythms in benthic ecosystems and their modulation by habitat cycles has important implications for resource and ecosystem management. The recent development of permanent, multi-sensor seafloor observatories in deep-water environments provides opportunities for the *in situ* investigation of the behaviour of benthic organisms in relation to habitat variability. This paper describes a multi-disciplinary investigation at the VENUS observatory platform in Saanich Inlet, an intermittently anoxic fjord (Vancouver Island, Canada). A remotely operated digital camera was used to document changes in the abundance of shrimp (*Spirontocaris* spp.) and the squat lobster (*Munida quadrispina*), as well as bacterial mat coverage (*Beggiatoa* spp.). These data were used as proxies of diel rhythms related to day-night and internal tidal cycles. Seafloor photos were acquired hourly during consecutive days, before, during and after oxygen intrusion events in the fall of 2009. In order to relate biological fluctuations with habitat cycles, bottom water pressure, temperature, dissolved oxygen, and nitrate data were also acquired. Periodogram analysis showed a weak internal-tide associated rhythmicity for *Spirontocaris* spp. that was absent in *M. quadrispina* and the bacterial mat coverage. Waveform analysis confirmed the absence of any day-night fluctuation in all tested species. However, punctual oxygen intrusion in the fjord influenced visual counts of species, possibly blurring detectable activity rhythms. Temperature and nitrate fluctuations were more accentuated during spring tides but cross-correlation analysis indicated an absence of species responses to these habitat variables. Results are discussed within the context of the complex oceanographic and ecosystem dynamics of Saanich Inlet.

Introduction

Biological rhythm modulation remains a poorly studied but important aspect of deep-water marine biology (Naylor 2005, Aguzzi & Company 2010). Behavioural rhythms result from the entrainment (modulation) of animals' physiology by predictable environmental fluctuations (i.e. geophysical cycles; Saunders (2002) and Dunlap et al. (2004)). Benthic species within the twilight zone, are contemporarily exposed to day-night light intensity cycles (Aguzzi et al. 2009c) and hydrodynamic-tidal fluctuations (Aguzzi et al. 2009d). In the dark deep-sea, photic modulation disappears and internal tides alone seem to modulate species behaviour (Aguzzi et al. 2011). Behaviour rhythms, if unknown, can have an unquantifiable influence on biomass and biodiversity estimations, directly affecting ecosystem management decisions and policies (Naylor 2005). For example, rhythmic movement of decapod populations in and out of burrows has been shown to generate uncertainties in benthic trawl surveys when time of day was not taken into account (Aguzzi & Bahamon 2009, Bahamon et al. 2009).

Marine chronobiologists have traditionally used laboratory approaches to study physiological processes in relation to endogenous circadian oscillators (e.g. for decapods see review in Aguzzi and Company (2010)). Laboratory results cannot be directly translated to the situation in the field without taking into account the complexity of interacting, multi-species communities. Similarly, ecological observations made with incomplete understanding of biological rhythm frequencies can miss important features of community and ecosystems dynamics (Marques & Waterhouse 2004, Morgan 2004). In deep-water habitats, technical and logistic limitations on repeated sampling and direct observation have hampered the study of activity rhythms of benthic organisms. Studying biological rhythms within a framework of regulating external influences is particularly

challenging in the case of deep-water benthos where continuous observations present many logistic challenges (Tunnicliffe et al. 2003, Aguzzi et al. 2009d, Aguzzi et al. 2011). We know little about the strength of behavioural rhythms in these environments in relation to geophysical cycles of conflictive periodicity (i.e. day-night 24-h based *versus* 12.4-h tidal based) and other more contingent habitat fluctuations. In most decapods, day-night based activity rhythms can be masked by competition for substrata (Aguzzi et al. 2009a), food availability (Fernandéz de Miguel & Aréchiga 1994) and dissolved oxygen fluctuations (Schurmann et al. 1998). Permanent cabled observatories offer one solution for this type of study. Cabled, multisensor demersal platforms can acquire continuous chemical and physical data and support real-time observation of seafloor organisms with video and still cameras. We present here the first results of a study of decapod activity (and microbial mat growth) in relation to environmental variables in a coastal fjord being monitored by the VENUS cabled observatory.

The VENUS cabled multisensory observatory allows remote, continuous, and real-time observation of plankton and seafloor organisms together with physical and chemical variables in Saanich Inlet, an intermittently anoxic fjord, located on southern Vancouver Island, British Columbia, Canada (Tunnicliffe et al. 2003). All sensor data are stored in an online archive. A shallow sill at the mouth of Saanich Inlet isolates the deep basin (215 m) that is subjected to a high vertical flux of organic matter (Herlinveaux 1962, Cohen 1978, Timothy & Soon 2001). During spring tides, the surface waters of the Inlet flow seaward, and are replaced by nutrient-rich sub-surface waters from outside of the fjord (Gargett et al. 2003). This supply of nutrients maintains high productivity throughout much of the fjord during spring and summer months, leading to deep-water

anoxia. Deep-water renewal occurs during the fall when dense oxygenated intermediate water masses formed in adjacent Haro Strait enter the Inlet (Anderson & Devol 1973). The VENUS camera platform was strategically located at 102.5 m depth (refer to Appendix C) on the edge of the main basin, slightly upslope from the anoxic waters, within a zone of fluctuating hypoxia. Dissolved oxygen, temperature, salinity and pressure sensors together with the camera platform's remotely controlled digital camera provided a unique suite of instruments for interdisciplinary studies of rhythmic behaviour of benthic organisms in relation to key environmental variables.

We examined activity rhythms in the demersal shrimp *Spirontocaris* spp. and the squat lobster *Munida quadrispina* in relation to conflictive geophysical cycles (i.e. diel fluctuations in sunlight and internal tides) and associated habitat variations (i.e. dissolved oxygen, nitrate and temperature). Seafloor images permitted visual counting of both species, and fluctuations in observed abundances were considered as proxies for population rhythms. We also estimated temporal variations in areal coverage by the sulphide oxidising bacteria (*Beggiatoa* spp.), which is known to effect diel cycles of emersion within the substratum in response to changing redox conditions (Nelson & Castenholz 1982). *Beggiatoa* spp. mats occupy extensive areas of seafloor in Saanich Inlet below 100 m depth, fluctuating in coverage with the cycle of anoxia and deep-water renewal (Juniper & Brinkhurst 1986).

Materials and Methods

VENUS Camera

The C-MAP Cyclops underwater camera used in this study was a modified Olympus® C8080 wide zoom camera (8 Megapixels, f-2.4, 5x optical zoom) that provided high-resolution still images and a lower resolution real-time video stream. The camera was mounted on a small, ROV-deployable tripod together with a Sidus SS209 pan and tilt unit (+/- 90˚ tilt and +/- 180˚pan). An Ikelite 200 Ws flash was used for still photos and three DeepSea Power and Light 100W incandescent lamps served as video lights. Two 10mW red lasers provided scale (10 cm separation) in the images. Image files had an associated meta-data file that included camera settings, pan and tilt position, light status, etc. For all image acquisition sessions, users logged in remotely to a shore-station computer that controlled all camera and accessory functions. Automated image acquisition was not available so that all imagery had to be acquired during scheduled user sessions. The 9-hour time difference between British Columbia and Europe permitted 24-hour time series, with camera control shifting from Victoria to Barcelona or Rome, and then back to Victoria.

Data Acquisition

We acquired digital photos at hourly intervals during three periods (November 2-9, 20-23 and November 30 to December 4) in the fall of 2009 that corresponded to before, during and after a major oxygen intrusion event at the camera site. Acquired still imagery was used to study behavioural rhythms of two abundant benthic species, the shrimp (*Spirontocaris* spp.) and the squat lobster (*Munida quadrispina*), and to quantify fluctuations in coverage of the sediment surface by microbial mats (*Beggiatoa* spp.).

Each image acquisition session began with a bacterial mat photo with the camera oriented vertically down, its home position. This was immediately followed by an oblique angle photo at fixed pan and tilt coordinates, of a larger seabed area (1200 cm^2) for faunal observations (Figure 16). Occasional video recordings were used to document locomotory and feeding behaviour of the two decapods.

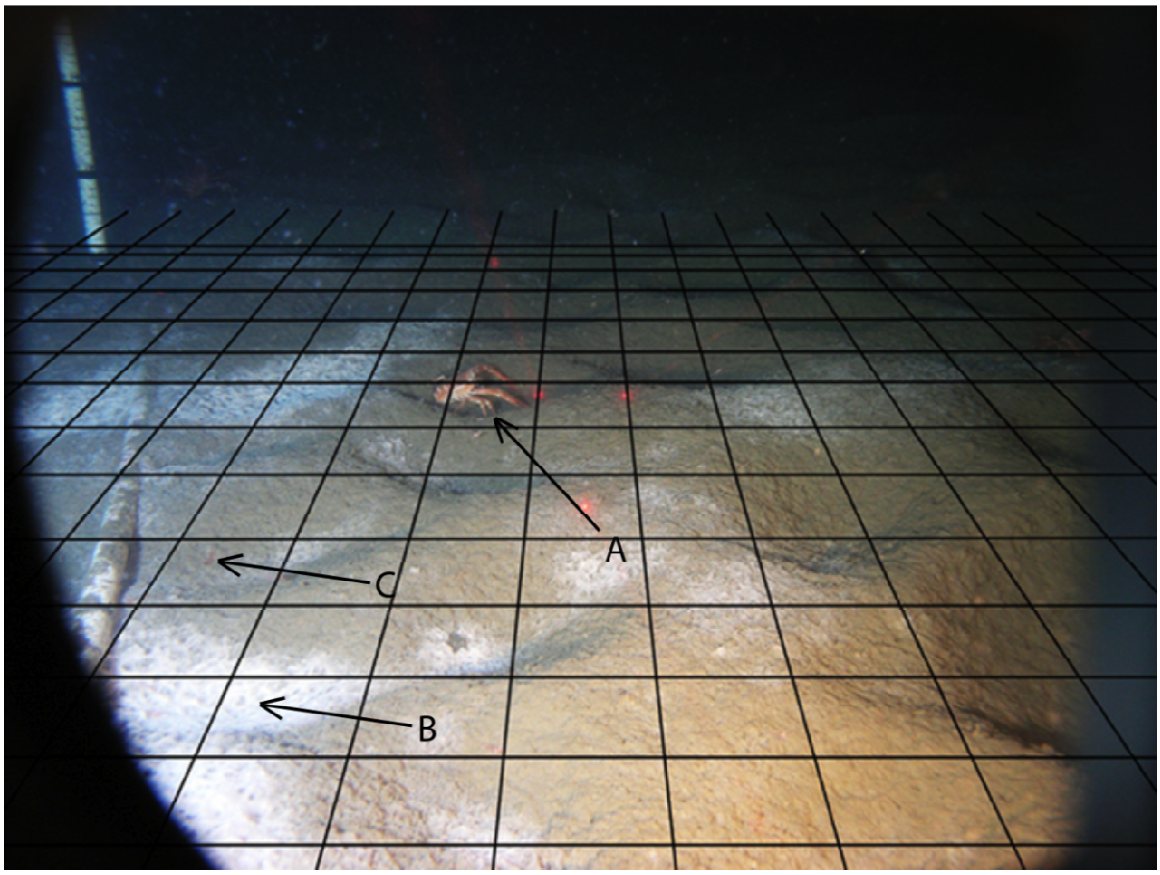

Figure 16: Example of a picture acquired at hourly interval during the experiment. The grid shows the surface area used for data acquisition. Each square is 10 cm x 10 cm, and the total surface area is 1200 cm^2. A) Shrimp, *Spirontocaris* sp. B) The galatheid squat lobster, *Munida quadrispina*. C) Bacterial mat, *Beggiatoa* spp.

In each photo the numbers of individuals were counted for each species and the total area of bacterial mat coverage was estimated as well as its fractal dimension (see below). Fluctuations in species abundances (or area coverage) were used as proxies of

biorhythms (i.e. population behavioural and metabolic rhythms respectively, for decapods and bacteria). Some hourly photos were missing as a result of technical problems or elevated water turbidity. Missing decapods counts or bacterial mat coverage estimates were then replaced by averaging values between immediately adjacent time intervals.

In order to correlate biological fluctuations with changes in habitat conditions, we used data from other VENUS sensors that recorded bottom pressure (i.e. tidal cycles) and temperature, as well as the concentrations of dissolved oxygen and nitrate. All oceanographic sensor data used in this study came from instruments mounted on the camera platform that was located at the same depth as the camera tripod to which it provided power and communications through a 15 m long cable. Oceanographic and chemical data were recorded at one-minute intervals for the entire study period (November 2 to December 4, 2009) and automatically archived by the VENUS system. Resulting time series were averaged over 60 min for statistical comparison with hourly biological data.

Bacterial Mat Coverage

During the first period of image acquisition, the seafloor was partially covered by white bacterial mat patches (*Beggiatoa* spp.), which subsequently decreased in area and disappeared from view. Lighting conditions were not constant across the image field of view (FOV), interfering with automated image analysis. We therefore selected the same image subsection (1500 x 1000 pixels), where lighting was uniform, for quantifying coverage by bacterial mats and sediments. This area of the image contained no other visible biological or substratum features. All images were converted to 8-bit greyscales

using the free-share image processing software, Image J (National Institutes of Health, USA; online ref. http://rsbweb.nih.gov/ij/). Image segmentation was manually conducted by setting a light intensity threshold in order to separate white bacterial mat patches from the grey background sediment. The resulting binarized images were analyzed for fractal dimension using Image J's 'Fractal Box Counter'. Fractal analysis is used to describe the shape of complex objects for which traditional geometric terms could not apply (Mandelbrot 1983). Fractal analysis has been used to describe branching patterns in tree roots (Oppelt et al. 2001) or in mussel bed associations (Kostylev & Erlandsson 2001). The fractal dimension provided a measure of how completely the bacterial mats filled space at increasingly smaller scales. It is represented by a quantity that varies between 1 and 2, where a fractal dimension of 1 represented a single bacterial filament while a value of 2 described a dense bacterial mat, fully covering the sediment. To determine the fractal dimension of the bacterial mats, a variable number of boxes (N) of different sizes (s) were overlaid over the image (i.e. pixels sizes of 2, 3, 4, 6, 8, 12, 16, 32, and 64). Image box fitting was reiteratively repeated with boxes of gradually decreasing s and the N required to obtain the maximum coverage of white spots was recorded at each time. The slope of the log(N) versus the log(s) gives the Box Dimension as a direct estimate of the Fractal Dimension (Fractal D-index) (Ott 1993, Walsh & Watterson 1993).

Statistical Analysis

In order to detect any significant relationships between habitat conditions and visual counts of shrimp and squat lobsters, cross-correlations were performed between the physico-chemical parameters and biological data, within corresponding temporal

windows, using the 'acf' function in R language (R Development Core Team, 2006, online ref.: http://www.r-project.org/). Since environmental data were continuously recorded, correlations among physico-chemical variables were also determined over the entire period (i.e. November 2nd to December 4th).

Regressive periodogram analysis (Klemfuss & Clopton 1993) can be used to screen for periodicity in time series of a few days duration (Chiesa et al. 2006, Costa et al. 2008)). The occurrence of significant ($p< 0.001$) periodicities in the recorded biological time series was screened using the periodogram in the El Temps software package (A. Díez-Noguera, University of Barcelona, UB). This method identifies the periodicity in a data set by subdividing it into subsets of increasing temporal length. It then calculates a variance for each group of data subsets. Finally, it compares each group variance to the total variance of the entire data set. We screened for periodicities of 600 min to 1,800 min, equivalent to 10 and 30 hours, respectively, in order to detect fluctuations related to day-night cycles or diurnal-semidiurnal tidal regimes.

Twenty-four-hour-based waveform analyses were carried out on visual count and physical (water pressure) data sets in order to evaluate the effect of day-night or tidal periodicity on rhythmic behaviour. Data sets were partitioned into subsets of 24 h duration for which values were averaged. All average values and their standard deviations were represented over a 'standard' 24 h interval, yielding a consensus curve describing the mean fluctuation of data within the whole set (Hammond & Naylor 1977). A horizontal threshold line was obtained for each waveform by averaging all constituting values. The resulting mean was added as a line to the plot. All values above that threshold represented a significant increment in data variation (Aguzzi et al. 2003b).

Night duration was indicated on the plot and corresponded to the first day of each recording period: 16:49-07:02 for the 1st period; 16:25-07:31 for the 2nd period; and finally, 16:17-07:45-for the 3rd period.

Results

Environmental Data

Time series of oceanographic, chemical and biological observations for the three recorded periods are presented in Figure 17. Water pressure recorded a variable tidal regime of spring (1st and 3rd periods) and intermediate between neap and spring tides (2nd period) (Fig. 2). A first oxygen intrusion event occurred on November 6th during the first period of the experiment and was followed by a second, more substantial event on November 9th. The higher oxygen concentrations of the 2nd and 3rd periods were also more variable (i.e. several hourly peaks; Figure 17). Temperature showed less variability (i.e. 9.2-9.5 ºC) over the entire experiment with a progressive decrease during the 1st period and an increase during the 3rd recording period (Figure 17). Dissolved nitrate concentrations displayed a similar trend. Temperature and nitrate concentration followed the tidal cycle with slightly higher values during spring tides (Figure 17).

Cross-correlations revealed significant correlations (i.e. 95% confidence level) between the variables and the time lag at which they occurred (Table 6). Because of the strong variance in oxygen data following the first intrusion event (see Figure 17), the time series was split in two halves: from Nov 2nd to Nov 16th and from Nov 16th to Dec 4th. There was a negative correlation between water pressure and oxygen during the first half ($r = -0.27$; 4 h lag) and a weaker negative correlation during the second one ($r = -0.18$; 5 h lag). Oxygen and temperature were positively correlated during the first

half (r = 0.37; 0 h lag) of the experiment, as well as in the second one (r = 0.25; 11 h lag). Oxygen and nitrate showed strong positive correlations for both halves (r = 0.38 and 0.51 respectively, with 1 h lag). While no correlations were apparent between water pressure and either temperature or nitrate, the latter two variables were positively correlated (r = 0.38; 0 h lag) (Table 6).

Table 6: Cross-correlations between the different environmental parameters: pressure, dissolved oxygen concentration, temperature and nitrates concentrations. Cross-correlations with dissolved oxygen concentrations were conducted on two different periods, before and after the first oxygen intrusion that occurred October 6th. The lower diagonal represent the time lag and is expressed in days, the upper diagonal give the significant r value ($p<0.05$).

r / **lag (h)**	**Water Pressure**	**Oxygen Nov 2-16**	**Oxygen Nov16-Dec 4**	**Nitrates**	**Temperature**
Water Pressure	-	-0.27	-0.18	ns	ns
Oxygen Nov 2-16	4	-	-	0.38	0.37
Oxygen Nov16-Dec 4	5	-	-	0.51	0.25
Nitrates	ns	1	1	-	0.38
Temperature	ns	0	0	0	-

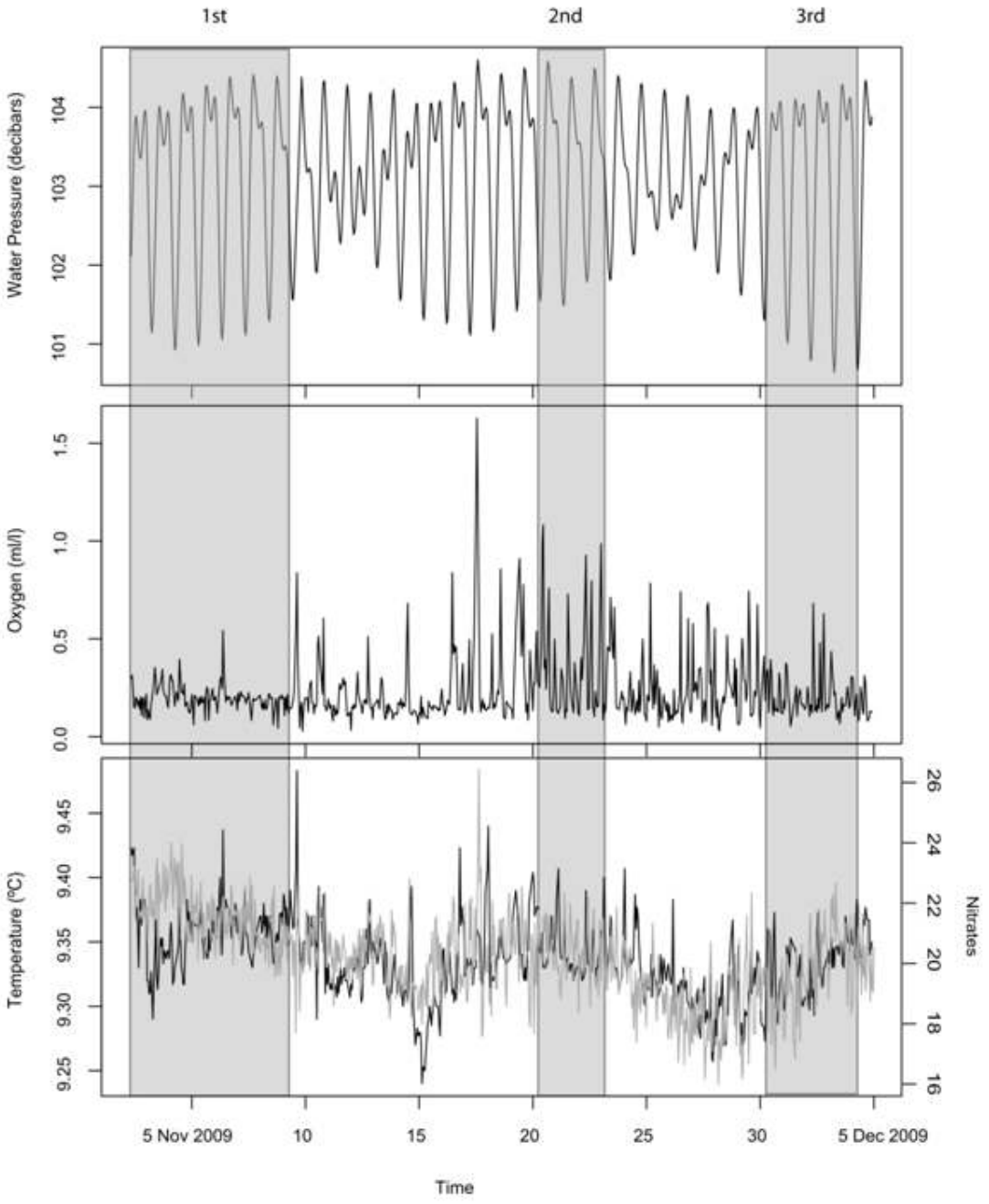

Figure 17: Time series of data for oceanographic (i.e. water pressure and temperature) and chemical (dissolved oxygen and nitrates) data are reported at the camera' VENUS location averaged by hour between November 2nd and December 4th 2009. Hourly pictures of the seafloor taken during the three video-recording periods are shaded in grey: 1st, Nov 2-9; 2nd, Nov 20-23 and 3rd, 30 Nov -4 Dec.

Behavioural Rhythms

A total of 12,278 shrimp (*Spirontocaris* spp.) and 452 squat lobsters (*Munida quadrispina*) were detected over the three experimental periods. Other species occasionally appeared in the FOV: the slender sole (*Lyopsetta exilis*) and the Pacific herring (*Cuplea pallasii*). In video recordings shrimp could be seen swimming within the benthic boundary layer, as well as resting on the bottom. Squat lobsters walked through the FOV but showed no burrowing activity. Behavioural observations documented two squat lobster feeding strategies: deposit feeding or foraging on the sediment surface and capturing zooplankton prey in the water column with their chelipeds.

The shrimp abundance time series (Figure 18) showed a progressive increase in visual counts over the three testing periods. The increase began in the final days of the 1st period and a peak in shrimp abundance was reached early in the 3rd period. Squat lobsters, on the other hand, maintained fairly constant numbers throughout the experiment (Figure 18), with a maximum of 6 individuals in a single photo.

Because of the shorter duration of the time series for the 2nd and 3rd periods, the periodogram analysis was only conducted for the first (Figure 19). Results suggested an overall weak but still significant ($p < 0.001$) tidal periodicity for both shrimp and squat lobsters. For the shrimp, we identified a weak rhythmicity closely matching the semi-diurnal regime (i.e. 736 min. equal to 12 h 26 min). Squat lobsters showed two periodicities not fully matching the tidal cycle: at 824 and 1,352 min, respectively equal to 13 h and 73 min and 22 h and 53 min. The squat lobster periodicities were probably an artefact of the time-series analysis related to the small number of counted individuals.

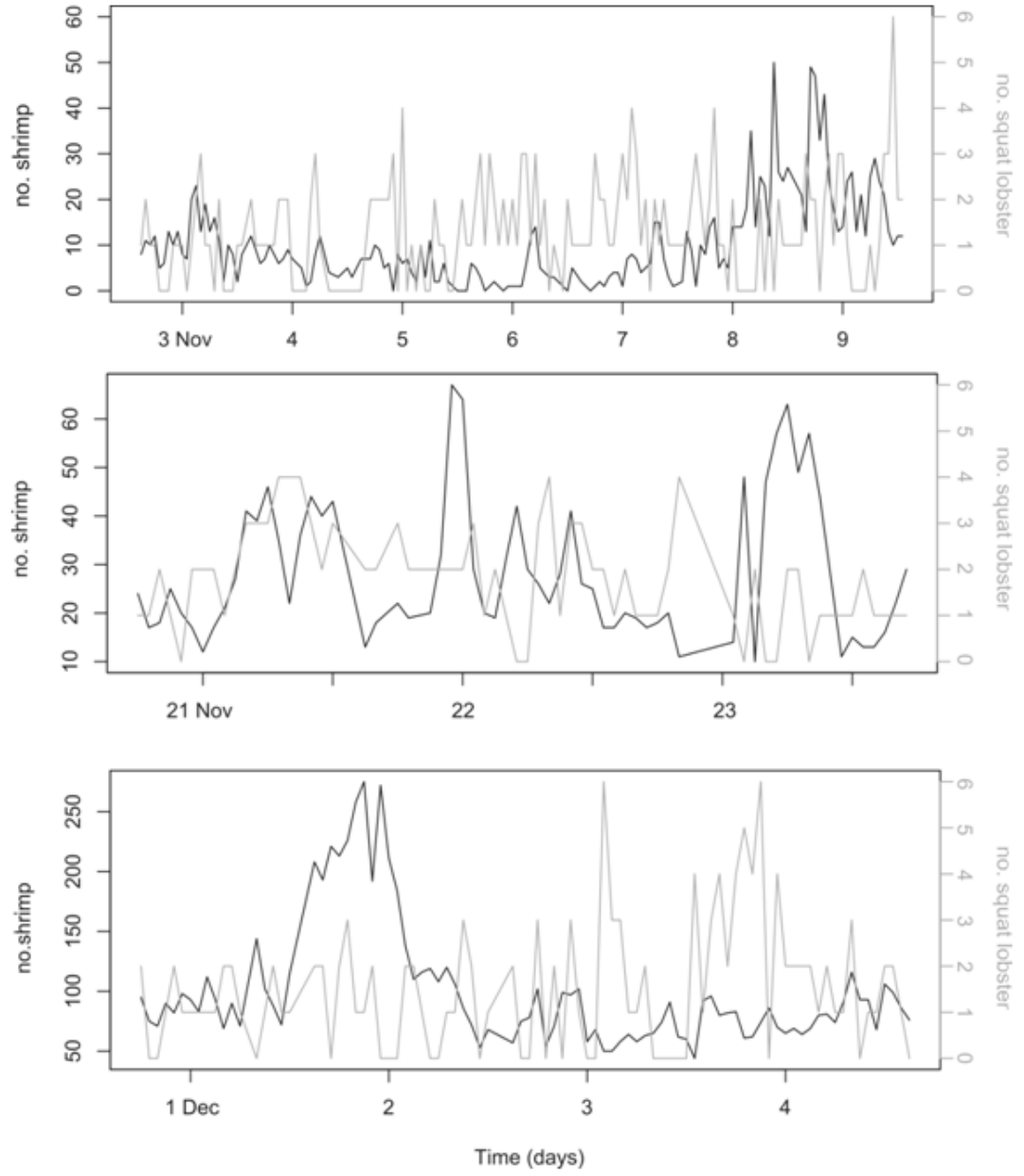

Figure 18: Time series of biological data (i.e. visual counts of the shrimp *Spirontocaris* spp. and the squat lobster *Munida quadrispina*) for the three recording periods.

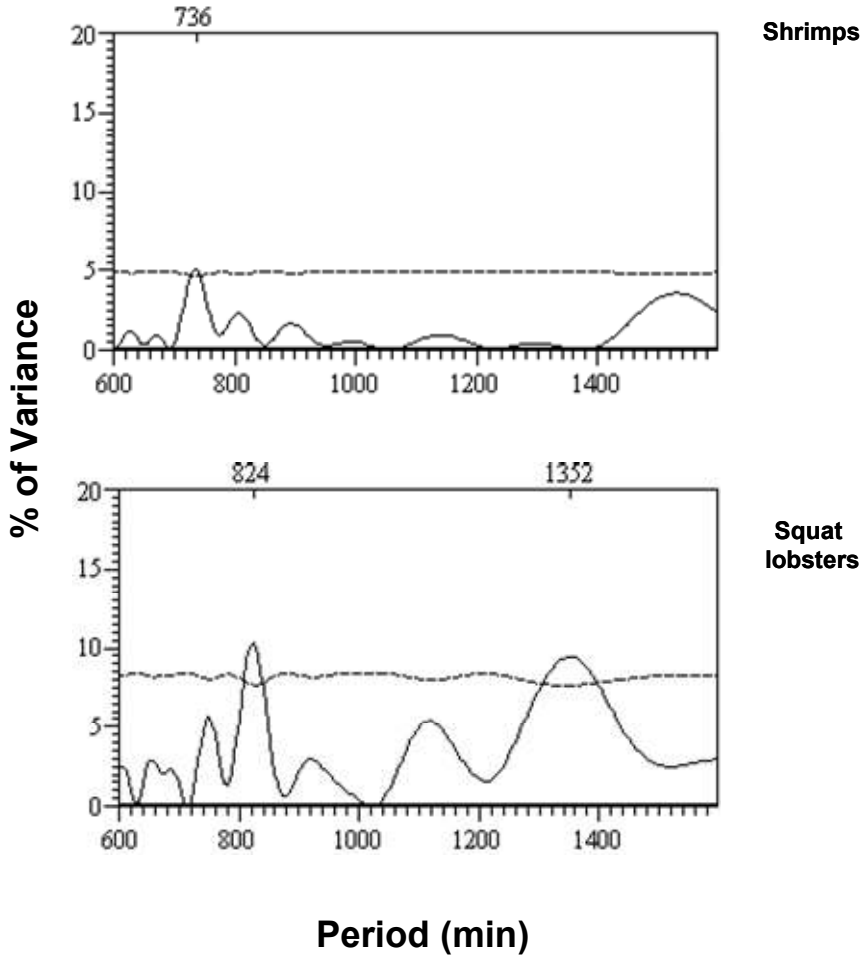

Figure 19: Regressive periodogram analysis outputs for time series of visual counts of shrimp (*Spirontocaris* spp.) and squat lobsters (*Munida quadrispina*) during the recording leg from the 2nd to the 9th of November. Significant ($p < 0.001$) inherent periodicities (in minutes) are indicated by peaks (and corresponding above values) that cross the horizontal dashed threshold.

Waveform analysis showed some level of phase relationships between diel fluctuations in visual counts for shrimp and squat lobsters and the tidal regime, and no apparent day-night fluctuations (Figure 20). Significant increases in counted specimens (i.e. mean values above the daily mean) showed variable timing in relation to the onset of night, as can be seen by comparing waveform plots for the 1st and the 3rd testing periods. This was visible in the plots of shrimp visual counts, where the timing variable increased

from night (Figure 20 A, B) to daytime (Figure 20 C). Similarly, squat lobsters showed a shift in abundance peaks from night in the 2nd recording period to fully diurnal and concomitant with shrimps in the 3rd period. The plot for the 1st period had poorly defined fluctuations, probably related to the small number of individuals per photo during this period.

There were weak but significant negative cross correlations between species counts and dissolved oxygen during the first period (r = -0.27 and r = -0.22 respectively, for *M. quadrispina* and *Spirontocaris* spp.; at a lag of 2 h) meaning that decapod species responded two hours after a change in dissolved oxygen concentration. This relationship was not significant for the other recording periods when oxygen concentrations were higher. A significant negative correlation was also found between shrimp counts and water pressure (i.e. tide) during the 1st (r = -0.18, 3 h lag) and 2nd (r = -0.5, 2 h lag) periods. The weak correlation during the 1st period and the absence of any correlations during the 3rd period were probably the result of high variability in shrimp counts (see Figure 18). A significant negative correlation was found between shrimp and nitrate (r = -0.33, 2 h lag) during the 1st and 2nd periods (r = -0.27, 0 h lag). There were no significant correlations between shrimp and temperature for any consistent time lags.

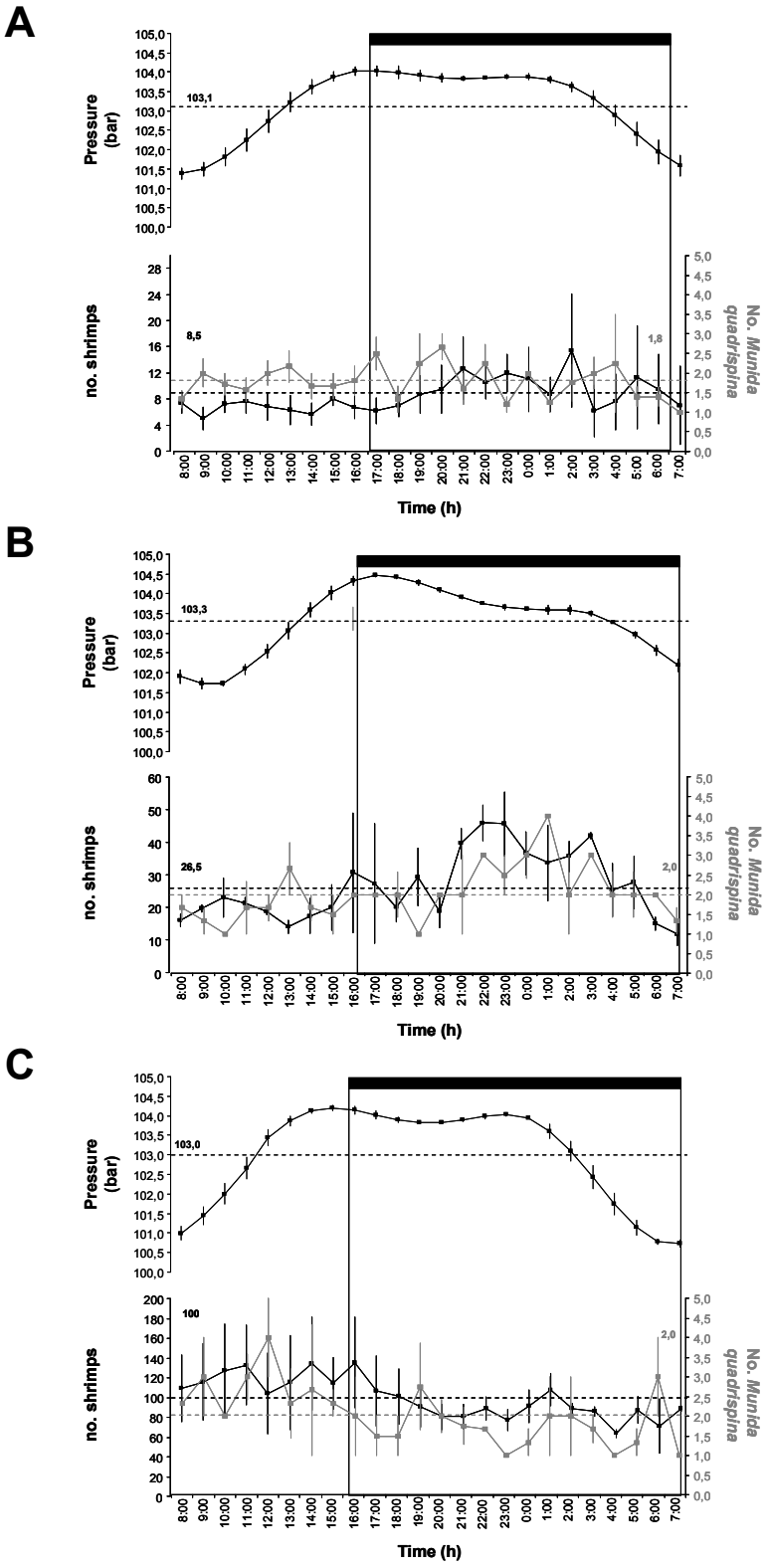

Figure 20: Waveform analysis output on time series for oceanographic (i.e. water pressure, temperature and speed), chemical (dissolved oxygen and nitrates), and finally, biological (i.e. visual counts of shrimps, *Spirontocaris* spp. and squat lobsters *Munida quadrispina*) time series obtained during different testing periods of November and the

beginning of December 2009 (A) from to Nov 2-9; B) from Nov 20-23; C) Nov 30-Dec 4). Small black and grey values within plots indicate the threshold (i.e. horizontal dashed line) as the daily mean computed form all averages of the waveform. Vertical rectangle with the black bar on top depicts the night duration at each recording period.

Bacterial Mat Coverage

Bacterial mat coverage was only analysed for the 1st recording period, since they were nearly absent during the 2nd period and completely absent during the 3rd, when oxygen concentrations increased (see Figure 17). The Fractal D-index time series (i.e. percentage of bacterial mat coverage) is presented in Figure 21 A. Fractal D-index showed a slight decrease (Figure 21 A), since the coverage was highly variable over the entire period. Fractal D-index and dissolved oxygen concentrations showed significant cross-correlations with positive and negative signs, depending on the time lag considered (Figure 21 B): positive ($r = 0.20$) for 1 h lag; negative ($r = -0.27$) for 6 h lag. Periodogram analysis did not reveal any significant periodicity in the Fractal D-index (results not shown). Cross-correlation analysis revealed a weak but significant negative correlation between shrimps counts and the bacterial mat Fractal D-index ($r = -0.17$, 0 h lag).

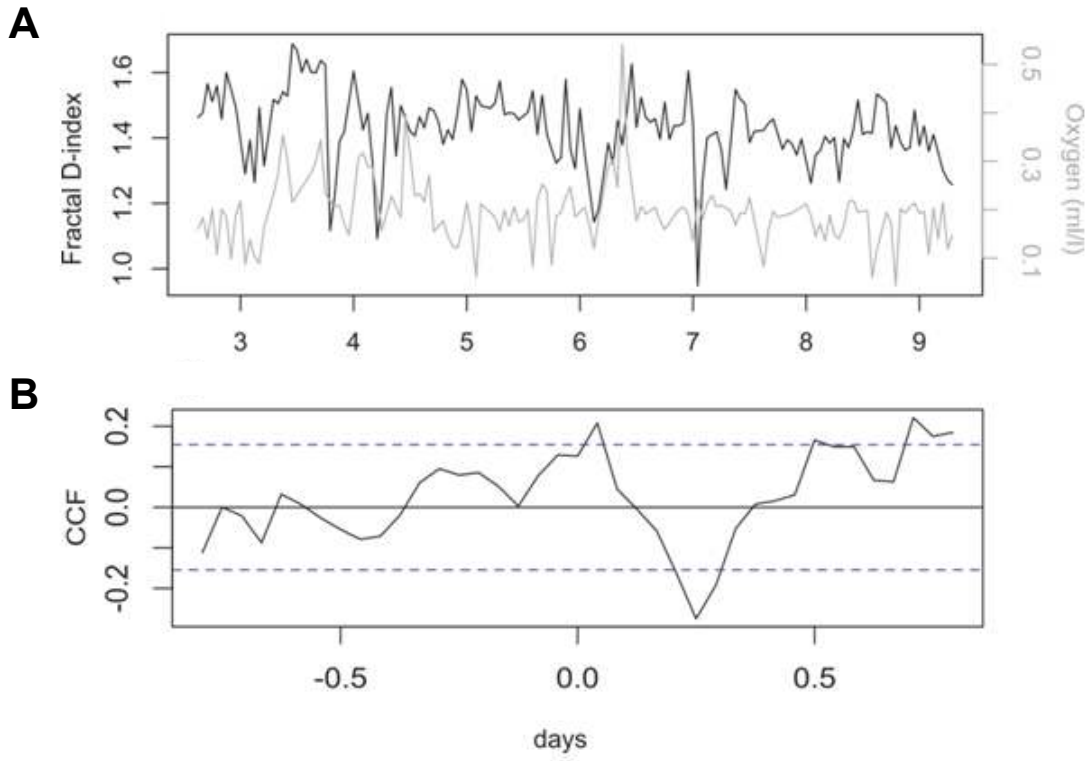

Figure 21: A) Evolution of Fractal D-index and dissolved oxygen concentration between November 2nd and 9th. B) Cross-correlation (CCF) between Fractal D-index and dissolved oxygen concentration. The x axis represent the time lag and is expressed in days, the dotted line represent the 95% confidence interval.

Discussion

This study made use of time-series imagery and oceanographic sensor data to explore potential cause and effect relationships between geophysical cycles, habitat dynamics and benthic community responses. In evaluating our results, it is important to consider methodological limitations as well as the particularities of the examined species and the study site. Fluctuations in visual counts in the camera FOV served as a proxy of population rhythms. Implicit in our analysis is the assumption that changes in abundance or coverage represented net movement of populations up or down the slope of the basin (decapods), in and out of the sediment (bacterial mats) or between the water column and the seafloor (shrimp). Changes in population size (or biomass) are unlikely at the time

scales considered except for the bacterial mats, although migration of shrimp populations in or out of the Inlet cannot be discounted. Another important consideration with respect to the image analysis results is the possibility of any uneven temporal distribution of error in our counts of shrimp and squat lobsters. Fixed camera settings, lighting and pan and tilt coordinates assured comparability of all images even though they were acquired by many different operators. All visual counts were done by the senior author, using archived images, to minimize (standardize) personal subjectivity. Occasional images that had reduced visibility because of particle resuspension were excluded from the analysis.

The observed weak tidal signal in shrimp activity could be the result of counting individuals belonging to a mixed species assemblage. Several morphologically similar shrimp species occur in the Strait of Georgia and associated fjords, including Saanich Inlet (Zimmermann 2006). Species belonging to the genus *Spirontocaris* can be difficult to distinguish by sight (Wicksten 1990). It is thus possible, that overall periodicity in our visual count data sets was influenced by a mixing of rhythmic patterns of different strengths (Kronfeld-Schor & Dayan 2003).

For the squat lobsters, the small sample size may have influenced our ability to detect diel rhythmicity. The VENUS camera photographed a limited area of seafloor (1200 cm^2) on which we observed between 0 and 6 squat lobsters. We therefore cannot exclude *a priori* the possibility of diel rhythms in this species.

Finally, although light may have attracted organisms toward the camera, lights-on periods were constant throughout all observations. Photos were taken within 5 minutes of turning on the camera lights, which were turned off at the end of the photo session. We are thus confident that changes observed in decapod abundance are linked to internal

or external factors other than the presence of the observing system. Light may, however, have introduced some artefacts in the bacterial mat studies since fish were sometimes quickly attracted by the light and their swimming activity disturbed the sediment surface colonized by the bacterial mats (K. Robert, pers. obs).

Saanich Inlet Habitat Dynamics

VENUS sensors recorded complex diel changes in seafloor habitat conditions at the Saanich Inlet study site. Throughout the entire study period, dissolved oxygen concentrations were typical of hypoxic conditions (i.e. <2 ml l^{-1}; Diaz & Rosenberg (1995)). The observed oxygen intrusions were characteristic of renewal events known to occur every year in Saanich Inlet when dense intermediate water masses form in Haro Strait in late summer, enter the fjord at the mouth and sink, replacing deep anoxic water (Anderson & Devol 1973). During this renewal, boluses of flushing water enter the Inlet with flood tides, explaining the occurrence of peaks in oxygen concentration (Anderson & Devol 1973). The 2009 renewal event was however significantly weaker compared to previous years (VENUS data). The intensity of renewal events can vary from year to year, depending on the upwelling regime in the adjacent Strait of Georgia, local atmospheric conditions and river discharge (Anderson & Devol 1973). Variability in temperature and nitrate also showed a tidal trend that may be related to another known fortnightly process in Saanich Inlet. Increased tidal mixing during spring tides in adjacent channels and passages reduces stratification outside of the Inlet, resulting in a density gradient that causes a weak outflow in surface waters of Saanich Inlet (Timothy & Soon 2001, Gargett et al. 2003). This outflow is replaced by a sub-surface inflow of well-mixed, nutrient-rich water that is eventually mixed upward through advection.

While we cannot identify a simple mechanism to explain observed variations in dissolved oxygen, nitrate and temperature at the study site, it is likely that the observed tidal components were related to the combined or individual effects of deep-water renewal events and spring tide forcing that dominated the oceanography of Saanich Inlet during the study period.

Diel and Tidal Rhythms

Periodogram and waveform analysis did not detect any day-night modulation of decapod abundance or in the coverage of sediments by bacterial mats. Although other studies at similar depths in less productive waters have detected diurnal light intensity fluctuations and biological responses (Aguzzi et al. 2003b), this result is not surprising for Saanich Inlet where the high productivity and particulate loading in surface waters severely limits light penetration. The lower limit of the photic zone (1% incident radiation) in Saanich Inlet is at < 20m depth (Grundle et al. 2009).

The shrimp (*Spirontocaris* spp.) showed a weak, tidally oriented periodicity, which was absent in the squat lobsters (*Munida quadrispina*). These differences may be partly related to their different forms of mobility (reviewed by Aguzzi & Company (2010)). Shrimp were observed to swim in the benthic boundary layer while squat lobster walked on the seabed. Swimmers are more exposed to hydrodynamic fluctuations than walkers as has already been observed in other deep-sea decapods with different displacement typologies (Aguzzi et al. 2010). However, since shrimp abundance was correlated to both the tide and oxygen concentrations, the identified activity rhythm could be directly related to tides (endogenous control) or indirectly through changes in oxygen

concentration (exogenous control). The time lags, 4 to 5h and 2h with the tide and oxygen, respectively, together with the significant correlation between the dissolved oxygen and the tides themselves, suggest that this species was more likely responding to changes in oxygen concentration as an external modulator. The squat lobster's known tolerance of low oxygen conditions (Burd & Brinkhurst 1984) may have contributed to its lack of response to minor, tidally driven changes in dissolved oxygen concentrations. In Saanich Inlet, *M. quadrispina* is very tolerant of hypoxia, with high densities found at DO_2 levels as low as 0.1 to 0.15 ml l^{-1} (Burd & Brinkhurst 1984). Levels of oxygen at the depth of the camera platform rarely dropped below 0.1ml l^{-1} during the period of this study.

Masking of Activity Rhythms by Dissolved Oxygen Variations

Circadian cycles, if present, can be blurred by higher frequency changes in environmental conditions (dissolved oxygen levels, other water mass properties) or by biological forcing (e.g. predation, competition) (Aguzzi et al. 2003a). The cross-correlation analysis showed dissolved oxygen to be the most important habitat factor influencing both decapod species and the bacterial mat coverage in Saanich Inlet. Changes in oxygen concentration differently affect the behaviour of benthic organisms, depending on their metabolism (Company & Sardà 1998). Blurring of circadian rhythms as a result of oxygen depletion is not limited to the benthos. For example, in Chesapeake Bay (US), hypoxia disrupts diel vertical migrations of species within different phyla such as fishes (Ludsin et al. 2009) and mesozooplankton (Pierson et al. 2009).

There is some indication that the response of the Saanich Inlet shrimp to changing oxygen concentrations may be complex, and possibly related to food requirements. Shrimp counts at our study site showed weak tidal associations but their numbers increased dramatically after the first oxygen intrusion. Yet in the overall data set, in which the majority of observations came after the first oxygen intrusion, there was a negative correlation between oxygen and shrimp counts. This indicates that the shrimp subsequently migrated away from the study area, possibly down slope following a deepening oxygenation front. This is supported by the observation of abundant shrimp at 120 m depth in an area covered by *Beggiatoa* spp. mats in February 2010, when dissolved oxygen concentration was higher at the depth of the camera platform (M. Matabos, pers. obs.).

The relationship of the shrimp to dissolved oxygen concentrations could also be influenced by food availability. They have been observed feeding on the *Beggiatoa* spp. bacterial mats in Saanich Inlet (V. Tunnicliffe, com. pers.). Bacterial mat coverage was significantly correlated with oxygen concentrations, in part as a result of their rapid disappearance following the first oxygen intrusion event. This disappearance was coincident with a rapid increase in shrimp abundance. However, *Beggiatoa* spp. mats are known to respond to changing oxygen availability by migrating vertically within sediments (or laboratory media), in order to remain at the interface of oxic and anoxic conditions where they oxidise reduced sulphur with molecular oxygen (Nelson et al. 1986). Thus they migrate downward (and out of sight) to avoid unfavourably high oxygen levels, and upward when oxygen levels decrease at depth (Nelson & Castenholz 1982, Nelson et al. 1986). It remains to be determined whether the disappearance of the

microbial mats was the result of vertical migration down into the sediments in response to an oxygen influx, or the result of grazing by the suddenly larger shrimp population. In either case, this disappearance could have contributed to the subsequent decrease in shrimp numbers if the shrimp were exploiting this food source.

Conclusion

This study provides a first demonstration of the use of cabled undersea observatories for studying how behavioural rhythms interact with habitat variations in deep-water environments. The availability of continuous data streams from oceanographic sensors at the camera site greatly facilitated the interpretation of the imagery data. The observed intrusions of oxygen at the beginning of November may have obscured the existence of biological rhythms in our relatively short time series, highlighting the problem of scale in studying these processes (Morgan 2004, Nevill et al. 2004). Nevertheless, our results highlight the importance of considering activity rhythms in the environment as well as the non-negligible influence of geophysical cycles on species auto-ecology and community dynamics.

Most studies of activity rhythms focus on the species alone with little regard to the surrounding ecosystem dynamic (Rona et al. 1986, Marques & Waterhouse 2004). At the other extreme, benthic ecology studies often disregard the existence of biological rhythm in populations and communities when reporting population size data. The online, community-scale collaborations that are encouraged by ocean observatories such as VENUS, offer opportunities for multi-investigator studies that can bridge disciplinary limitations.

Acknowledgments

M. Matabos is a post-doctoral fellow funded by the Canadian Healthy Ocean Network (CHONe). J. Aguzzi is a post-doctoral fellow in the *Ramón y Cajal* Program (MICINN). K. Robert benefited from scholarships from the Natural Sciences and Engineering Research Council of Canada (NSERC), the Fond québécois de la recherche sur la nature et les technologies (FQRNT) and the University of Victoria. The authors would like to thank J. Rose, K. Nicolich and E. Ramirez-Llodra for their help with image acquisition. We also would like to thank the VENUS and ROV ROPOS teams for their helpful collaboration. This research was made possible through funding from NSERC Canada (S.K. Juniper, V. Tunnicliffe), the Canada Foundation for Innovation (VENUS project, University of Victoria) and the HIGHVISION program (grant #19177-7303-08 from the Italian Ministero delle Politiche Agricole; Decreto Ministeriale MIPAFF).

Chapter 5
Conclusion

Applications and Implications

The development of an adaptive methodological approach to initiate the quantitative study of benthic ecological processes using imagery was a necessary step to improve the efficiency of observatory systems and increase our ability to test hypotheses using the collected images. This is particularly true in understudied environments such as the deep sea where prior knowledge has been limited due to restricted, weather dependent access and where new knowledge acquisition continues to require expensive equipment. As such, a maximal quantity of information needs to be extracted as quickly as possible and employed efficiently to build models describing ecosystem functioning.

However, this can prove challenging when first approaching a new ecological question or a new study site. As exemplified in this thesis, sampling frequencies need to be closely tailored to the ecosystem processes of interest and an increased understanding of processes occurring at various temporal scale is currently needed to characterize the baseline state of the deep sea. For example, in Barkley Canyon, 2hr sampling intervals were sufficient to describe sea urchin movement patterns, but to achieve the same result with vent endemic polynoids; a 6sec sampling frequency was required, while in Saanich Inlet, sweeps carried three times per week adequately captured trends in bacterial mat coverage. Hence, studies aiming at observation protocol optimization are very useful in the long term and the initial time investment required should be compensated by the increased efficiency of the information gathering process. With the proposed step-wise methodological approach, the initial information first collected was incorporated into

preliminary models whose results informed subsequent sampling decisions. The aim was always to find a sampling frequency which ensured that the parameters of interest could be measured accurately all the while ensuring that it remained feasible for a single observer to manually process all the acquired imagery.

The use of cabled observatories facilitated the application of a step-wise procedure as they permit interactive setting of sampling frequencies; greatly reducing the number of deployments needed to reach optimized observation protocols. Low sampling frequencies were first employed to gain familiarity with the deployment site and experimentally increased until the observer obtained a representative view of the ecosystem. However, underwater observatory cameras are fixed in position, providing only a spatially limited view of the seafloor. The complementary use of previous knowledge acquired via remotely operated vehicle (ROV) video transects and autonomous camera systems ensured that spatial variation was taken into account and ensured optimal camera placement. In the case of autonomous camera systems, an initially high sampling frequency which could then be subsampled during the analysis phase was favoured. This ensured that sufficient information was captured to allow determination of optimal sampling frequencies for application in future deployments. With standardized approaches, both the required ROV infrastructure maintenance (Jones 2009) and optimized autonomous camera deployments will provide an extended observatory footprint yielding meaningful ecological insights at a larger scale and improving predictive models.

Before such models can be built, techniques allowing quantitative information to be extracted from the collected imagery need to be developed. We proposed a diversified

array of techniques (perspective grids, polar coordinate systems, automated color selection and thresholding routines, particle tracking, temperature interpolation and fractal analysis) whose main advantages were their simplicity and inexpensiveness. Their implementation was demonstrated using specific ecological processes, but their applications are much broader. Extension to other ecological studies in other environments, even coastal and terrestrial, should only require minimal adjustments; particularly as long as the step-wise methodological approach suggested is conserved.

These initial deployments also served to build a baseline level of information needed to inform subsequent deployments. In all three systems considered, longer term deployments are currently planned. In Barkley Canyon, it will now be possible to monitor seasonal responses of benthic organisms to variations in organic matter inputs resulting from surface water phytoplankton blooms. Since additional cameras are deployed deeper within the canyon, depth related differences will also be examined. The summer 2011 deployment of a remotely operated camera connected to the NEPTUNE Canada cabled observatory at Main Endeavour Vent Field will permit refined characterization of thermal responses using movement pattern analyses for a variety of taxa. This new camera system will increase the FOV and allow for interactive control, ensuring that specific individuals can be accurately tracked and that shifts in species assemblages are followed over longer time scales. A year-long monitoring scheme is also presently underway in Saanich Inlet and should yield additional information regarding the relationship between biological community structures and complex oceanographic dynamics (Matabos et al. 2011b).

For these long-term projects, observation schedules were optimized to examine specific processes which will improve our understanding of how ecosystems are likely to respond to predicted global level changes in the ocean. With climate change, sea surface temperatures are expected to vary leading to alterations in global circulation patterns and upwelling strength; influencing offshore primary productivity in the upper water column and altering the amount of organic matter reaching the bottom (Danovaro et al. 2001, Danovaro et al. 2004, Behrenfeld et al. 2006, Smith et al. 2009, Billett et al. 2010). By examining the natural response of the benthos when poorer years are encountered, we will be in a better position to predict how ecosystem functions and services such as bioturbation may be affected in the long term. The planned start to extract copper, zinc, gold and silver from hydrothermal sulphide deposits will alter the flow discharge regime and incidentally the thermal environment for the associated benthic biota (Nautilus Minerals Niugini 2008, Van Dover 2011). Knowing the strategies employed by specific taxa to cope with thermal variability will ensure that the species more likely to be impacted are identified *a priori* and that adequate management is devised (Dancette 2008). Another increasing threat to our ocean is the spreading of anoxic zones brought on by increased heterotrophic bacterial activity following eutrophication or water-column stratification related to climate change (Diaz & Rosenberg 2008). This depletion in benthic oxygen levels will create shifts in community structure, not inconsistent with the ones naturally occurring in Saanich Inlet and described in Matabos et al. (2011b). As such, Saanich Inlet provides a natural laboratory to study short and long-term ecosystem responses to oxygen depletion, test for the existence of threshold levels or measure ecosystem resilience.

The optimization and standardization of observation protocols should reduce the time necessary to carry out specific studies in new environments while at the same time improving our ability to make comparisons between study sites. The deep seafloor represents the largest biome on the planet and a more integrated multi-disciplinary approach is necessary to understand and predict the impact of global level changes. The implementation of long-term studies involving both optimized *in situ* observations of benthic communities and real-time high frequency monitoring of environmental variables through cabled observatories will enhance our ability to characterize natural ecosystem variability and establish the baseline state needed for early detection of anthropogenically induced changes.

.

Bibliography

Aguzzi J, Bahamon N (2009) Modeled day-night biases in decapod assessment by bottom trawling survey. Fisheries Research 100:274-280

Aguzzi J, Bahamon N, Marotta L (2009a) The influence of light availability and predatory behavior of the decapod crustacean *Nephrops norvegicus* on the activity rhythms of continental margin prey decapods. Marine Ecology 30:366-375

Aguzzi J, Company JB (2010) Chronobiology of deep-water decapod crustaceans on continental margins. Advances in marine biology 58:155-225

Aguzzi J, Company JB, Costa C, Menesatti P and others (2011) Activity rhythms in the deep-sea: A chronobiological approach. Frontiers in Biosciences 16:131-150

Aguzzi J, Company JB, Sardà F, Abelló P (2003a) Circadian oxygen consumption patterns in continental slope *Nephrops norvegicus* (Decapoda: Nephropidae) in the Western Mediterranean. Journal of Crustacean Biology 23:749-757

Aguzzi J, Costa C, Fujiwara Y, Iwase R, Ramirez-Llorda E, Menesatti P (2009b) A novel morphometry-based protocol of automated video-image analysis for species recognition and activity rhythms monitoring in deep-sea fauna. Sensors 9:8438-8455

Aguzzi J, Costa C, Furushima Y, Chiesa JJ and others (2010) Behavioural rhythms of hydrocarbon seep fauna in relation to internal tides. Marine Ecology Progress Series 418:47-56

Aguzzi J, Costa C, Menesatti P, García JA, Chiesa JJ, Sardà F (2009c) Monochromatic blue light entrains diel activity cycles in the Norway lobster, *Nephrops norvegicus* (L.) as measured by automated video-image analysis. Scientia Marina 73:773-783

Aguzzi J, Puig P, Company JB (2009d) Hydrodynamic, non-photic modulation of biorhythms in the Norway lobster, *Nephrops norvegicus* (L.). Deep Sea Research Part I: Oceanographic Research Papers 56:366-373

Aguzzi J, Sarda F, Abello P, Company JB, Rotllant G (2003b) Diel and seasonal patterns of *Nephrops norvegicus* (Decapoda: Nephropidae) catchability in the western Mediterranean. Marine Ecology Progress Series 258:201-211

Aller RC (1982) The effcet of macrobenthos on chemical properties of marine sediment and overlying water. In: McCall PL, Tevesz MJS (eds) Animal-sediment relations. Plenum Press, New York, p 53-102

Anderson JJ, Devol AH (1973) Deep water renewal in Saanich Inlet, an intermittently anoxic basin. Estuarine and Coastal Marine Science 1:1-10

Angilletta MJJ, Huey RB, Frazier MR (2010) Thermodynamic effects on organismal performance: Is hotter better? Physiological and Biochemical Zoology 83:197-206

Auffret Y, Coail J-Y, Delauney L, Legran J and others (2010) Tempo-Mini: A Custom-designed instrument for real-time monitpring of hydrothermal vent ecosystems. Instrumentation Viewpoint 8:17

Auster P, Malatesta R, LaRosa S (1995) Patterns of microhabitat utilization by mobile megafauna on the southern New England (USA) continental shelf and slope. Marine Ecology Progress Series 127:77-85

Bahamon N, Sardà F, Aguzzi J (2009) Fuzzy diel patterns in catchability of deep-water species on the continental margin. ICES Journal of Marine Science: Journal du Conseil 66:2211-2218

Bailey DM, Bagley PM, Jamieson AJ, Collins MA, Priede IG (2003) *In situ* investigation of burst swimming and muscle performance in the deep-sea fish *Antimora rostrata* (Günther, 1878). Journal of Experimental Marine Biology and Ecology 285-286:295-311

Bates AE, Lee RW, Tunnicliffe V, Lamare MD (2010) Deep-sea hydrothermal vent animals seek cool fluids in a highly variable thermal environment. Nature Communications 1:1-6

Bates AE, Robert K, Onthank KL, Quinn G, Juniper SK, Lee RW (submitted) Thermoregulation in the hydrothermal vent sulphide worm: Behavioural response to extreme temperature variability. Marine Ecology Progress Series

Bates AE, Tunnicliffe V, Lee RW (2005) Role of thermal conditions in habitat selection by hydrothermal vent gastropods. Marine Ecology Progress Series 305:1-15

Bayes T (1763) An essay towards solving a problem in the doctrine of chances. Philosophical Transactions of the Royal Society of London 53:370-418

Beaumont NJ, Austen MC, Atkins JP, Burdon D and others (2007) Identification, definition and quantification of goods and services provided by marine biodiversity: Implications for the ecosystem approach. Marine Pollution Bulletin 54:253-265

Behrenfeld MJ, O'Malley RT, Siegel DA, McClain CR and others (2006) Climate-driven trends in contemporary ocean productivity. Nature 444:752-755

Belley R, Archambault P, Sundby B, Gilbert F, Gagnon J-M (2010) Effects of hypoxia on benthic macrofauna and bioturbation in the Estuary and Gulf of St. Lawrence, Canada. Continental Shelf Research 30:1302-1313

Bergquist DC, Eckner JT, Urcuyo IA, Cordes EE, Hourdez S, Macko SA, Fisher CR (2007) Using stable isotopes and quantitative community characteristics to determine a local hydrothermal vent food web. Marine Ecology Progress Series 330:49-65

Bett BJ (2001) UK Atlantic Margin Environmental Survey: Introduction and overview of bathyal benthic ecology. Continental Shelf Research 21:917-956

Bett BJ, Malzone MG, Narayanaswamy BE, Wigham BD (2001) Temporal variability in phytodetritus and megabenthic activity at the seabed in the deep Northeast Atlantic. Progress in Oceanography 50:349-368

Billett DSM, Bett BJ, Reid WDK, Boorman B, Priede IG (2010) Long-term change in the abyssal NE Atlantic: The '*Amperima* Event' revisited. Deep Sea Research Part II: Topical Studies in Oceanography 57:1406-1417

Billett DSM, Bett BJ, Rice AL, Thurston MH, Galéron J, Sibuet M, Wolff GA (2001) Long-term change in the megabenthos of the Porcupine Abyssal Plain (NE Atlantic). Progress in Oceanography 50:325-348

Billett DSM, Lampitt RS, Rice AL, Mantoura RFC (1983) Seasonal sedimentation of phytoplankton to the deep-sea benthos. Nature 302:520-522

Bizzarro JJ, Robinson HJ, Rinewalt CS, Ebert DA (2009) Comparative feeding ecology of four sympatric skate species off central California, USA. In: Ebert DA, Sulikowski JA (eds) Biology of Skates, Vol 27. Springer Netherlands, p 91-114

Boolootian RA, Giese AC, Tucker JS, Farmanfarmaian A (1959) A contribution to the biology of a deep sea Echinoid, *Allocentrotus fragilis* (Jackson). Biological Bulletin 116:362-372

Bradshaw C, Kumblad L, Fagrell A (2006) The use of tracers to evaluate the importance of bioturbation in remobilising contaminants in Baltic sediments. Estuarine, Coastal and Shelf Science 66:123-134

Burd BJ, Brinkhurst RO (1984) The distribution of the galatheid crab *Munida quadrispina* (Benedict 1902) in relation to oxygen concentrations in British Columbia fjords. Journal of Experimental Marine Biology and Ecology 81:1-20

Busby MS, Mier KL, Brodeur RD (2005) Habitat associations of demersal fishes and crabs in the Pribilof Islands region of the Bering Sea. Fisheries Research 75:15-28

Chiesa JJ, Araujo JF, Díez-Noguera A (2006) Method for studying behavioural activity patterns during long-term recordings using a force-plate actometer. Journal of Neuroscience Methods 158:157-168

Choy SL, O'Leary R, Mengersen K (2009) Elicitation by design in ecology: Using expert opinion to inform priors for Bayesian statistical models. Ecology 90:265-277

Cline DE, Edgington DR, Mariette J (2008) An automated visual event detection system for cabled observatory video. 3rd International Conference on Computer Vision Theory and Applications, Funchal, Madeira Portugal, p 22-28

Cohen Y (1978) Consumption of dissolved nitrous oxide in an anoxic basin, Saanich Inlet, British Columbia. Nature 272:235-237

Company JB, Sardà F (1998) Metabolic rates and energy content of deep-sea benthic decapod crustaceans in the western Mediterranean Sea. Deep Sea Research Part I: Oceanographic Research Papers 45:1861-1880

Costa C, Aguzzi J, Chiesa JJ, Magnifico G, Cascione D, Rimatori V, Caprioli R (2008) Evidences on the transient disruption of *Sabella spallanzanii* (Polychaeta, Sabellidae) fan activity rhythm in laboratory constant darkness. Italian Journal of Zoology 75:337 - 344

Craig CL, Ebert K (1994) Colour and pattern in predator–prey interactions: The bright body colours and patterns of a tropical orb-spinning spider attract flower-seeking prey. Functional Ecology 8:616-620

Dancette R (2008) La biodiversité et les imapcts de la recherche aux champs hydrothermaux Main Endeavour et Mothra de la zone de protection marine des Sources Hydrothermales d'Endeavour. Université du Québec à Montréal

Danovaro R, Dell'Anno A, Fabiano M, Pusceddu A, Tselepides A (2001) Deep-sea ecosystem response to climate changes: The eastern Mediterranean case study. Trends in Ecology & Evolution 16:505-510

Danovaro R, Dell'Anno A, Pusceddu A (2004) Biodiversity response to climate change in a warm deep sea. Ecology Letters 7:821-828

Davies AJ, Roberts JM, Hall-Spencer J (2007) Preserving deep-sea natural heritage: Emerging issues in offshore conservation and management. Biological Conservation 138:299-312

Delaney J, Heath GR, Chave A, Kirkham H and others (2000) NEPTUNE: Real-time, long-term ocean and earth studies at the scale of a tectonic plate. Oceanography 13:71-79

Delaney JR, Robigou V, McDuff RE, Tivey MK (1992) Geology of a vigorous hydrothermal system on the Endeavour Segment, Juan de Fuca Ridge. Journal of Geophysical Research 97:19663-19682

Dennis B (1996) Discussion: Should ecologists become Bayesians? Ecological Applications 6:1095-1103

Desbruyères D, Segonzac M, Bright M (2006) Handbook of deep-sea hydrothermal vent fauna, Denisia 18, Plouzané, France

Diaz RJ, Rosenberg R (1995) Marine benthic hypoxia: A review of its ecological effects and the behavioural responses of benthic macrofauna. In: Oceanography and marine biology - an annual review, Vol 33. UCL Press Ltd, London, p 245-303

Diaz RJ, Rosenberg R (2008) Spreading dead zones and consequences for marine ecosystems. Science 321:926-929

Ding K, Seyfried Jr WE, Tivey MK, Bradley AM (2001) *In situ* measurement of dissolved H_2 and H_2S in high-temperature hydrothermal vent fluids at the Main Endeavour Field, Juan de Fuca Ridge. Earth and Planetary Science Letters 186:417-425

Dover CV (2000) The ecology of deep-sea hydrothermal vents, Princeton University Press, Princeton , New Jersey

Drazen JC, Baldwin RJ, Smith Jr KL (1998) Sediment community response to a temporally varying food supply at an abyssal station in the NE pacific. Deep Sea Research Part II: Topical Studies in Oceanography 45:893-913

Dunlap JC, Loros JJ, DeCursey P (2004) Chronobiology: Biological timekeeping, Sinauer, Sunderland, MA

Dusenbery DB (1989) Ranging strategies. Journal of Theoretical Biology 136:309-316

Ellison AM (1996) An introduction to Bayesian inference for ecological research and environmental decision-making. Ecological Applications 6:1036-1046

Ellison AM (2004) Bayesian inference in ecology. Ecology Letters 7:509-520

Fernandéz de Miguel F, Aréchiga H (1994) Circadian locomotor activity and its entrainment by food in the crayfish *Procambarus clarkii*. Journal of Experimental Biology 190:9-21

Furrer R, Nychka D, Sain S (2010) Fields: Tools for spatial data, http://wwwimageucaredu/Software/Fields

Gargett AE, Stucchi D, Whitney F (2003) Physical processes associated with high primary production in Saanich Inlet, British Columbia. Estuarine, Coastal and Shelf Science 56:1141-1156

Gelman A, Carlin J, Stern H, Rubin D (1995) Bayesian data analysis, Chapman & Hall, London

Gerino M, Aller RC, Lee C, Cochran JK, Aller JY, Green MA, Hirschberg D (1998) Comparison of different tracers and methods used to quantify bioturbation during a spring bloom: 234-thorium, luminophores and chlorophyll a. Estuarine, Coastal and Shelf Science 46:531-547

Giese AC (1961) Further studies on *Allocentrotus fragilis*, a deep-sea Echinoid. Biological Bulletin 121:141-150

Gillibrand E, Bagley P, Jamieson A, Herring P and others (2007) Deep sea benthic bioluminescence at artificial food falls, 1,000–4,800 m depth, in the Porcupine Seabight and Abyssal Plain, North East Atlantic Ocean. Marine Biology 150:1053-1060

Girguis PR, Lee RW (2006) Thermal preference and tolerance of Alvinellids. Science 312:231

Glover AG, Smith CR (2003) The deep-sea floor ecosystem: Current status and prospects of anthropogenic change by the year 2025. Environmental Conservation 30:219-241

Gobi AF (2010) Towards generalized benthic species recognition and quantification using computer vision. 4th Pacific-Rim Symposium on Image and Video Technology (PSIVT), p 94-100

Gregory MR, Ballance PF, Gibson GW, Ayling AM (1979) On how some rays (Elasmobranchia) excavate feeding depressions by jetting water. Journal of Sedimentary Research 49:1125-1129

Grelon D, Morineaux M, Desrosiers G, Juniper SK (2006) Feeding and territorial behavior of *Paralvinella sulfincola*, a polychaete worm at deep-sea hydrothermal vents of the Northeast Pacific Ocean. Journal of Experimental Marine Biology and Ecology 329:174-186

Grundle DS, Timothy DA, Varela DE (2009) Variations of phytoplankton productivity and biomass over an annual cycle in Saanich Inlet, a British Columbia fjord. Continental Shelf Research 29:2257-2269

Hammond RD, Naylor E (1977) Effects of dusk and down on locomotor activity rhythms in the Norway lobster *Neprhops norvegicus*. Marine Biology 39:253-260

Herczeg G, Kovács T, Hettyey A, Merilä J (2003) To thermoconform or thermoregulate? An assessment of thermoregulation opportunities for the lizard *Zootoca vivipara* in the subarctic. Polar Biology 26:486-490

Herlinveaux RH (1962) Oceanography of Saanich Inlet in Vancouver island, British Columbia. Journal of the Fisheries Research Board of Canada 19:1-37

Herring PJ, Gaten E, Shelton PMJ (1999) Are vent shrimps blinded by science? Nature 398:116-116

Hollertz K, Duchêne J-C (2001) Burrowing behaviour and sediment reworking in the heart urchin; *Brissopsis lyrifera*, Forbes (Spatangoida). Marine Biology 139:951-957

Howard JD, Mayou TV, Heard RW (1977) Biogenic sedimentary structures formed by rays. Journal of Sedimentary Research 47:339-346

Huey RB, Slatkin M (1976) Cost and benefits of lizard thermoregulation. The Quarterly Review of Biology 51:363-384

Isern AR, Clark HL (2003) The Ocean Observatories Initiative: A continued presence for interactive ocean research. Marine Technology Society Journal 37:26-41

Jamieson AJ, Fujii T, Solan M, Matsumoto AK, Bagley PM, Priede IG (2009) First findings of decapod crustacea in the hadal zone. Deep Sea Research Part I: Oceanographic Research Papers 56:641-647

Jannasch HW, Mottl MJ (1985) Geomicrobiology of deep-sea hydrothermal vents. Science 229:717-725

Jeffreys RM, Lavaleye MSS, Bergman MJN, Duineveld GCA, Witbaard R (2011) Do abyssal scavengers use phytodetritus as a food resource? Video and biochemical evidence from the Atlantic and Mediterranean. Deep Sea Research Part I: Oceanographic Research Papers 58:415-428

Jones DOB (2009) Using existing industrial remotely operated vehicles for deep-sea science. Zoologica Scripta 38:41-47

Juniper SK, Brinkhurst RO (1986) Water-column dark CO_2 fixation and bacterial-mat growth in intermittently anoxic Saanich Inlet, British Columbia. Marine Ecology Progress Series 33:41-50

Kaufmann RS, Smith KL (1997) Activity patterns of mobile epibenthic megafauna at an abyssal site in the eastern North Pacific: Results from a 17-month time-lapse photographic study. Deep Sea Research Part I: Oceanographic Research Papers 44:559-579

Klemfuss H, Clopton P (1993) Seeking tau: a comparison of six methods. Journal of interdisciplinary cycle research 24:1–16

Kostylev, Erlandsson (2001) A fractal approach for detecting spatial hierarchy and structure on mussel beds. Marine Biology 139:497-506

Kronfeld-Schor N, Dayan T (2003) Partitioning of time as an ecological resource. Annual Review of Ecology, Evolution, and Systematics 34:153-181

Lampitt RS, Bett BJ, Kiriakoulakis K, Popova EE, Ragueneau O, Vangriesheim A, Wolff GA (2001) Material supply to the abyssal seafloor in the Northeast Atlantic. Progress in Oceanography 50:27-63

Lard M, Bäckman J, Yakovleva M, Danielsson B, Hansson L-A (2010) Tracking the small with the smallest: Using nanotechnology in tracking zooplankton. Plos One 5:e13516-e13516

Larkin K, Ruhl HA, Bagley P, Benn A and others (2010) Benthic biology time series in the deep sea: Indicators of change OceanObs'09

Lauerman LML, Kaufmann RS (1998) Deep-sea epibenthic echinoderms and a temporally varying food supply: Results from a one year time series in the N.E. Pacific. Deep Sea Research Part II: Topical Studies in Oceanography 45:817-842

Lee RW (2003) Thermal tolerances of deep-sea hydrothermal vent animals from the Northeast Pacific. The Biological Bulletin 205:98-101

Levesque C, Kim Juniper S, Limén H (2006) Spatial organization of food webs along habitat gradients at deep-sea hydrothermal vents on Axial Volcano, Northeast Pacific. Deep Sea Research Part I: Oceanographic Research Papers 53:726-739

Lohrer AM, Thrush SF, Gibbs MM (2004) Bioturbators enhance ecosystem function through complex biogeochemical interactions. Nature 431:1092-1095

Lohrer AM, Thrush SF, Hunt L, Hancock N, Lundquist C (2005) Rapid reworking of subtidal sediments by burrowing spatangoid urchins. Journal of Experimental Marine Biology and Ecology 321:155-169

Ludsin SA, Zhang X, Brandt SB, Roman MR, Boicourt WC, Mason DM, Costantini M (2009) Hypoxia-avoidance by planktivorous fish in Chesapeake Bay: Implications for food web interactions and fish recruitment. Journal of Experimental Marine Biology and Ecology 381:S121-S131

Maire O, Duchêne JC, Rosenberg R, Braga de Mendonça Jr. J, Grémare A (2006) Effects of food availability on sediment reworking in *Abra ovata* and *A nitida*. Marine Ecology Progress Series 319:135-153

Maire O, Lecroart P, Meysman F, Rosenberg R, Duchêne JC, Grémare A (2008) Quantification of sediment reworking rates in bioturbation research: A review. Aquatic Biology 2:219-238

Mandelbrot BB (1983) Fractal geometry of nature, W. H. Freeman, New York

Marques MD, Waterhouse J (2004) Rhythms and ecology - Do chronobiologists still remember nature? Biological Rhythm Research 35:1-2

Martinell J, de Gibert JM, Domenech R, Ekdale AA, Steen PP (2001) Cretaceous ray traces?: An alternative interpretation for the alleged dinosaur tracks of La Posa, Isona, NE Spain. Palaios 16:409-416

Masson DG (2001) Sedimentary processes shaping the eastern slope of the Faeroe-Shetland Channel. Continental Shelf Research 21:825-857

Matabos M, Aguzzi J, Robert K, Costa C, Menesatti P, Company JB, Juniper SK (2011a) Multi-parametric study of behavioural modulation in demersal decapods at the VENUS cabled observatory in Saanich Inlet, British Columbia, Canada. Journal of Experimental Marine Biology and Ecology 401:89-96

Matabos M, Dean C, Juniper K, Tunnicliffe V (2011b) A year of benthic community responses to fluctuating oxygen levels assessed through online observations Canadian Meteorological and Oceanographic Society, Victoria, Canada

Mermillod-Blondin F, Rosenberg R (2006) Ecosystem engineering: The impact of bioturbation on biogeochemical processes in marine and freshwater benthic habitats. Aquatic Sciences - Research Across Boundaries 68:434-442

Meysman FJR, Malyuga VS, Boudreau BP, Middelburg JJ (2008) Quantifying particle dispersal in aquatic sediments at short time scales: Model selection. Aquatic Biology 2:239-254

Meysman FJR, Middelburg JJ, Heip CHR (2006) Bioturbation: A fresh look at Darwin's last idea. Trends in Ecology & Evolution 21:688-695

Morgan E (2004) Ecological significance of biological clocks. Biological Rhythm Research 35:3-12

Myrick JL, Flessa KW (1996) Bioturbation rates in Bahia la Choya, Mexico. Ciencias Marinas 22:23-46

Nautilus Minerals Niugini (2008) Coffey Natural Systems environmental impact statement: Solwara 1 project, Brisbane, Australia

Naylor E (2005) Chronobiology: Implications for marine resource exploitation and management. Scientia Marina 69:157–167

Nelson DC, Castenholz RW (1982) Light responses of *Beggiatoa*. Archives of Microbiology 131:146-155

Nelson DC, Jorgensen BB, Revsbech NP (1986) Growth pattern and yield of a chemoautotrophic *Beggiatoa* sp. in oxygen-sulfide microgradients. Applied and Environmental Microbiology 52:225-233

Nevill AM, Teixeira LV, Marques MD, Waterhouse JM (2004) Using covariance to unravel the effects of meteorological factors and daily and seasonal rhythms. Biological Rhythm Research 35:159-169

Norcross BL, Mueter F-J (1999) The use of an ROV in the study of juvenile flatfish. Fisheries Research 39:241-251

Norris JG, Wyllie-Echeverria S, Mumford T, Bailey A, Turner T (1997) Estimating basal area coverage of subtidal seagrass beds using underwater videography. Aquatic Botany 58:269-287

Ogle K (2009) Hierarchical Bayesian statistics: Merging experimental and modeling approaches in ecology. Ecological Applications 19:577-581

Oppelt AL, Kurth W, Godbold DL (2001) Topology, scaling relations and Leonardo's rule in root systems from African tree species. Tree Physiology 21:117-128

Ott E (1993) Chaos in dynamical systems, Cambridge University Press, UK

Patterson TA, Basson M, Bravington MV, Gunn JS (2009) Classifying movement behaviour in relation to environmental conditions using hidden Markov models. Journal of Animal Ecology 78:1113-1123

Pettibone MH (1988) New species and new records of scaled Polychaetes (Polychaeta: Polynoidae) from hydrothermal vents of the Northeast Pacific Explorer and Juan De Fuca Ridges. Proceedings of the Biological Society of Washington 101:192-208

Pierson JJ, Roman MR, Kimmel DG, Boicourt WC, Zhang X (2009) Quantifying changes in the vertical distribution of mesozooplankton in response to hypoxic bottom waters. Journal of Experimental Marine Biology and Ecology 381:S74-S79

Priede IG, Solan M, Mienert J, Person R and others (2004) ESONET - European Sea Floor Observatory Network. Oceans '04 MTS/IEEE Techno-Ocean '04, p 2155-2163 Vol.2154

Purser A, Bergmann M, Lundalv T, Ontrup J, Nattkemper TW (2009) Use of machine-learning algorithms for the automated detection of cold-water coral habitats: A pilot study. Marine Ecology Progress Series 397:241-251

Raymond E, Widder E (2007) Behavioral responses of two deep-sea fish species to red, far-red, and white light. Marine Ecology Progress Series 350:291-298

Raymond EH (2008) Unobtrusive observations in the deep sea. The Johns Hopkins University

Rhoads DC, Boyer LF (1982) The effect of marine benthos on physical properties of sediment: A successional perspective. In: McCall PL, Tevesz MJS (eds) Animal-sediment relations. Plenum Press, New York, p 3-52

Rinke C, Lee RW (2009) Macro camera temperature logger array for deep-sea hydrothermal vent and benthic studies. Limnology and Oceanography: Methods 7:527-534

Robert K, Matabos M, Sarrazin J, Sarradin PM, Lee RW, Juniper K (2010) Cameras on the NEPTUNE Canada seafloor observatory: Towards monitoring hydrothermal vent ecosystem dynamics American Geophysical Union, Fall Meeting 2010, San Francisco

Rona PA, Klinkhammer G, Nelsen TA, Trefry JH, Elderfield H (1986) Black smokers, massive sulphides and vent biota at the Mid-Atlantic Ridge. Nature 321:33-37

Rowe GT, Sibuet M, Vangriesheim A (1986) Domains of occupation of abyssal scavengers inferred from baited cameras and traps on the Demerara Abyssal Plain. Deep Sea Research Part A Oceanographic Research Papers 33:501-522

Ruhl HA, Smith KL, Jr. (2004) Shifts in deep-sea Community structure linked to climate and food supply. Science 305:513-515

Salazar MH (1970) Phototaxis in the deep-sea urchin *Allocentrotus fragilis* (Jackson). Journal of Experimental Marine Biology and Ecology 5:254-264

Sarrazin J, Blandin J, Delauney L, Dentrecolas S and others (2007) TEMPO: A new ecological module for studying deep-sea community dynamics at hydrothermal vents Oceans '07 IEEE, Aberdeen

Sarrazin J, Juniper SK, Massoth G, Legendre P (1999) Physical and chemical factors influencing species distributions on hydrothermal sulfide edifices of the Juan de Fuca Ridge, northeast Pacific. Marine Ecology Progress Series 190:89-112

Sarrazin J, Levesque C, Juniper SK, Tivey M (2002) Mosaic community dynamics on Juan de Fuca Ridge sulphide edifices: Substratum, temperature and implications for trophic structure. Cahiers de Biologie Marine 43:275-279

Sarrazin J, Robigou V, Juniper S, Delaney J (1997) Biological and geological dynamics over four years on a high-temperature sulfide structure at the Juan de Fuca Ridge hydrothermal observatory. Marine Ecology Progress Series 153:5-24

Saunders DS (2002) Insect clocks, Elsevier Science BV, London, Amsterdam

Schurmann H, Claireaux G, Chartois H (1998) Change in vertical distribution of sea bass (*Dicentrarchus labrax* L.) during a hypoxic episode. Hydrobiologia 371-372:207-213

Service RF (2007) Oceanography's third wave. Science 318:1056-1058

Sherman AD, Smith KL (2009) Deep-sea benthic boundary layer communities and food supply: A long-term monitoring strategy. Deep Sea Research Part II: Topical Studies in Oceanography 56:1754-1762

Smith CR, Jumars PA, DeMaster DJ (1986) *In situ* studies of megafaunal mounds indicate rapid sediment turnover and community response at the deep-sea floor. Nature 323:251-253

Smith CR, Pope RH, DeMaster DJ, Magaard L (1993a) Age-dependent mixing of deep-sea sediments. Geochimica et Cosmochimica Acta 57:1473-1488

Smith KL, Kaufmann RS (1999) Long-term discrepancy between food supply and demand in the deep Eastern North Pacific. Science 284:1174-1177

Smith KL, Kaufmann RS, Baldwin RJ, Carlucci AF (2001) Pelagic-benthic coupling in the abyssal eastern North Pacific : An 8-year time series study of food supply and demand. 46:543-556

Smith KL, Kaufmann RS, Wakefield WW (1993b) Mobile megafaunal activity monitored with a time-lapse camera in the abyssal North Pacific. Deep Sea Research Part I: Oceanographic Research Papers 40:2307-2324

Smith KL, Ruhl HA, Bett BJ, Billett DSM, Lampitt RS, Kaufmann RS (2009) Climate, carbon cycling, and deep-ocean ecosystems. Proceedings of the National Academy of Sciences 106:19211-19218

Smith KL, Ruhl HA, Kaufmann RS, Kahru M (2008) Tracing abyssal food supply back to upper-ocean processes over a 17-year time series in the Northeast Pacific. Limnology and Oceanography 53:13

Snelgrove PVR (1999) Getting to the bottom of marine biodiversity: Sedimentary habitats: Ocean bottoms are the most widespread habitat on Earth and support high biodiversity and key ecosystem services. BioScience 49:129-138

Solan M, Germano JD, Rhoads DC, Smith C and others (2003) Towards a greater understanding of pattern, scale and process in marine benthic systems: A picture is worth a thousand worms. Journal of Experimental Marine Biology and Ecology 285-286:313-338

Solan M, Kennedy R (2002) Observation and quantification of *in situ* animal-sediment relations using time-lapse sediment profile imagery (t-SPI). Marine Ecology Progress Series 228:179-191

Solan M, Wigham BD, Hudson IR, Kennedy R and others (2004) *In situ* quantification of bioturbation using time lapse fluorescent sediment profile imaging (f SPI), luminophore tracers and model simulation. Marine Ecology Progress Series 271:1-12

Stoner AW, Spencer ML, Ryer CH (2007) Flatfish-habitat associations in Alaska nursery grounds: Use of continuous video records for multi-scale spatial analysis. Journal of Sea Research 57:137-150

Stuurman N (2003) MTrack2, http://valelabucsfedu/~nico/IJplugins/MTrack2html

Szewczyk R, Osterweil E, Polastre J, Hamilton M, Mainwaring A, Estrin D (2004) Habitat monitoring with sensor networks. Communications of the ACM 47:34-40

Taylor R, Vine N, York A, Lerner S and others (2008) Evolution of a benthic imaging system from a towed camera to an automated habitat characterization system Oceans '08 IEEE, p 1-7

Teal LR, Bulling MT, Parker ER, Solan M (2008) Global patterns of bioturbation intensity and mixed depth of marine soft sediments. Aquatic Biology 2:207-218

Thrush SF, Pridmore RD, Hewitt JE, Cummings VJ (1991) Impact of ray feeding disturbances on sandflat macrobenthos: Do communities dominated by polychaetes or shellfish respond differently? Marine Ecology Progress Series 69:245-252

Timothy DA, Soon MYS (2001) Primary production and deep-water oxygen content of two British Columbian fjords. Marine Chemistry 73:37-51

Tivey MK, Bradley AM, Joyce TM, Kadko D (2002) Insights into tide-related variability at seafloor hydrothermal vents from time series temperature measurements. Earth and Planetary Science Letters 202:693-707

Tunnicliffe V, Dewey R, Smith D (2003) Research plans for a mid-depth cabled seafloor observatory in Western Canada. Oceanography 16:53-59

Turchin P (1998) Quantitative analysis of movement: Measuring and modeling population redistribution in animals and plants, Sinauer Associates Inc, Sunderland, MA

Van Dover CL (2011) Tighten regulations on deep-sea mining. Nature 470:31-33

Wakefield WW, Genin A (1987) The use of a Canadian (perspective) grid in deep-sea photography. Deep Sea Research Part A Oceanographic Research Papers 34:469-478

Walsh JJ, Watterson J (1993) Fractal analysis of fracture patterns using the standard box-counting technique: valid and invalid methodologies. Journal of Structural Geology 15:1509-1512

Walther D, Edgington DR, Koch C (2004) Detection and tracking of objects in underwater video. IEEE Computer Society Conference on Computer Vision and Pattern Recognition (CVPR), p I544-I549

Walther D, Edgington DR, Salamy KA, Risi M, Sherlock RE, Koch C (2003) Automated video analysis for oceanographic research. IEEE Computer Society Conference on Computer Vision and Pattern Recognition (CVPR), Madison, WI

Wicksten MK (1990) Key to the hippolytid shrimp of the eastern Pacfic ocean. Fishery Bulletin 88:587-598

Widder EA, Robison BH, Reisenbichler KR, Haddock SHD (2005) Using red light for *in situ* observations of deep-sea fishes. Deep Sea Research Part I: Oceanographic Research Papers 52:2077-2085

Witte U (1999) Consumption of large carcasses by scavenger assemblages in the deep Arabian Sea: Observations by baited camera. Marine Ecology Progress Series 183:139-147

Yahel G, Yahel R, Katz T, Lazar B, Herut B, Tunnicliffe V (2008) Fish activity: A major mechanism for sediment resuspension and organic matter remineralization in coastal marine sediments. Marine Ecology Progress Series 372:195-209

Zimmermann M (2006) Benthic fish and invertebrate assemblages within the National Marine Fisheries Service US west coast triennial bottom trawl survey. Continental Shelf Research 26:1005-1027

Appendix A
NEPTUNE Canada case study of observational approaches

Contribution to *Chapter 14: Seafloor observatories*

Matabos, M.[1*], Best, M.M.R.[1, 2], Blandin, J.[3], Hoeberechts, M.[1], Juniper, S.K.[2, 4], Pirenne, B.[1], Robert, K.[4], Ruhl, H.A.[5],Sarrazin, J.[6], and Vardaro, M.F.[7]

[1]NEPTUNE Canada, University of Victoria, PO Box 1700 STN CSC, Victoria, BC V8W 2Y2 Canada

[2] School of Earth and Ocean Sciences, University of Victoria, PO Box 3065 STN CSC, Vic, B.C. V8W 3V6, Canada

[3] Institut Français de Recherche pour l'Exploitation de la MER, Département Recherches et Développements Technologiques, BP 70 - 29280 Plouzané, France

[4] Department of Biology, University of Victoria, University of Victoria, PO Box 3020 STN CSC, Vic, B.C. V8W 3N5, Canada

[5] National Oceanography Centre, University of Southampton Waterfront Campus, European Way, Southampton SO14 3ZH, United Kingdom

[6]Institut Français de Recherche pour l'Exploitation de la MER, Département Etudes des Ecosystèmes Profonds, BP70, F-29280 Plouzané, France

[7]College of Oceanic and Atmospheric Sciences, Oregon State University, Corvallis, OR 97331-5503, USA

In *Biological sampling in the deepsea*

Mireille Consalvey and Malcolm Clark (Editors)
Wiley-Blackwell

*Corresponding author: mmatabos@uvic.ca
NEPTUNE Canada
University of Victoria
PO Box 1700 STN CSC
Victoria, BC V8W 2Y2 Canada
Tel: (+1) 250 472 5089
Fax: (+1) 250 472 5370

Abstract

While the deep sea covers approximately 60% of the Earth's surface, much of what we know about the ocean is the result of ship-based expeditionary science whose origins date back to the late 19th century leading to a really fragmented and limited knowledge of our oceans. In consequence, the idea of deploying instruments on the seafloor for a long period is not new and has been already developed since the early 80s (e.g. landers, moorings, time-lapse cameras) even though those systems had limited power autonomy, local data storage and a very limited set of sensors. In parallel, the idea of seafloor observatories grew fast in the scientific community. Seafloor observatories offer Earth and Ocean scientists unique new opportunities to study multiple, interrelated processes over time scales ranging from seconds to decades and to conduct comparative studies of regional processes. The Earth and its oceans are dynamic at many temporal and spatial scales. As such, the significant advantage that observatories have over traditional sampling methods lies in their enabling long-term interdisciplinary monitoring of ocean processes where researchers from diverse fields combine their efforts to understand ecosystem functioning and ecosystem changes in a comprehensive manner. The first 'observatories' started in the 1950's with the Sound Surveillance System (SOSUS), developed by the U.S. Navy to follow Soviet submarines using hydrophone arrays connected by a submarine cable off the coast of Washington State. Quickly observatories designed for seismic surveys in active regions were developed (DONET-Japan). More recently integrated observatories to conduct research across multiple disciplines form geophysics to biology were deployed on the North American Pacific coast (MARS - US, VENUS and NEPTUNE Canada – Canada). However, cabled

observatories are emerging technologies, and scientists are still on a learning curve in terms of engineering, technology development and research methodologies.

This chapter gives insight on the existing observatories, not only in terms of organization, implementation, and technology but most importantly on how they can be used to conduct biology and ecology in the deep-sea. The two first sections give an introduction and strategy plans for seafloor observatories design. The third section details cabled observatories with some study cases from two cabled observatories: VENUS and NEPTUNE Canada. The fourth section is devoted to the diversity of autonomous observatories on the example of the European setting, and provides an overlook of the various observatories in place and the diversity of research areas offered. Finally the fifth section gives an overview on data management and archiving, and the sixth section depicts the importance and potential for outreach and education using online tools.

Chapter Content

* Contributions

Introduction

Cabled observatories provide a new and unique laboratory for studies of benthic processes. Monitoring of the benthic fauna provides a tool for documenting how individual species and benthic communities respond to environmental variability, which is essential for understanding how they will be affected by global ocean change (Larkin et al. 2010). Methodological approaches to the study of such questions are currently being developed (Robert et al. 2010, Matabos et al. 2011a) and will help optimize the use of the unique capabilities offered by cabled observatories, particularly high resolution sampling, long-term monitoring, real-time event detection and interactive observing. The following approaches and results exemplify work currently underway using the remotely operated camera systems installed at the Barkley Canyon site of the NEPTUNE Canada regional network, West Coast of Canada.

At Barkley Canyon, the locations of four different instrument pods were determined by the requirements of a multidisciplinary project involving ecologists, physical oceanographers and geologists. The deployed instruments include a sediment trap, plankton pump, ADCPs, CTDs, cameras, hydrophones and high resolution sonars. This setting provides opportunities to study the responses of benthic communities to variations in organic input from the daily to inter-annual and even decadal scales, and to distinguish input from the surface from organic matter advected through the canyon. The sonars allow the study of seafloor bed from dynamics related to benthic faunal activity or transport processes within Barkley Canyon (upwelling and downwelling currents, slumps, slides, gravity flows).

Site Selection

An important first step in the deployment of camera systems is site selection, which should be based on prior knowledge of the study area. Site selection can also be constrained by technical considerations. The deployment of the mid-canyon instrument pods in Barkley Canyon illustrates the various technical and ecological trade-offs that need to be taken into account when selecting sites for seafloor cameras. The initial experimental design required that all instrument pod locations be representative of major physical habitat types in Barkley Canyon, rather than any special localized phenomena such as the gas hydrate field in the mid-canyon area. The presence of the hydrate field posed a special problem for placement of the mid-canyon instrument pods. Logistic requirements of hydrate-focused experiments and a need to minimize the complexity and cost of the mid-canyon deployment meant that the mid-canyon instrument pods had to connect to a junction box in the hydrate field. Since cable length from junction boxes is limited by data and power transmission constraints, the mid-canyon pods could be no more than a few hundred metres away from the 870 m deep hydrate field, on the same plateau that hosted the hydrates. Yet the experimental design required the mid-canyon pods to be placed in an area that was representative of the mid-canyon ecosystem and not a marginal area of the hydrate field. A pre-deployment ROV video survey was analyzed to determine the limits to the influence of the hydrate field, in terms of the composition of the benthic megafauna. Megabenthic organisms were identified to the lowest taxonomic unit and their position on the seafloor was georeferenced and mapped.

With the exception of a field of vesicomyid clams and shell debris in the vicinity of the exposed hydrates, no further effect of the hydrate field was observed on megabenthic species composition. On the other hand, deep-water corals and tanner crabs

occurred predominantly near the edge of the plateau (Figure 22) where water currents likely differed from the inside of the plateau. With this knowledge in mind and within the physical limitations of the cable length, the mid-canyon instrument pods were deployed away from the edge of the plateau.

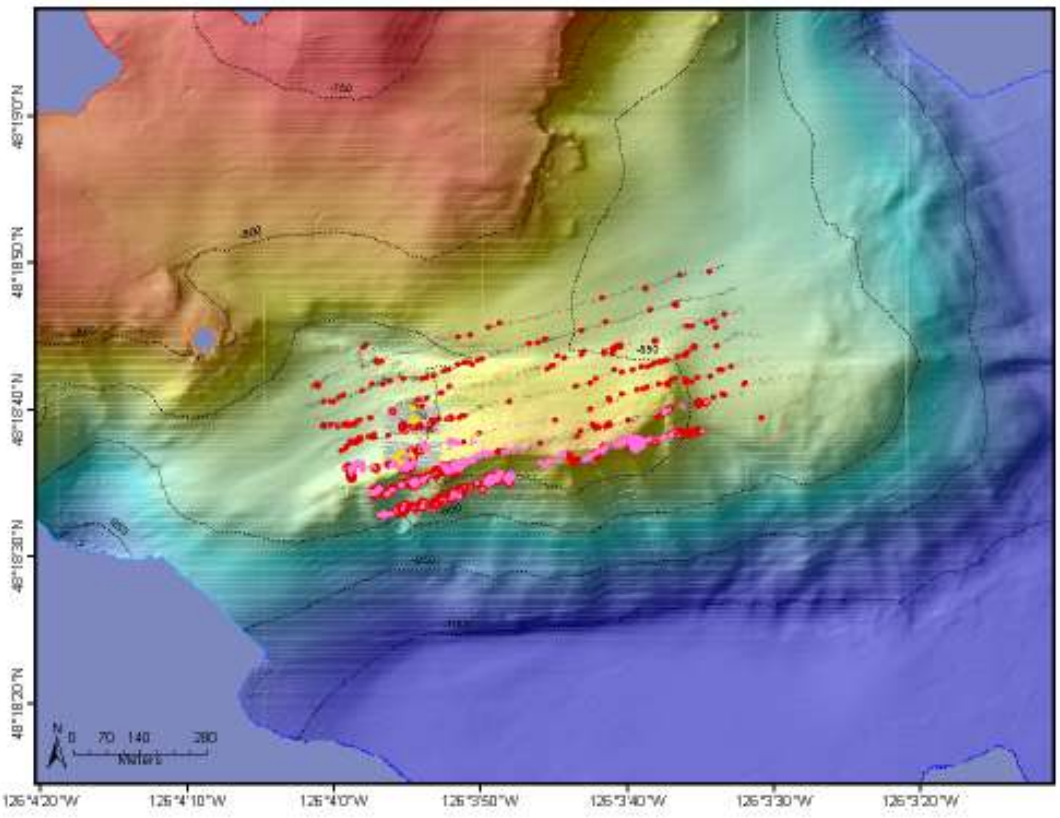

Figure 22: Distribution of tanner crabs (red) and deep-water corals (pink) along the edge of the plateau at the Mid-Canyon site in Barkley Canyon. Bathymetric layer provided by Monterey Bay Aquarium Research Institute 2006.

Deep-sea Bioturbation

One of the camera-equipped instrument pods was deployed at a 400 m depth location on the outer continental shelf away from the edge of Barkley Canyon. This camera was used to develop methods for the study of bioturbation by the benthic megafauna. The continuous power supply provided by the cabled observatory meant that

it was theoretically possible to record seafloor imagery without interruption, 24 hours a day. However, the manual analysis of such a large quantity of video would be impossibly time-consuming. In addition, the impact of the artificial lighting required for making observations in aphotic environments has not been well documented. As a precautionary approach, one hour of lighting was allotted per day. We therefore undertook to develop observational protocols that would make optimal use of the 60 min per day of observation, to quantify the activities of the two main groups of bioturbating megafaunal organisms found at this site, sea urchins and flatfish. Below we describe the approach used for the sea urchins.

An iterative method was employed to determine the observation frequency best suited to estimate each of the parameters of interest: bioturbation footprint of individual sea urchins, sea urchin abundance, and movement rates. During initial hour-long observation periods, it became apparent that echinoderm movements could rarely be observed. Infrequently, high bursts of activity were recorded, but were not representative of sustained movement rates. Increasing to two, 30-min observation periods yielded a higher number of sightings, but organisms usually resided for less than 12 hrs within the field of view (FOV). In order to take maximum advantage of the increased FOV provided by the pan and tilt mechanisms, the camera was swept almost 360° at specific tilt angles to cover the seafloor from the horizon to the Nadir point. As these sweeps took 5 min, the sampling rate could be increased to a maximum of 12 times daily and still remain within the lighting time limit. At this observation frequency, the locomotory path of individual sea urchins could be tracked and measured.

The extraction of quantitative information from the imagery involved the use of laser pointers and scaling rulers to build perspective grids (see Wakefield & Genin (1987) as well as a polar coordinate system to track organisms across the FOV. The laser points, set 10 cm apart, provided a horizontal scale for all tilt angles and were used to trace meridian lines for the perspective grid. To draw the horizontal lines, a ruler marked at 10 cm intervals, laid beneath the camera, provided the vertical scale. With this information, we were able to build perspective grids (Figure 23 A) without knowing the exact height of the camera from the seafloor. This normally required information could not be obtained in the current situation because the platform's feet sank to unknown depths within the sediments. Positions of organisms within the FOV were mapped using a polar coordinate system based on the pan and tilt angles of the camera (Figure 23 B).

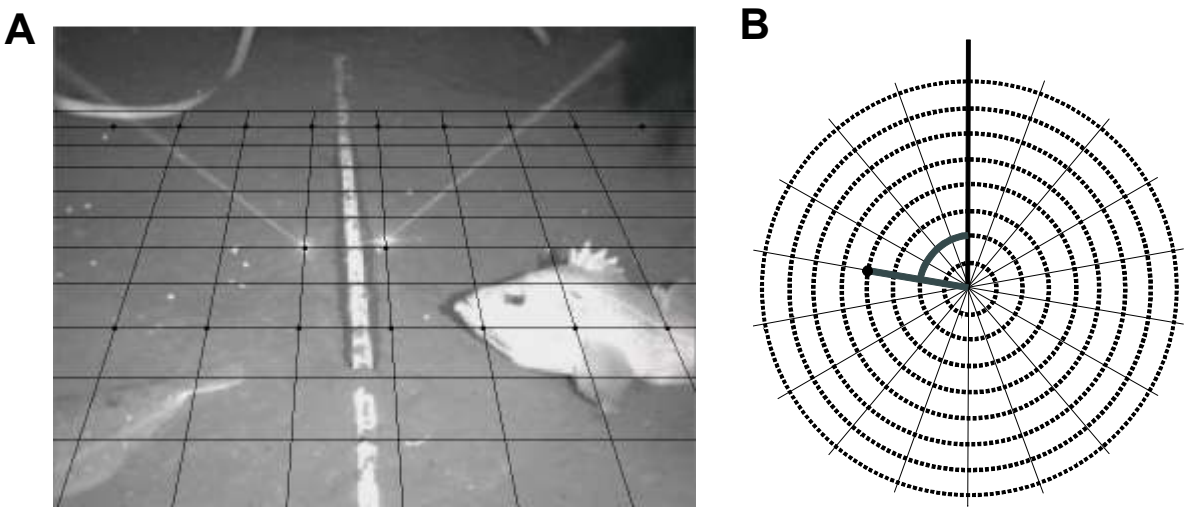

Figure 23: A) Perspective grid built with the help of the scaling ruler and the two laser beams and overlain over an extracted video frame. B) Polar coordinate system representing the field of view of the camera.

Once a protocol for bioturbation monitoring has been implemented, it is possible to document temporal variations over long time scales. Information from other sensors may be useful in relating bioturbation rates to environmental fluctuations. For example,

benthic processes are known to vary with respect to phytodetrital accumulations which follow surface water phytoplankton blooms (Bett et al. 2001, Smith et al. 2001). Such blooms are already being monitored through satellite imagery from which chlorophyll-a concentrations can be extracted.

For Barkley Canyon, for example, complementary information on surface chlorophyll levels was obtained through imagery from the SeaWiF satellite (Figure 24), and assembled using the Ocean Color Radiometry Online Visualization and Analysis tool from NASA's web-based GIOVANNI application developed by GES DISC (http://daac.gsfc.nasa.gov/giovanni/). Monthly averages in chlorophyll-a concentration are being compiled for the 600 km^2 area overlying Barkley Canyon and will eventually be compared to the monthly estimates of bioturbation rates currently being collected.

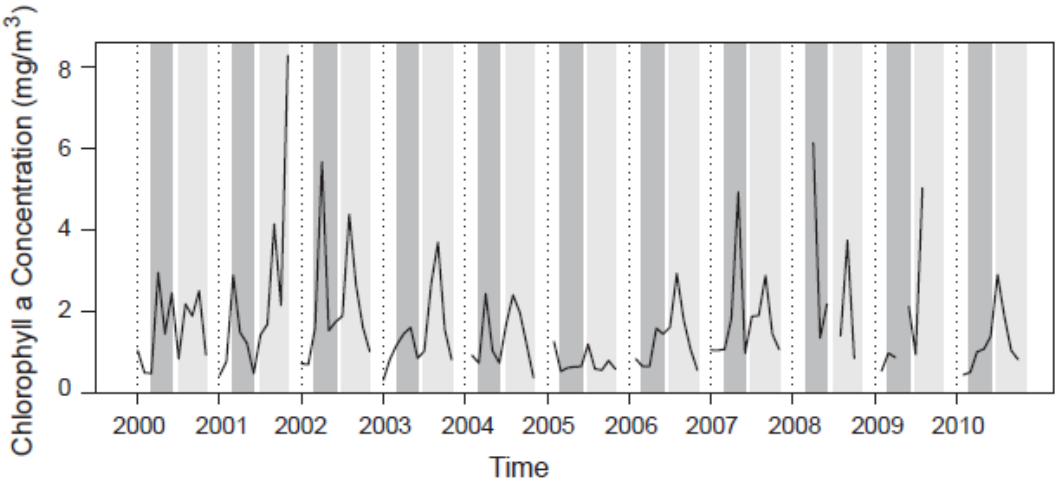

Figure 24: Historical trend in chlorophyll-a concentration for the last decade as obtained through ocean colour monitoring from the SeaWiF satellite. Dark grey bars represent April-May and light grey, August-September.

Establishment of a regular monitoring program greatly facilitates the observation of rare, unpredictable or episodic events whose significance may arise. This is where the

interactive capability of cabled observatories is particularly valuable. Once an event has been detected, observation protocols can be immediately modified to better capture the outcome of the event.

The arrival of phytodetrital accumulations has previously been observed *a posteriori* with time-lapse cameras (Billett et al. 1983). With the current NEPTUNE Canada system, such an occurrence would be detected in real-time and updates to the observation schedule could be implemented within hours. Even more sophisticated, co-located sensors such as fluorometers could be programmed to trigger an event response sampling protocol once chlorophyll levels surpass a predetermined threshold (Figure 25).

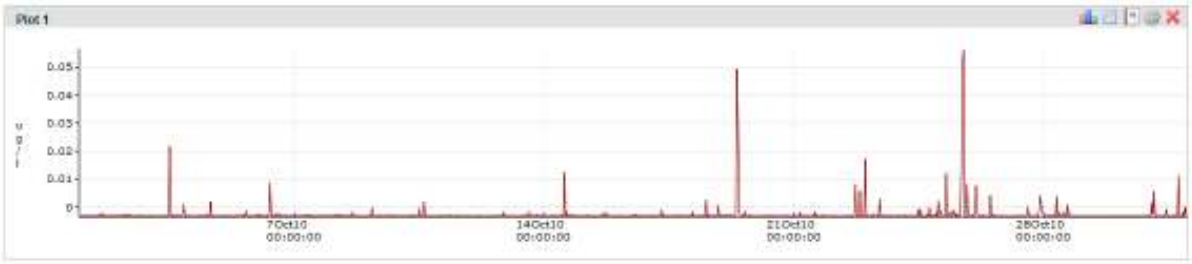

Figure 25: At-depth (871m) chlorophyll measurements as measured by the Seapoint Fluorometer 3125 and plotted using the utility developed by DMAS.

Appendix B
Thermoregulation in the hydrothermal vent sulphide worm: Behavioural response to extreme temperature variability

Bates, A.E. [1*], Robert, K.[2], Onthank, K.L.[3], Quinn, G.[1], Juniper, S.K.[2] and Lee, R.W.[3]

[1] School of Life and Environmental Sciences, Deakin University, P.O. Box 423, Warrnambool, 3280, Australia

[2] Department of Biology, University of Victoria, PO Box 3020 STN CSC, Victoria, B.C., V8W 3N5, Canada

[3] School of Biological Sciences, Washington State University, Pullman, Washington, 99164-4236, USA

Submitted to Marine Ecology Progress Series, May 2011

*Corresponding Author: bates.amanda@gmail.com
Deakin University
School of Life and Environmental Sciences
PO Box 423
Princes Highway
Warrnambool, Victoria 3280
Australia
61 +3 5563 3021

Abstract

Genotypes adapted to high versus low temperatures can have relatively higher performance (e.g., activity, growth, fitness) because biochemical reaction rates increase with temperature, selecting for warm-adapted genotypes. However, environmental variability also selects for broader biochemical adaptation within a species, which in turn can compensate for thermodynamic effects on performance. Here, we questioned whether the highly heat tolerant hydrothermal vent worm, *Paralvinella sulfincola*, is a thermal specialist. We first confirmed that the critical thermal maximum of this species falls within 55-66 ºC using a heating experiment executed remotely on the seafloor. We then tested whether extreme thermotolerance in *P. sulfincola* corresponds with specialization of activity to warm temperatures. We predicted, if warmer habitats within the range of temperatures preferred by this worm are selectively advantageous, that individuals would adjust their position to exploit available thermal gradients to achieve relatively warm body temperatures. Our results indicate that *P. sulfincola* is remarkably eurythermal with a thermal breadth exceeding 40 ºC. Even so, in contrast to our predictions, worms did not select the warmest fluids, although the temperatures of these fluids were well within the worm's preferred range. Instead, in localities with the greatest temperature variability, worms positioned their brachial tentacles to minimize their experienced temperature variability. The sulphide worm appears to be the first species from a subtidal habitat to use postural adjustments as a thermoregulatory mechanism, presumably a response to the extreme temporal and spatial variability of hydrothermal vent habitats. Our results highlight the role that abiotic variability plays in limiting the distributions of fauna in hydrothermal vent habitats and in selecting for broader adaptation to temperature in animals.

Contributions

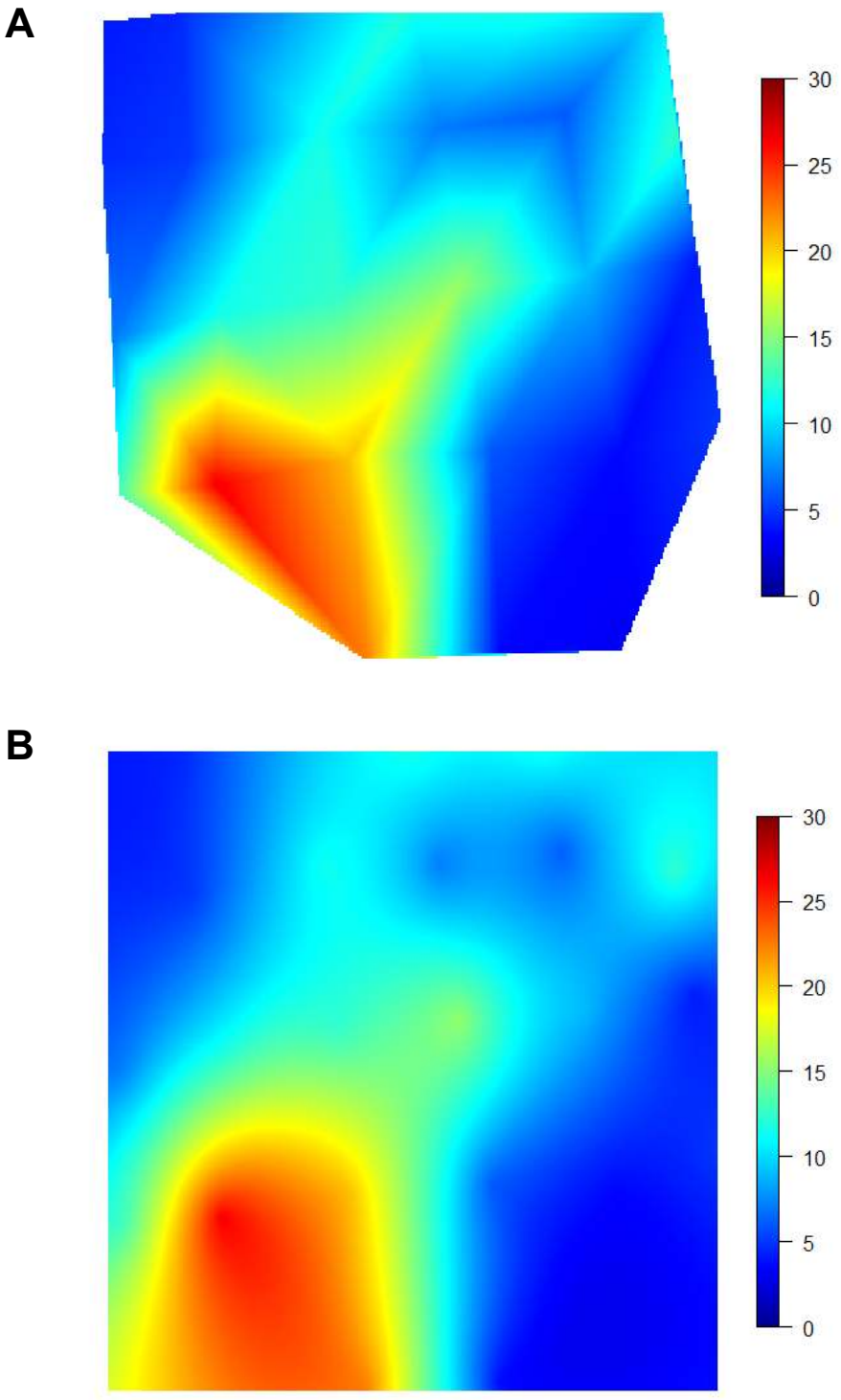

Figure 26: Comparison of temperature maps obtained using two interpolation techniques; A) linear and B) ordinary kriging.

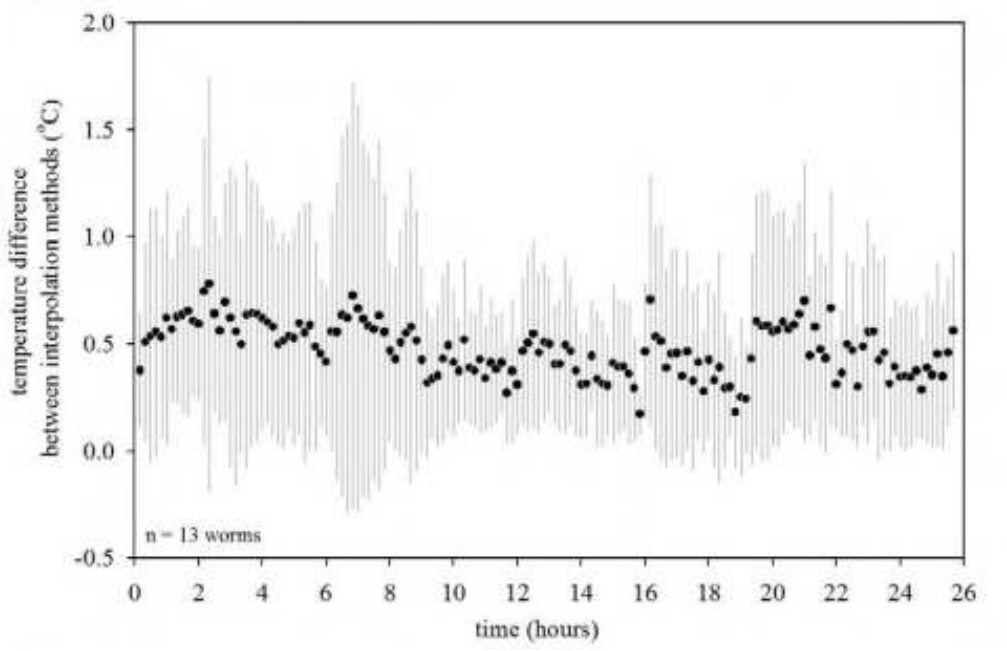

Figure 27: Mean (± 1SD) temperature difference between predictions made by simple linear and ordinary kriging spatial interpolation methods at the tube opening positions (n = 13 worms) for each observation period.

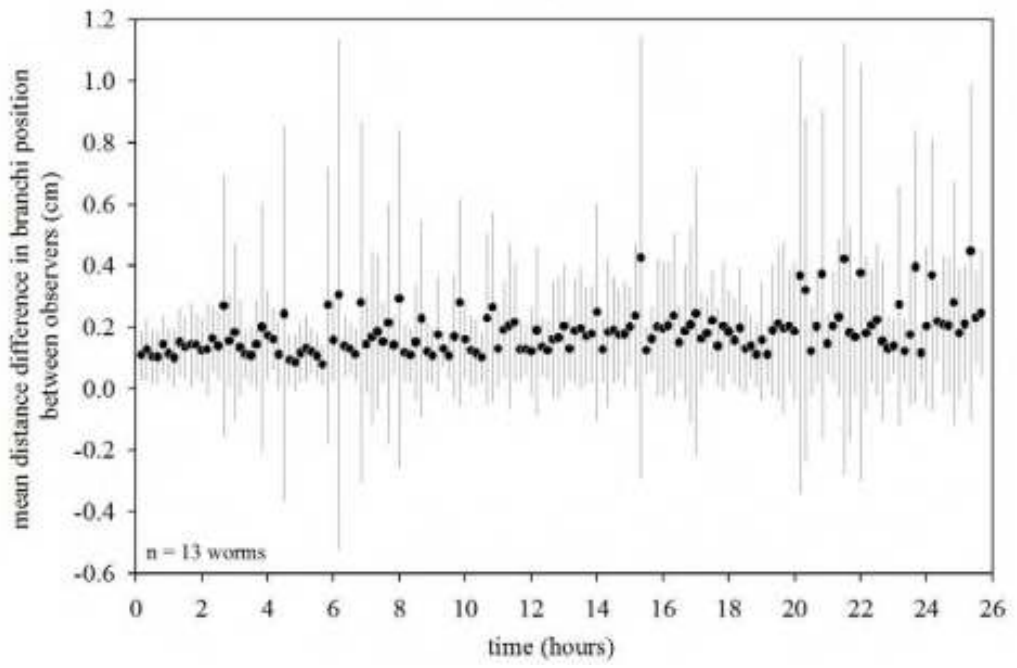

Figure 28: Mean (± 1SD) distance differences returned for two independent observers of worm branchi positions over time.

Table 7: Temperature (ºC) that each worm was observed displaying each of three behavioural categories (see below) for 154 observations made at 10 min intervals over 25 hrs, pooled and averaged for each category. Sample size is reported in brackets beside each mean temperature value.

	Behavioural Category		
Worm#	**1**	**2**	**3**
1	5.33 (24)	5.04 (87)	4.78 (43)
2	7.66 (2)	8.51 (112)	11.23 (40)
3	7.51 (10)	10.91 (70)	9.45 (74)
4	8.82 (13)	8.69 (112)	9.26 (29)
5	n/a (0)	10.60 (45)	9.74 (109)
6	8.75 (28)	8.23 (85)	8.51 (41)
7	12.06 (9)	10.92 (96)	10.21 (49)
8	6.39 (15)	6.56 (114)	6.85 (25)
9	3.82 (7)	4.28 (128)	4.44 (19)
10	7.63 (10)	7.49 (89)	8.41 (55)
11	10.34 (14)	8.96 (124)	9.85 (16)
12	12.76 (18)	9.85 (101)	10.51 (35)
13	9.81 (57)	9.78 (97)	n/a (0)

Behavioural categories assigned on an image-by-image basis for each specimen based on whether the worm, its branchi and/or body were visible;

1) Worm located entirely within its tube (tube maintenance)
2) Worm branchi visible at the tube opening (resting)
3) Worm branchi and body extended (foraging)

(Grelon et al. 2006)

Appendix C
Short methodological note on the positioning of the VENUS remotely operated camera tripod in Saanich Inlet

Introduction

A remotely operated camera tripod connected to the VENUS (Victoria Experimental Network Under the Sea, 2006) cabled observatory was deployed in Saanich Inlet, a fjord on southern Vancouver Island. This cabled observatory made it possible to carry real-time *in situ* monitoring of benthic megafauna and obtain data streams of nearby sensors measuring the physical proprieties of the surrounding environment (Tunnicliffe et al. 2003). This fjord is particularly well suited to the study of megabenthic responses to environmental variability because it undergoes natural hypoxic cycles due to the presence of a sill near its entry which isolates the deeper waters from adjacent water masses (Anderson & Devol 1973). Resulting changes in megabenthic community composition and bacterial mat growth have been described (Juniper & Brinkhurst 1986). To determine the depth at which the camera tripod should be deployed in order to observe maximal community change and bacterial mat growth, we examined within and between year variations in species distribution and bacterial mat substratum cover using video surveys acquired via remotely operated vehicle (ROV). Optimal positioning of the camera tripod was also constrained by the location of the seafloor node that provided power and communications to the camera and fixed lengths of cable connecting the camera to the node via the intermediate 'camera platform'.

Methods

Video transects recorded using a front-mounted camera on the ROV ROPOS (Figure 29) were analyzed for the distribution of the three most common megabenthic subgroups observed; small flatfishes, (English, *Parophrys vetulus*, Rock, *Lepidopsetta* sp., and Slender Sole, *Lyopsetta exilis*), squat lobsters (*Munida quadrispina*) and small pelagic fishes (Pacific Herring, *Clupea pallasii* and Walleye Pollock, *Theragra chalcogramma*) (Yahel et al. 2008). The position of individuals belonging to each subgrouping was georeferenced by coupling the time-stamped video to the ROV's navigation system which recorded coordinates and depth for every second. Two laser beams separated by 10 cm were used for scaling of the collected imagery.

The video transects analyzed were conducted as part of the VENUS cabled observatory maintenance cruises from 2005 to 2009 (Table 8). Except for Dive R-1035, these generally covered overlapping area of the seafloor, starting deeper within the Saanich Inlet channel and steadily moving upslope. Whenever possible, transects were carried twice a year, once during the oxic state and once under the hypoxic state (see Matabos et al. (2011a), Chapter 4, for a more complete description).

Table 8: Summary of the ROPOS dives for which video transects were analyzed

Dive No.	Year	Month	State
R-902	2005	July	Hypoxic
R-948	2006	February	Oxic
R-986	2006	August	Hypoxic
R-1035	2007	February	Oxic
R-1101	2007	September	Hypoxic
R-1129	2008	February	Oxic
R-1176	2008	September	Hypoxic
R-1197	2009	February	Oxic

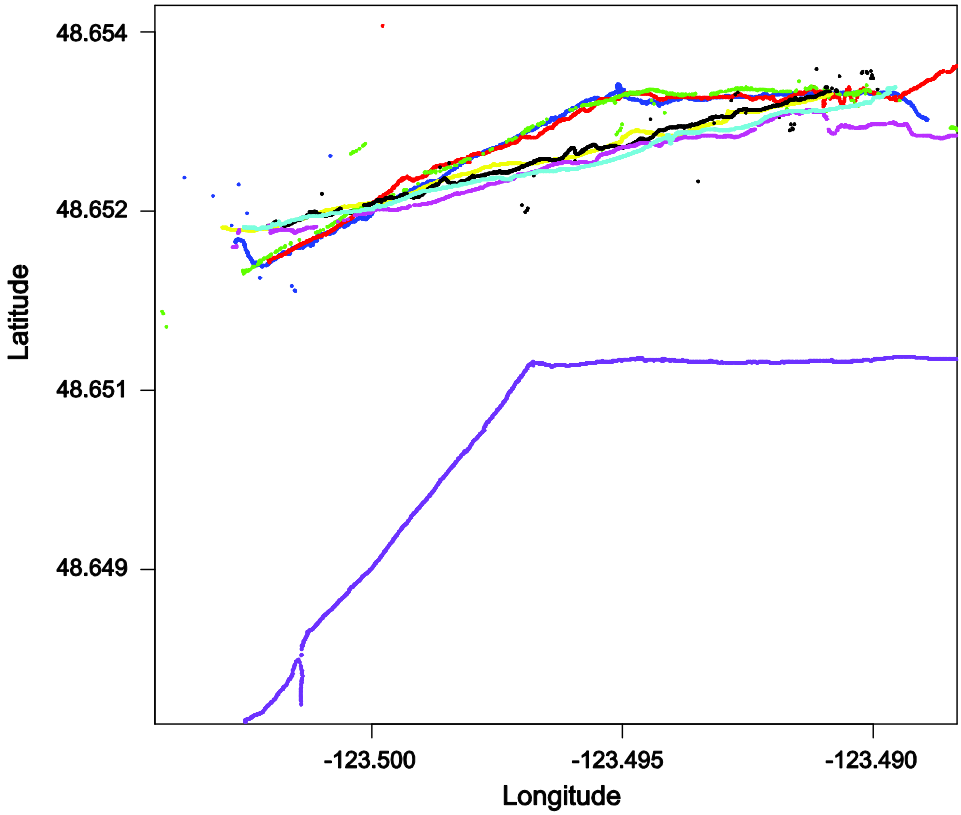

Figure 29: Location of the eight ROV video transects; R-902 (blue), R-948 (red), R-986 (green), R-1035 (purple), R-1101 (yellow), R-1129, (black), R-1176 (pink) and R-1197 (cyan).

Visibility varied along the transects and affected the likelihood of accurately detecting individual animals. We therefore recorded visibility over the length of each transect using a qualitative scale ranging from 0 to 3 (0 → Unable to see substratum, 1 → Substratum visible, but organisms unlikely to be detected, 2 → Organisms can be detected, but identification unreliable, 3 → Identification possible).

A qualitative index of 0 to 6 was also used to describe the substratum (0 → Old grey mat, 1→ Old grey mat, with discontinuous patches of new white mat, 2 → New white mat, with discontinuous patches of old grey mat, 3 → Old grey mat covered by

mostly continuous new white mat, 4 → Thick covering of new white mat, 5 → Sediments covered by a light sheet of new white mat, 6→ Sediments only).

Results

Small flatfishes were generally occurred deeper along the transects than squat lobsters or small pelagic fishes. Dive R-1035 was an exception as a surprising number of pollock were observed at unexpected depths. Small flatfishes and squat lobsters tended to occur at deeper depths under hypoxic conditions, but the opposite trend was observed for pollock (Figure 30).

The depth at which the first individual of each subgroup was recorded varied between years and likely resulted from yearly variations in the strength of the hypoxic cycle. Time-series oxygen measurements from optodes located at the Central Node (97 m in depth) are reported in Figure 31. No clear depth pattern between oxic and hypoxic states was observed with respect to substratum cover (Figure 32). However, the same progression was observed across years; from substratum dominated by old mat or small patches of new mat at the deepest end, increasing in new mat coverage and density until only sediments were observed at shallow oxygenated depths.

No difference in visibility was observed between oxic and hypoxic states. Generally, visibility tended to be poorer in the lower and upper regions of the transects. Visibility for dives R948 and R1035 was poorer than for other dives.

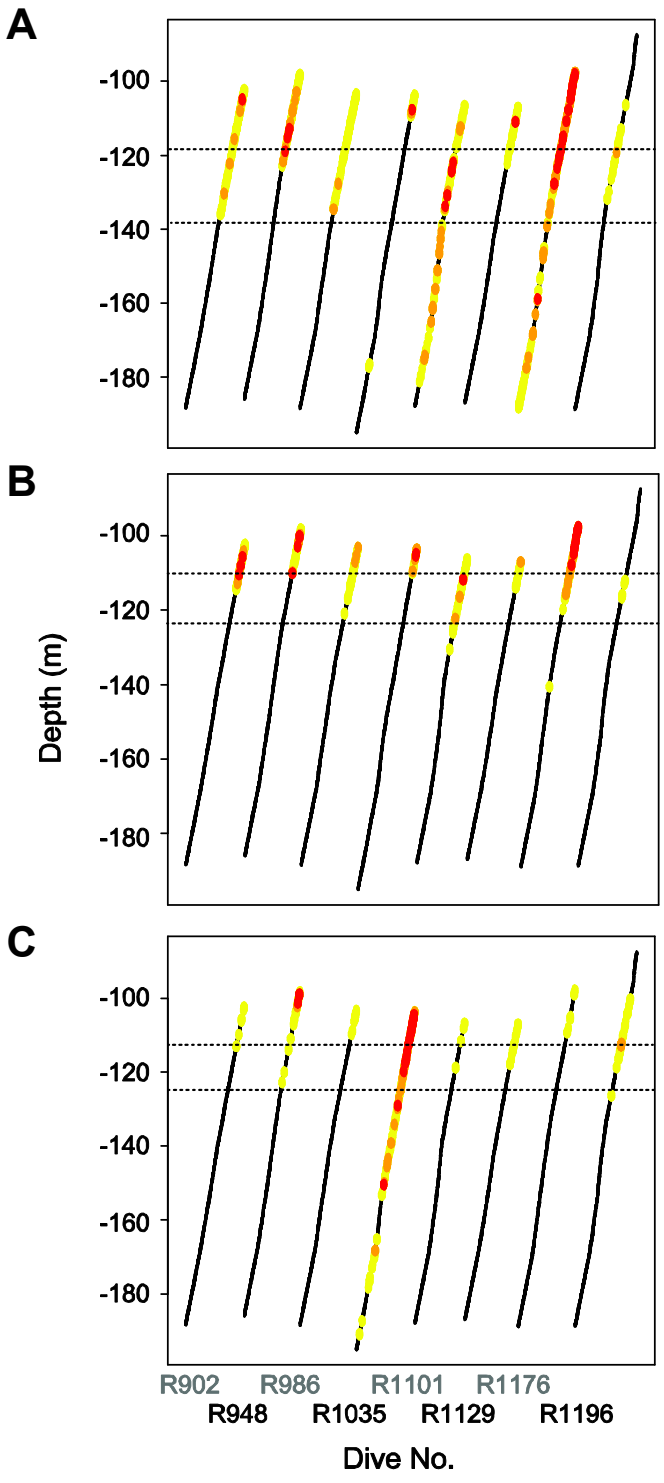

Figure 30: The density of individuals observed over depth for the eight ROV dives; A) small flatfishes, B) squat lobsters and C) small pelagic fishes. Yellow, orange and red colours represent the average number of individuals observed per seconds spent at that depth;] 0, 0.5],]0.5, 1] and >1 respectively. Dives during oxic and hypoxic states are indicated in black and grey respectively. The dotted lines represent the optimal depth range for camera placement.

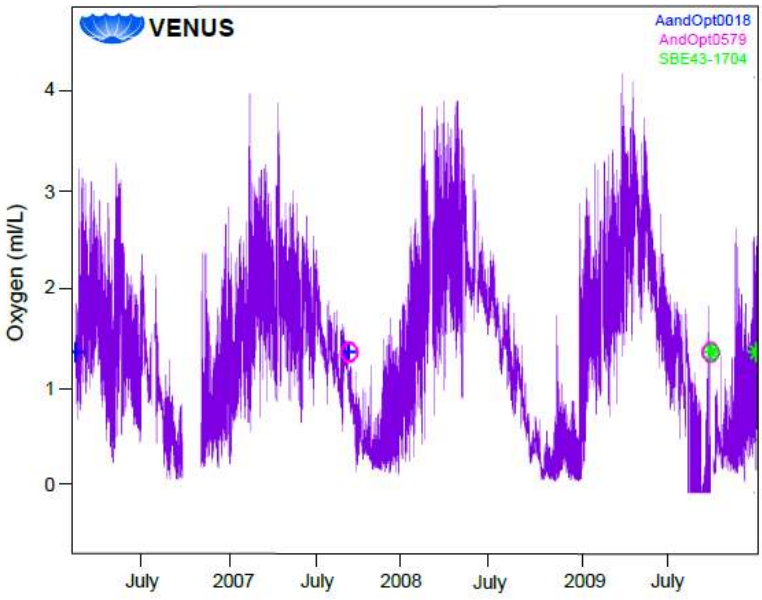

Figure 31: Cyclic trend in oxygen concentration from February 2006-2009 concatenated from multiple devices deployed at the VENUS Central Node (97m in depth) in Saanich Inlet. The data are freely available online (http://venus.uvic.ca/data/).

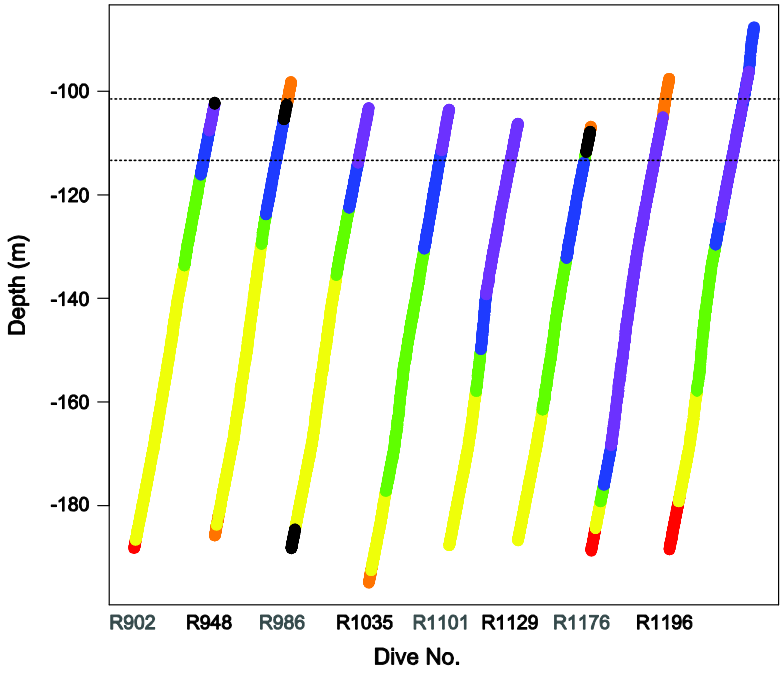

Figure 32: Qualitative index describing substratum cover over depth for the eight ROV dives; 0 (red), 1 (yellow), 2 (green), 3 (blue), 4 (purple), 5 (black) and 6 (brown). Refer to method section for description of the index used. Dives during oxic and hypoxic states are indicated in black and grey respectively. The dotted lines represent the optimal depth range for camera placement.

Outcome

Based on the ROV transect analysis, the depth range for which the greatest seasonal (oxic versus hypoxic periods) variation could be observed varied depending on the class of organism; flatfishes (119 to 139 m), squat lobsters (115 to 122 m), small pelagic fishes (117 to 124 m) and bacterial mat (101 to 116 m). However, cable length limitations and the need for a firm sediment substratum to support the camera tripod (sediments below 110 metres were very soft) forced selection of a fall 2009 deployment site at 102.5m depth (123° 29.2486 W, 48° 39.0505 N). Although suboptimal for monitoring megabenthic community shifts, this placement was strategic for observing maximal changes in bacterial mat percent cover. This deployment was the start of a year-long monitoring program whereby image sweeps of the FOV were collected three times a week. Results of the study on behavioural activity rhythms were published in Matabos et al. (2011a), presented in Chapter 4. Results from the year-long monitoring will be forthcoming.

Appendix D
Short Methodological note on a simulation to quantify the effect of observation window size on bacterial mat percent cover estimates

Introduction

The remotely operated camera tripod of the VENUS (Victoria Experimental Network Under the Sea, 2006) cabled observatory was deployed at 102.5m in depth where maximal changes in megabenthic community composition and bacterial mat growth could be observed (see Appendix C). Sweeps of the field of view (FOV) were carried out three times per week from October 6th 2009 to October 18th 2010, yielding 161 sweeps, each consisting of 7-13 images. To analyze the acquired imagery, perspective grids were constructed (Wakefield & Genin 1987) (see Chapter 2 for description of methodology). Although the accuracy of the pan and tilt mechanism was unreliable, efforts were made to sample the same area of seafloor over time. Bacterial mat was quantified in a central, near-field sector of each image. This fixed 'observation window' was chosen to avoid two possible sources of error: 1) The uneven lighting field in each image made it difficult to distinguish bacterial mat from sediment in more distant, poorly-lit portions of the FOV; 2) Overlap between consecutive images of the same sweep, together with the often featureless nature of bacterial mat coverage, made it difficult to avoid quantifying the same area twice, in overlapping images. Since bacterial mats were frequently patchy and not uniformly distributed throughout the FOV, the precision and accuracy of the bacterial mat percent cover estimates could be influenced by the size of the observation window. We therefore undertook a numerical simulation to theoretically quantify this effect and create confidence intervals around our observations.

Methods

Two window sizes were compared, each consisting of adjacent rows of 10 x 10 cm squares in the perspective grid (Figure 33). The 5 x 3 window afforded the best lighting and resolution, but the 5 x 6 window provided a larger counting area. A simulation was created using the statistical package R (freely available online; http://www.r-project.org/) whereby a 10 x 10grid (total of 100 grid squares) was subjected to increasing bacterial mat percentage cover (P%) (1-99%). The squares with bacterial mat were chosen randomly and for each P%, 1,000 iterations were conducted. The two candidate observation window sizes, 5 x 3squares and 5 x 6 squares, were overlain (Figure 33) and the number of squares with mat present (N) for each window size was recorded. For each N observed, the range in P% inputted was recorded and used to build 95% exact Poisson confidence limits. These confidence limits were assigned to N values recorded using the VENUS camera in Saanich Inlet.

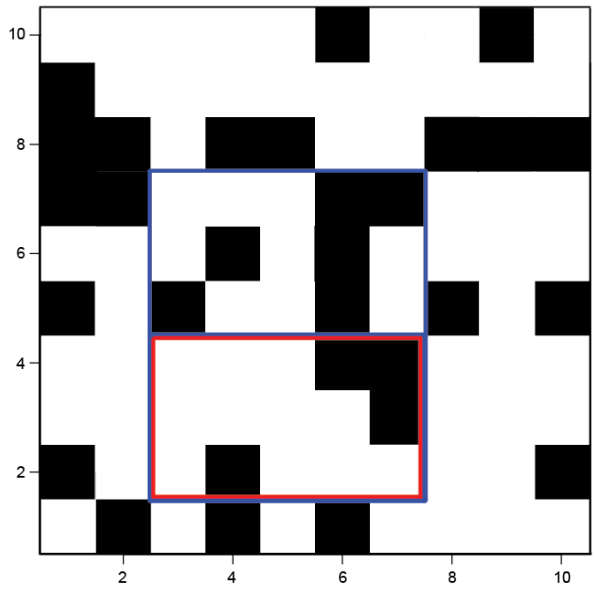

Figure 33: Example of the grid with a simulated 33% bacterial mat (black squares) cover. The 15-square (red) and 30-square (blue) observation windows are visible in the lower half of the grid. N_{15}= 4 and N_{30}= 10; representing a $P\%_{15}$= 26.7% and $P\%_{30}$= 33.3%.

Results

Bacterial mat percent cover estimates obtained based on the number of squares with mat within the 15-square window were generally higher than the estimates obtained using the 30-square window (Figure 34 A). Increasing window size did not significantly affect precision of the estimate (Figure 34 B). To validate this with field data, we determined bacterial mat percent cover using the entire 10 x 10 grid (100 squares) for nine images. All values were contained within the predicted 95% exact Poisson confidence limits for the 30-square window size while only one value fell outside the estimated range of the 15-square window.

Outcome

As the 30-square window took longer to analyze, but did not significantly improve bacterial mat percent coverage estimates, the 15-square window was used for subsequent faunal analysis and cross-correlations with environmental variables such as oxygen concentration.

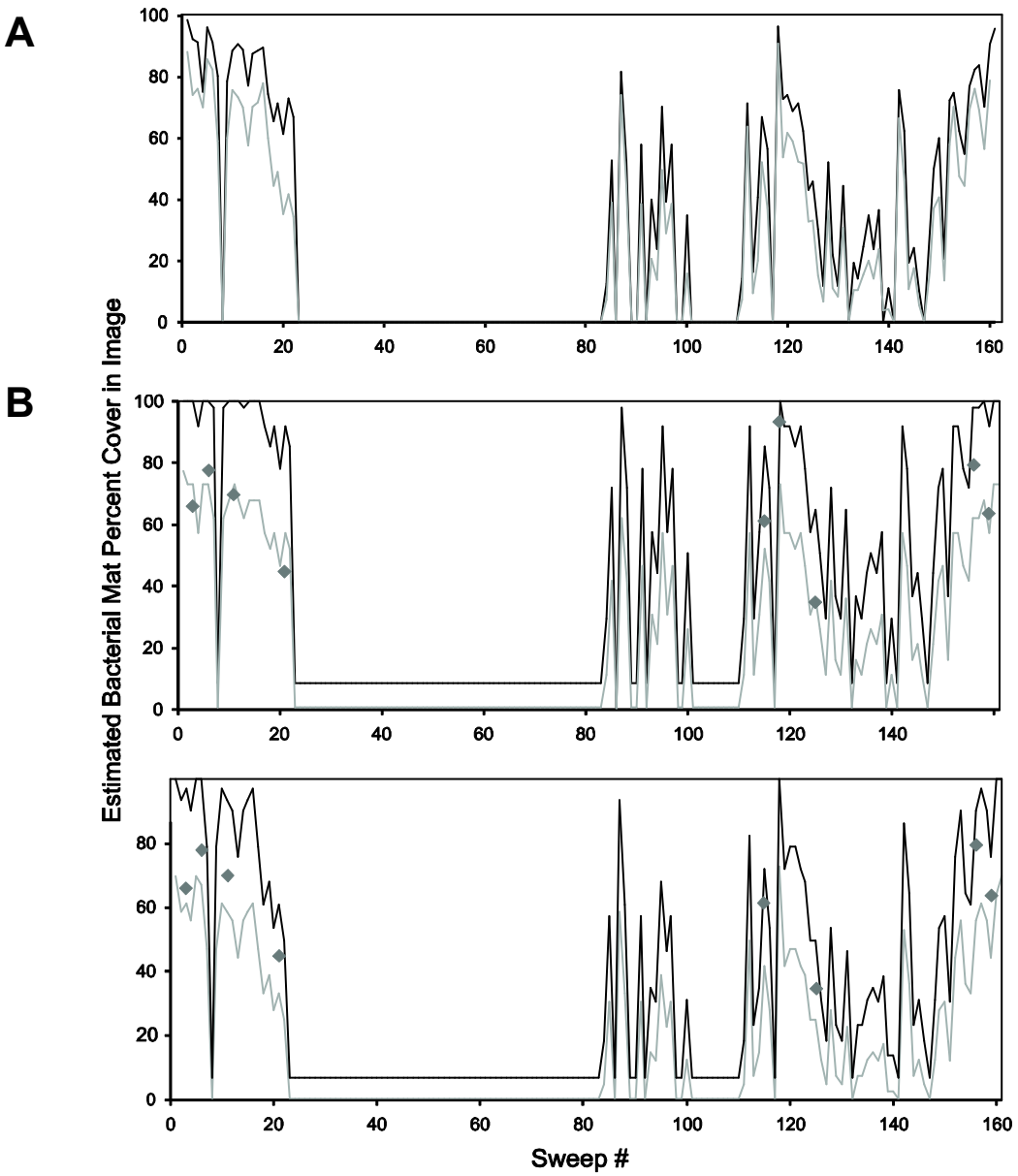

Figure 34: A) The estimated bacterial mat percent cover based on the number of squares with mat recorded in the 15-square window (black) and 30-square window (gray). B) The 95% exact Poisson confidence limits as obtained using the simulation; 15-square window (upper) and 30-square window (lower). The black lines represent the upper and grey lines the lower. The diamonds represent the nine images for which percent cover for the entire image was collected.

Supplementary Material

R code used to randomly generates squares with bacterial mat given a percent cover ranging from 1-99%. The function 'Patches' returns the number of square with mat in the two windows

```
library (rgdal)
library (maptools)
library (gstat)
library (RSAGA)
library (lattice)

Patches= function (Number) {

# Builds the grid
grd <- expand.grid (x= seq (from= 1, to= 10, by= 1), y= seq (from= 1, to= 10, by= 1))
N= sample (seq (1, 100), Number)
seq= numeric (100)
seq [N]= 1
table= cbind (grd, seq)

 # Plots the image
 ## 15 square window
 image (table, col= c ("white", "black"), xlim= c (1, 10), ylim= c (1, 10))
lines (c (2.5, 7.5), c (1.5, 1.5)) #Lower
lines (c (2.5, 7.5), c (4.5, 4.5)) #Upper
lines (c (7.5, 7.5), c (1.5, 4.5)) #Right
lines (c (2.5, 2.5), c (1.5, 4.5)) #Left
## 30 square window
lines (c (2.5, 7.5), c (1.5, 1.5)) #Lower
lines (c (2.5, 7.5), c (7.5, 7.5)) #Upper
lines (c (7.5, 7.5), c (1.5, 7.5)) #Right
lines (c (2.5, 2.5), c (1.5, 7.5)) #Left

# Selects the coordinates making up the window
## 15 square window
var1= which (table [, 1]== 3 | table [, 1]== 4 | table [, 1]== 5 | table [, 1]== 6 | table [, 1]== 7)
table2= table [var1,]
var2= which (table2 [, 2]== 2 | table2 [, 2]== 3 | table2[, 2]== 4)
table3= table2 [var2,]
Estimate= sum (table3 [, 3])
## 30 square window
var1= which (table [, 1]== 3 | table [, 1]== 4 | table [, 1]== 5 | table [, 1]== 6 | table [, 1]== 7)
table2= table [var1,]
var2= which(table2 [,2]== 2 | table2 [, 2]== 3 | table2 [, 2]== 4 | table2 [, 2]== 5 | table2 [, 2]== 6 |
  table2 [, 2]== 7)
table6= table2 [var2,]

return (Estimate)
}
```